2003

Performance evaluation of diesel particulate filters on heavy-duty vehicles

Stephen George Rosepiler
West Virginia University

Performance Evaluation of Diesel Particulate Filters on Heavy Duty Vehicles

Stephen G. Rosepiler

Thesis submitted to the
College of Engineering and Mineral Resources
at West Virginia University
in partial fulfillment of the requirements
for a degree of

Master of Science
in
Mechanical Engineering

W. Scott Wayne, Ph.D., Chair
Nigel N. Clark, Ph.D.
Mridul Gautum, Ph.D.
Ralph D. Nine, MSME

Department of Mechanical and Aerospace Engineering

Morgantown, WV
2003

Keywords: exhaust after-treatment, diesel emissions, particulate matter

Abstract

Performance Evaluation of Diesel Particulate Filters on Heavy Duty Vehicles

Stephen G. Rosepiler

Diesel particulate filters, or DPFs, are exhaust aftertreatment devices used to reduce exhaust emissions from diesel powered vehicles. Typical designs have a wall flow filter element downstream of an oxidation catalyst, which oxidizes a portion of the NO present in the exhaust stream to form NO_2. The resulting NO_2 aides in the combustion of the soot collected in the wall flow filter element allowing for the complete breakdown of the soot within typical diesel exhaust temperatures, thus limiting the required maintenance on the filter elements to the removal of non-combustible ash.

Three aspects of DPF performance were investigated: cold start performance, filter durability, and general efficiencies. The cold start performance evaluation determined that the filter elements trapped particulate matter prior to the DPF light-off temperature being reached, however there was no significant impact on white smoke emissions at any temperature range. The DPF light-off temperature was determined to be between 330°F and 450°F for the Engelhard DPX and between 375°F and 450°F for the Johnson-Matthey CRT.

The filter durability study showed a slight degeneration of DPF performance as age and accumulated mileage increased. However, a definitive DPF life span could not be determined due to inconsistencies in the data from one testing round to the next.

In the general efficiencies evaluation, CO emissions were reduced by greater than 84% for both DPF styles tested. HC emissions were reduced by 76% with the Engelhard DPX and by 81% with the Johnson-Matthey CRT. PM emissions were reduced by 94% and 82% by the Engelhard DPX and the Johnson-Matthey CRT respectively. No significant changes were recorded for total NO_X (NO + NO2) or CO_2 emissions.

Acknowledgements

I would like to thank my committee members, Scott Wayne, Nigel Clark, Mridul Gautum, and Ralph Nine, for their professional guidance and support. Additionally, I would like to thank Scott Wayne for giving me the opportunity to continue my education through graduate school and for the opportunity to work with the Transportable Emissions Lab.

Also, I would like to thank all of the engineers and technicians of the WVU Transportable Heavy-Duty Vehicle Emissions Testing Laboratory. Without your knowledge and expertise, the data collection for this thesis would have been impossible.

I would also like to thank all of my friends and office-mates, especially Nick. You have made the last several months much more enjoyable, both at work and outside of work.

Finally, I would like to thank my parents, brother, Joe, and fiancée, Amy. Without your continuing and never-ending encouragement, I would not have successfully made it through this part of my life. You will never understand how much your encouragement and support mean to me. Thank You!

Table of Contents

List of Figures

List of Tables

Nomenclature

AC	Alternating Current
ADC	Analog to Digital Converter
BDL	Below Detectable Limits
CARB	California Air Resources Board
CBD	Central Business District
CFR	Code of Federal Regulations
CFV	Critical Flow Venturi
CO	Carbon Monoxide
CO_2	Carbon Dioxide
CRT	Johnson-Matthey Continuously Regenerating Technology
CSHVR	City-Suburban Heavy Vehicle Route
DC	Direct Current
DE	Diesel Exhaust
DF	Dilution Factor
DOC	Diesel Oxidation Catalyst
DPF	Diesel Particulate Filter
DPX	Engelhard Diesel Particulate Filter
ECD	Emission Control Diesel
ECM	Engine Control Module
EGR	Exhaust Gas Recirculation
EPA	United States Environmental Protection Agency
EUI	Electronic Unit Injection
FTP	Federal Test Procedure
g/bhp-hr	grams per brake horsepower-hour
GPS	Global Positioning System
GVWR	Gross Vehicle Weight Rating
HC	Hydrocarbon
HCO	High Level Carbon Monoxide
HFID	Heated Flame Ionization Detector
LCO	Low Level Carbon Monoxide
LED	Light Emitting Diode
MPG	Miles Per Gallon
NDIR	Non-Dispersive Infrared Analyzer
NMHC	Non-Methane Hydrocarbon
NO_2	Nitrogen Dioxide
NO	Nitric Oxide
NOx	Oxides of Nitrogen
NREL	National Renewable Energy Laboratory
NYCDOS	New York City Department of Sanitation
PAH	Polyclic Aromatic Hydrocarbon
PM	Particulate Matter
QCS	Quiescent Combustion System
RMS	Root Mean Square
SCR	Selective Catalytic Reduction
SMD	Sauter Mean Diameter

SOF	Soluble Organic Fraction
TEOM	Tapered Element Oscillating Microbalance
Translab	WVU Transportable Heavy-Duty Vehicle Emissions Testing Laboratory
USDOE	United States Department of Energy
VOC	Volatile Organic Compound
WCTA	Westchester Count Transit Authority
WMATA	Washington Metropolitan Area Transit Authority
WVU	West Virginia University

Chapter 1 – Introduction

Diesel engines are well known for durability, excellent fuel economy, and unmatched torque generation at low engine speeds. For these reasons, diesel engines have long been the workhorses of the commercial transit and freight industries. Over 95 percent of all transit buses and virtually all over-the-road tractors on the road today are equipped with diesel engines (Kilcarr, 2001).

Despite their overwhelming popularity and widespread use, diesel engines face an uncertain future as emissions regulations become ever more stringent. The United States Environmental Protection Agency (EPA) has listed diesel exhaust emissions as a "cancer-causing carcinogen". The EPA, California Air Resources Board (CARB), and various other international regulatory agencies have been regulating diesel exhaust emissions, particularly carbon monoxide, hydrocarbons, oxides of nitrogen, and particulate matter, for several decades in order to protect the environment and human health. These regulations have forced engine manufacturers to greatly reduce engine-out emissions through optimization of internal engine designs. However as reductions gained through continued design improvements began to stabilize, it was realized that exhaust aftertreatment might be the only way to meet or exceed the fast approaching 2007 EPA emissions standards. Chapter 2 of this thesis, the Literature Review, contains a review of existing and future emissions standards and techniques engine manufacturers have used to optimize engine designs to minimize engine out emissions.

Many types of aftertreatment devices have been developed for application to heavy-duty diesel engines, however the most popular of these devices are diesel oxidation catalysts and diesel particulate filters. Diesel oxidation catalysts, or DOCs,

greatly reduce carbon monoxide and hydrocarbons, however they have little effect on oxides of nitrogen (NO_X) and particulate matter (PM), although the soluble organic fractions in the PM are reduced. These and other aftertreatment systems are discussed in Chapter 2 – Literature Review.

Diesel particulate filters, or DPFs, significantly reduce emissions of carbon monoxide, hydrocarbons, and particulate matter; yet still have little effect on total NO_X. Although total NO_X emissions remain virtually unchanged, NO is reduced by conversion to NO_2. The resultant NO_2 produced is used to aid in the oxidation of the particulate matter that is collected on the internal filter walls. Although NO_2 is reduced, NO and NO_2 are not independently regulated by the EPA or CARB.

The main objective of this thesis was to investigate the operational performance of diesel particulate filters. To accomplish this, three aspects were investigated: cold start performance, durability, and general performance with a comparison of two DPF styles. The DPF styles studied were the Engelhard DPX and the Johnson-Matthey CRT.

The Johnson-Matthey Corporation claims their CRT reduces particulate matter, hydrocarbon, and carbon monoxide emissions by greater than 90% while reducing NO_X levels by 5-10%. For passive regeneration, the CRT requires an exhaust temperature of greater than 260°C (500°F) for a minimum of 40% of the operating time and a NO_X/PM ratio of at least 20. Additionally, the Johnson-Matthey CRT requires less than 15 ppm sulfur fuel and requires general maintenance and cleaning between every 60,000 and 100,000 miles (Johnson-Matthey, 2001).

The Engelhard Corporation claims their diesel particulate filter, the DPX, can reduce particulate matter, carbon monoxide, and hydrocarbon emissions by up to 90%.

Additionally, they claim the DPX regenerates within normal diesel operating temperatures and does not require low sulfur fuel. Engelhard makes no claims to NO_X reductions and does not specify a routine maintenance schedule (Engelhard, 2002).

Each of the three investigation areas within the scope of this thesis had individual objectives. The intended purpose of performing cold start testing was to determine an approximate light-off temperature for the catalyst within the DPF, to quantify the general performance of the DPF before this light-off temperature was reached, and to determine if white smoke emissions were reduced by the DPFs. The durability study was performed in order to estimate the life cycle of each particulate filter type and to determine if a relation exists between DPF performance and accumulated vehicle mileage. The general performance study and product comparison was performed to evaluate the overall performance of the diesel particulate filters being tested and to determine if the corporate claims to performance were reasonable.

All tests for this evaluation were performed using the West Virginia University Transportable Heavy-Duty Vehicle Emissions Testing Laboratory (Translab). It is known that chassis dynamometer testing more accurately simulates "real world" engine emissions than does engine dynamometer testing, as engine dynamometer testing does not account for losses due to transmissions, differentials, and vehicle accessories, nor does it mimic engine transients sufficiently well. Details of the WVU Transportable Heavy-Duty Vehicle Emissions Testing Laboratory are given in Chapter 3 of this thesis, Experimental Procedures and Equipment.

Test vehicles for this evaluation included transit buses, over-the-road tractor trucks, and refuse trucks taken from five independent fleets. The fleets included West

Virginia University (WVU), the Washington Metropolitan Area Transit Authority (WMATA), the Westchester County Transit Authority (WCTA), the New York City Department of Sanitation (NYCDOS), and Ralph's Grocery fleet in Riverside, California. Multiple driving schedules were utilized through out this testing. Most driving schedules were cycles or routes developed to simulate the duty cycle of a specific fleet, although some driving schedules were standard cycles, such as the Central Business District (CBD) cycle. Details pertaining to the test vehicles, the driving schedules, and experimental results are given in Chapter 4 of this thesis, Test Vehicles, Driving Schedules, and Results. Conclusions drawn from this data about the performance of diesel particulate filters are shown in Chapter 5 – Conclusions.

Chapter 2 – Literature Review

2.1 Introduction

Diesel engines have long been known for their fuel economy and reliability. For these reasons, they have become the workhorses of the commercial trucking industry. Diesel engines are used to power the transportation of 94% of all freight shipped in the United States, and 95% of all transit buses and heavy construction equipment are diesel powered (Kilcarr, 2001).

In spite of this, diesel exhaust emissions have been found to have a great environmental impact and continue to be of concern to state, federal, and international air quality agencies. In 1998, the California Air Resources Board, or CARB, designated diesel particulate matter to be a toxic air contaminant (Chandler, et al., 2002). In the 2002 Health Assessment Document for Diesel Exhaust, the United States Environmental Protection Agency (EPA) listed diesel exhaust as a cancer causing carcinogen, finding "considerable evidence demonstrating an association between DE (diesel exhaust) exposure and increased lung cancer risk among workers in varied occupations where diesel engines historically have been used."

In this same report, the EPA listed the major gaseous components of diesel exhaust as carbon dioxide, oxygen, nitrogen, water vapor, carbon monoxide, nitrogen compounds, sulfur compounds, and numerous molecular weight hydrocarbons, including, but not limited to, aldehydes, benzene, 1,3-butadiene, polyclic aromatic hydrocarbons (PAHs), and nitro-PAHs. Additionally, diesel particulate matter was defined as solid particles having a center core of elemental carbon and absorbed organic compounds, as well as small amounts of sulfate, nitrate, metals, and other trace elements (EPA, 2002).

2.1.1 Emissions Standards

Emissions regulation first began in 1955 with the passage of the Air Pollution Control Act of 1955. This was followed by the passage of various legislation throughout the 1960's, which included the creation of the 13 mode gaseous emissions cycle and the development of the first smoke standards (Richards and Sibley, 1988). The legislation increase of the 1960's lead to creation of the United States Environmental Protection Agency, EPA, through the Clean Air Act of 1970.

In an effort to standardize emissions testing procedures, the EPA developed the Code of Federal Regulations, Title 40: Protection of Environment, Part 86: Control of Emissions from New and In-Use Highway Vehicles and Engines (40CFR-PART 86). This document contains all of the testing procedures which must be followed by an emissions testing facility, as well as all federally mandated emissions standards.

The EPA has specified four diesel emissions components for regulation. They are carbon monoxide (CO), hydrocarbon (HC or NMHC for Non-Methane Hydrocarbon), oxides of nitrogen (NO_X), and particulate matter (PM). The present and future emissions standards are shown in Table 2.1. Emissions standards apply to an engine based on its original manufacture model year. The EPA mandates that all emissions must be reported in units of grams per brake horsepower-hour (g/bhp-hr).

Table 2.1: EPA Emissions Standards for Heavy Duty Diesel Engines (g/bhp-hr) (Dieselnet, 2002)

Year	HC	CO	NO_x	PM
Heavy-Duty Diesel Truck Engines				
1988	1.3	15.5	10.7	0.60
1990	1.3	15.5	6.0	0.60
1991	1.3	15.5	5.0	0.25
1994	1.3	15.5	5.0	0.10
1998	1.3	15.5	4.0	0.10
2004	*See note*			
2007	0.14	15.5	0.2	0.01
Urban Bus Engines				
1991	1.3	15.5	5.0	0.25
1993	1.3	15.5	5.0	0.10
1994	1.3	15.5	5.0	0.07
1996	1.3	15.5	5.0	0.05*
1998	1.3	15.5	4.0	0.05*
2004	*See note*			
2007	0.14	15.5	0.2	0.01

* - in-use PM standard 0.07

***note** The 2004 emissions standard called for a reduction in NO_X emissions, however two options are available for certification. These options are shown in Table 2.2. Again, all data is shown in g/bhp-hr.

Table 2.2: Options for Engine Certification for 2004 NO_X Emissions (Dieselnet, 2002)

Option	NMHC + NO_x	NMHC
1	2.4	n/a
2	2.5	0.5

The 2007 NO_X and NMHC standards are to be phased in on a percent-of-sales basis. Fifty percent for each from 2007 to 2009 and reaching 100% compliance by 2010. The 2007 PM standard will take immediate effect in 2007 (Dieselnet, 2002).

2.1.2 Cold Start Emissions and White Smoke

Cold start emissions concentrations, especially white smoke, hydrocarbons, and particulate matter, can vary significantly from emissions concentrations from a

sufficiently warmed-up engine. These emissions need to be controlled in order to meet future emissions standards (Yassine, et al., 1996).

White smoke, often appearing as a white or blue haze in direct sunlight, consists of a mixture of fuel and lubricating oil particles in an unburned or partially burned state. The blue component is a result of excess lubricating oil in the combustion chamber caused by engine wear such as deteriorating piston rings or worn valve guides. The white component consists mainly of unburned hydrocarbons resulting from low gas temperatures in the combustion chamber during cold starts.

Black/gray smoke is essentially composed of carbon particles resulting from incomplete combustion of fuel. Incomplete combustion is often a result of an excessively rich condition caused by malfunctioning or dirty fuel injectors, restricted airflow into the engine, or from excessive cranking during cold start-up.

During engine start-up, fuel is injected into the combustion chambers during misfire cycles while the engine is being cranked by the starter motor. This fuel accumulates on the cylinder walls and piston bowls until the in-cylinder temperature reaches the combustion temperature of the fuel and combustion occurs. Upon combustion, the high temperature of the combustion products increases the rate of evaporation of the accumulated fuel and causes high concentrations of fuel vapor emission, part of which condenses into white smoke (Yassine, et al., 1996).

Some of the hydrocarbons and particulates remaining after combustion might be oxidized during the expansion and exhaust strokes. The rate of oxidation is dependent on the gas temperature and local equivalence ratio. Under warm-up conditions, oxidation reactions can be effective in reducing HC concentrations. However, during cold start

conditions, the oxidation reactions are not effective due to the low in-cylinder temperatures (Yassine, et al., 1996).

NO_X emissions can also be affected under cold start conditions, particularly in engines which have advanced timing when cold. By lengthening the ignition delay, timing advancement can cause an increase in NO_X levels while other emission species remain relatively affected (Heywood, 1988).

2.2 Diesel Engine Technology

In efforts to control engine-out emissions in order to meet the new more stringent standards, engine manufacturers and researchers have made design changes to both engine designs, such as combustion chamber configuration, and to the design of many engine components, including fuel injectors and turbochargers.

2.2.1 Improved Combustion Chamber Design

Combustion chamber modifications are crucial to increasing the performance of a diesel engine, from an emissions standpoint as well as a reliability issue. Engine designers have at their disposal technological and computational advancements never before seen in the industry. These include computers and computer models which aid in testing, modeling, and optimization of new designs. These modifications and optimizations, which include reducing oil consumption, increasing the compression ratio, and improving combustion, are responsible for lowering both gaseous and particulate emissions.

2.2.1.1 Reduced Oil Consumption

Engine lubricating oil which remains on the cylinder walls during the expansion stroke, or oil which is otherwise introduced into the combustion chamber, can

significantly influence engine-out PM emissions. Precision bore honing and enhanced piston ring designs can considerably reduce the amount of lubrication oil consumed during the expansion stroke, however modifications of this nature must be made very carefully as too little oil remaining on the cylinder walls can have a detrimental effect on engine reliability (Browning, 1997). For this reason, other mechanical components, such as valve guides, valve guide seals, and turbocharger seals, should be investigated for reducing oil consumption.

Another design aspect that should be addressed in an effort to reduce oil consumption is bore distortion. Bore distortion is a result of localized distortions caused by thermal and mechanical expansion of the cylinder walls due to the internal temperatures and pressures inside the combustion chamber. To prevent or cure bore distortion, significant and costly changes may be required in the cylinder block, cylinder sleeve, and cylinder head gasket designs. For this reason, this design aspect should be addressed in the early design stages of a new engine and is not a suitable area for retrofits to existing engines (Zelenka, et al., 1990).

2.2.1.2 Increased Compression Ratio

Increasing the compression ratio in a diesel engine has many favorable results. The increased compression ratio reduces the ignition delay period, thus reducing the amount of fuel burned in the premixed region and allowing increased injection timing retard. The increased injection timing retard allows for greater control over NO_X production.

Additionally, an increased compression ratio increases the combustion temperature, thus reducing cold start PM and white smoke production. High compression

ratios are most beneficial under a high speed / light load condition when ignition delay is the longest and under cold operating conditions (Browning, 1997).

2.2.1.3 Improved Combustion

There are two methods for improving combustion characteristics through intake air motion. They are intake swirl and quiescent combustion. Intake swirl focuses on forcing rotational motion in the intake air to increase air/fuel mixing and fuel atomization. The resultant completeness of combustion lowers PM output, allowing designers to take a more aggressive approach in reducing NO_X.

Quiescent combustion has been used in marine diesel applications where fuel consumption is of the utmost importance. Mitsubishi Motors Corporation has been working on an improved quiescent combustion system (QCS) for on-road heavy-duty diesel applications. This system does not rely on air motion to promote fuel atomization, but rather fuel spray momentum with a high-pressure fuel injection system. Engineers investigated both fuel system requirements, which will be discussed later in this thesis, and combustion chamber geometry in order to optimize the fuel efficiency and emissions production of this system.

After much calculation and modeling, researchers from Mitsubishi Motors Corporation decided that the optimum combustion chamber geometry was a large-diameter toroidal type combustion chamber with a low swirl ratio. The low swirl ratio is associated with a smaller pressure loss across the intake port and had a higher flow coefficient, therefore the air flow could be enhanced and fuel consumption reduced. The large diameter bowl helped to prevent fuel spray from impinging on the cylinder walls prior to ignition, resulting in lower black smoke and HC emissions. It was also shown

that a larger radius in the combustion chamber bottom (the piston bowl) is associated with lower smoke emissions under the low load condition. Thus implying that the fuel being injected into the chamber is being spread-out over the entire combustion chamber and burned more completely (Mori, et al., 2000)

2.2.2 Improved Fuel Injection

Fuel injection parameters can greatly impact the combustion process. Injection delay and air/fuel mixing can be affected by injection timing, pressure, duration, and rate, consequently having a large effect on engine-out emissions. In efforts to optimize the fuel injection systems, manufacturers will continue to investigate nozzle geometry, multiple injection and rate shaping, and electronic unit injection.

2.2.2.1 Nozzle Geometry

Nozzle hole diameter, the number of nozzle holes, spray angle, and the Sauter Mean Diameter are all important aspects to consider when reviewing nozzle geometry.. The Sauter Mean Diameter (SMD or D_{SM}) is the diameter of the fuel droplet that has the same surface/volume ratio as the entire spray volume and is related to the atomization of the fuel. Hiroyasu and Kadota developed equation 2.1 as an empirical expression for the SMD.

$$D_{SM} = A(\Delta p)^{-0.135} \rho_a{}^{0.121} V_f^{0.131} \tag{2.1}$$

where Δp is the mean pressure drop across the nozzle, ρ_a is the density of the intake air, V_f is the volume of fuel delivered per cycle per cylinder, and A is a nozzle dependent constant (23.9 for hole nozzles) (Heywood, 1988).

Researchers from the University of Wisconsin-Madison and Caterpillar Inc. found that the injection spray angle was directly related to the SMD and to NO_X and PM

formation. They found that a larger injection angle produces a narrower spray angle and a larger overall average SMD. Also, they found that the injection angle is proportional to NO_X formation, yet has little effect on PM emission (Su, et al., 1995).

Similarly, a relation exists between nozzle hole size, hole number, and injection pressure. Small nozzle hole sizes, used in conjunction with high injection pressures, produce a small overall average SMD and reduce particulate emissions significantly. It was also shown that as injection pressure increases, NO_X formation increases at almost the same rate. However, if the injection duration is extended while using a small hole diameter nozzle, the NO_X production is decreased. Additionally, the number of nozzle holes should be matched to the fuel injection pressure and combustion chamber geometry to best utilize the intake air for fuel atomization (Browning, 1997; Mori, et al., 2000; Su, et al., 1995).

2.2.2.2 Multiple Injections and Rate Shaping

Rate shaping is a process used to optimize combustion and reduce emission production by manipulating the rate at which fuel is injected into the cylinder. The amount of fuel injected at the onset of injection is decreased to reduce NO_X formation. The latter portion of injection is characterized by a fast injection rate, for particulate control, as the piston approaches top-dead-center and the highest combustion temperatures are reached. This method of rate shaping is known as pilot injection and has shown 50% reductions in ignition delay, allowing increased injection timing retard and good combustion stability (Khair, 1997).

A different approach to rate shaping employs multiple or split injections. Multiple injections have been shown to simultaneously reduce NO_X and PM emissions by

15% and 40% respectively. These results were demonstrated in the previously mentioned study performed by the University of Wisconsin-Madison and Caterpillar Inc. using a setup characterized by a double injection of 50% of fuel mass evenly distributed to two injections separated with a 10° crank angle dwell (Su, et al., 1995).

2.2.2.3 Electronic Unit Injection

Electronic unit injection (EUI) possesses the ability to achieve high injection pressures, in the 1400-1900 bar range, and can specify injection parameters such as start of injection, injection duration, and rate shaping as a function of engine speed and load. These systems are often mechanically driven from the camshaft or fully electronically controlled by the engine control module. Electronically controlled common rail systems offer the advantage over the mechanical systems of being independent of engine speed, however they often have lower overall peak injection pressures.

The high injection pressure offered by these systems aid in fuel atomization and completeness of combustion, resulting in reductions in particulate emissions. However, the increased injection pressures often increase the accessory loading on the engine. In spite of this, it is felt that the improved combustion due to the higher injection pressures should counter this effect and result in no net increase in brake specific fuel consumption (Browning, 1997).

2.2.3 Turbocharger Improvements

Turbochargers have been proven to improve engine performance and brake horsepower without adversely affecting fuel consumption or emissions. Technological advancements in turbocharger design, including two-stage turbocharging and variable geometry turbocharging, have increased effectiveness in providing leaner air/fuel ratios

under full load conditions and improving transient response at lower loads and speeds (Browning, 1997).

Researchers at the University of Wisconsin-Madison are also looking into the effects of boost pressure on emissions reductions. They have found that optimizing boost pressure leads to significant improvements in brake specific fuel consumption and particulate emissions. The decrease in particulate emissions is accredited to the increased availability of air for soot oxidation at elevated intake pressures from increased boost levels. It should be noted that the decrease in PM emissions was accomplished while holding brake specific NO_X constant. It should also be noted that there exists a point at which boost pressures is optimized, and continued increase of boost pressures has a detrimental effect on particulate emissions as a result of reduced liquid spray and vapor penetration lengths within the combustion chamber (Tanin, et al., 1999).

2.3 Exhaust Aftertreatment

In spite of the advances in diesel engine design, manufacturers are looking to after-treatment to bring the emission levels to within acceptable limits. As emission regulations become more stringent, especially for NO_X and PM emissions, aftertreatment will be the only way to build certifiable engines. There are numerous types of after-treatment systems including diesel oxidation catalysts, lean NO_X catalysts, selective catalytic reduction, exhaust gas recirculation, non-thermal plasma catalysts, and diesel particulate filters (Johnson, 2002). Each system has advantages and disadvantages which must be weighted before selecting an after-treatment system, however their use is inevitable.

2.3.1 Oxidation Catalysts

Diesel oxidation catalysts (DOC) were once the premier choice for diesel exhaust after-treatment, however with ever tightening emissions standards, they are quickly becoming obsolete. DOCs are very effective in reducing CO, HC, aldehydes, and the soluble organic fraction (SOF), however they have little effect on NO_X and limited effect on particulate emissions (Zelenka, et al., 1990). Additionally, oxidation catalysts produce sulfates through the oxidation of SO_2 when exhaust temperatures exceed the 400° centigrade unless fuel sulfur content is kept to a minimum; this drawback is quickly lessening in importance with the introduction and mandated use of ultra-low sulfur diesel fuel by 2006.

In a study performed in Europe, diesel oxidation catalysts were shown to greatly reduce HC, CO, and formaldehyde emissions by 86%, 93%, and 81% respectively. However, this study also demonstrated the DOCs lack of ability to substantially reduce particulate matter and NO_X emission. PM was reduced by a mere 17% when using Swedish Class 1 fuel without sulfur and 19% when the same fuel was doped to 0.05 wt% sulfur. No measurable NO_X reduction was reported with either fuel (Hammerle, et al., 1995).

With the sizable emission reductions in HC, CO, and aldehydes, DOCs are good candidates for after-treatments systems when combined with another form of after-treatment or with fuel-borne catalysts. A study performed by the Southwest Research Institute saw PM reductions from 0.073 g/bhp-hr to 0.042 g/bhp-hr, a 42% reduction, using a fuel-borne catalyst. However this study also reported that for a diesel oxidation

catalyst to be most effective, it must be approximately equal in volume to the engine displacement, meaning that for large diesel engines, the catalyst would be quite large and cumbersome (Khair & McKinnon, 1999).

2.3.2 Lean NO_X Catalysts

Lean NO_X catalysts provide a catalytic reduction of NO_X through a lean-fuel environment. Copper zeolite catalysts use hydrocarbons in the exhaust stream to reduce NO_X emission at high temperatures, ranging from 425 to 550 degrees centigrade. This system has two major problems: 1) the system requires a significant amount of hydrocarbons in the exhaust stream to reduce NO substantially, approximately an HC to NO ratio of 4 to 1. 2) The system is very sensitive to sulfur poisoning from the absorption of SO_2 and water inhibition (Browning, 1997). It has been determined that sulfur degrades the oxygen storage media, which in turn inhibits the formation of hydrogen in the water gas shift reaction. This, in turn, greatly detracts from the lean NO_X catalyst's efficiency and requires a desulfation process to recover some of the lost efficiency. The catalysts never fully regenerate to 100% capacity, thus suggesting that they have a finite life (Johnson, 2002).

Another type of lean NO_X catalyst utilizes a platinum based catalyst. This system operates at a lower temperature than the previously discussed system (200 to 300 degrees centigrade) and requires less HC to reduce the NO_X (a 2 to 1 ratio). However, the platinum in this system produces sulfates from the fuel sulfur, increasing the particulate matter emission (Browning, 1997).

The significant problem with any lean NO_X catalyst is the need for large amounts of hydrocarbons. Three systems have been developed to supplement the exhaust stream

with the necessary HC's. The first strategy is to place an additional fuel injector into the exhaust pipe up-stream of the catalyst and inject diesel fuel directly into the exhaust stream. This system, however, encourages tampering since removal of the injector would not influence engine performance and would enhance fuel economy. Some promise has been shown utilizing this injection method, but substituting urea for the diesel fuel injected into the exhaust. This urea system has shown NO_X reduction of 69 to 84% depending on the testing cycle being utilized (Hammerle, et al., 1995). The urea being injected does however pose its own set of drawbacks which will be discussed in section 2.3.3 – Selective Catalytic Reduction.

The second method of fuel supplementation is to increase the fuel volume being injected into combustion chamber during the normal injection process. Although potential tampering of this method is much less, large fuel penalties and increased HC emissions are likely.

The third, and most feasible, method is to inject additional fuel into the cylinder during the exhaust stroke. A more complex electronic fuel injection system would be needed to accomplish this method of fuel supplementation. It is estimated that a five percent increase in fuel consumption would be necessary to provide enough hydrocarbons for sufficient NO_X reduction (Browning, 1997).

2.3.3 Selective Catalytic Reduction

Selective Catalytic Reduction (SCR) is an after-treatment system commercially applied to stationary diesel installations. It is being researched as a possible on-road method of reducing NO_X production from heavy-duty diesel vehicles. This system injects ammonia in the form of a urea solution into the raw exhaust in order to

supplement the exhaust hydrocarbons (Khair, 1997). The ammonia injection forces the chemical reactions necessary for the nitrogen oxides in the exhaust to convert to harmless nitrogen and water. The process has demonstrated NO_X reductions as high as 90% in both the EPA's Federal Test Procedure (FTP) cycle and the New European Driving Cycle (Auto Emissions Magazine, Fall 1999).

SCR systems, in combination with diesel particulate filters, have also shown promise in simultaneously reducing diesel particulate matter and NO_X+NMHC (Non-Methane Hydrocarbon) emissions. Southwest Research Institute reported PM emissions of 0.01 g/bhp-hr and NO_X + NMHC emissions of 1.1 g/bhp-hr using 368 ppm sulfur fuel, an 86% and 73% reduction over the baseline measurements respectively. These data were recorded while testing a 1998 Detroit Diesel Series 60 12.7L turbocharged engine rated at 400 hp at 1800 rpm. Khair & McKinnon, 1999).

As promising as this system appears, it is not without its drawbacks. SCR systems produce highly elevated levels of N_2O when compared to a standard diesel and over injection of urea leads to ammonia emissions. Also, vehicles utilizing an SCR system would have to be equipped with a bulky urea storage tank, on-board monitoring system, and precise control to avoid ammonia slip. Additionally, the urea solution utilized by this system is not commercially available at every refueling station and would require a large capital investment and infrastructure development in order to change this realization (Auto Emissions Magazine, Fall 1999).

2.3.4 Exhaust Gas Recirculation

Exhaust gas recirculation (EGR) has been around for many years in spark ignition applications and is, in fact, the principle technique for NO_X emission control in these

applications. However, with the increasingly stringent NO_X limits being imposed in heavy-duty diesel engines, engine manufacturers are developing a sophisticated EGR system for direct-injected heavy-duty diesel engines.

EGR systems recycle exhaust gases into the air intake where it acts as a heat sink reducing the peak combustion temperature. The heat absorbed by the recirculated exhaust gases is thought to be proportional to the EGR flow rate ($\dot{m}$), the specific heat at constant pressure (C_P), and the temperature gradient (Δt). This relation is shown in equation 2.2. (Heywood, 1988; Khair, 1997)

$$Q = \dot{m} C_P (\Delta t) \tag{2.2}$$

The second positive aspect of EGR is its ability to effectively lower NO_X concentrations in the vehicle exhaust. The burned gases that are introduced into the air intake displace oxygen introduced with the fresh air charge. NO_X is formed as a function of nitrogen (N_2), oxygen (O_2), combustion temperature, and residence time in the NO_X formation environment. This relation is quantified in equation 2.3.

$$\frac{d(NO)}{dt} = K_1(N_2, O_2) - K_2(NO, NO_2) \tag{2.3}$$

where K_1 and K_2 are combustion temperature dependent reaction rate constants. Controlling any of these basic variables will have a great effect on NO_X formation, therefore reducing the oxygen content in the fresh air intake charge through displacement with exhaust gas will substantially lower NO_X formation. Additionally, with EGR cooling, the temperature differential term of equation 2.2 can be increased, thus increasing the EGR heat absorption capacity and further reduce NO_X formation. (Khair, 1997)

However, exhaust gas recirculation has an adverse effect on particulate formation. EGR reduces the combustion rate making stable combustion more difficult to achieve. The stability of combustion is inversely proportional to particulate formation. Thus, in order for EGR to be effective in all aspects of emission reduction, it must be utilized with some other form of after-treatment, most likely diesel particulate filters. (Heywood, 1988; Khair, 1997)

2.3.5 Non-Thermal Plasma Catalysts

Non-thermal plasma catalysts are an after-treatment system that is still in the experimental stages. In these systems, exhaust gases pass through an intense field of charged particles, a plasma field, and are dissociated and ionized into more reactive particles. These particles are easily catalyzed downstream. A pair of electrodes is used to generate the plasma field with at least one electrode covered by a dielectric barrier such as alumina. A high voltage alternating current (AC) is placed across the electrodes causing the gas in the gap between them to break down resulting in the formation of discharge streamers. The streamers rapidly travel across the gap creating electrons with a mean energy of three to four electron volts (eV). When the streamers reach the barrier, charge accumulates on the surface and cancels the electric field so that the streamers are extinguished. (Hoard, 2001)

The electrons released by the plasma discharge result in a radical chemistry between species resulting the dissociation of gases in the exhaust. The predominant dissociation that takes place is that of oxygen (O_2). This is shown in equation 2.4.

$$O_2 + e^- \rightarrow O + O + e^- \qquad (2.4)$$

The oxygen dissociation is the primary initiator of the plasma exhaust chemistry because of its rapid reaction rate with the hydrocarbons (HC) present in the exhaust. These reactions are very similar to those initiated by ultra-violet radiation in the atmosphere. The hydrocarbon-oxygen reactions result in the formation of aldehydes, including formaldehyde (CH_2O) and acetaldehyde (CH_3CHO), peroxy radicals (RO_2), and hydroxyl radicals (OH).

Nitric oxide (NO) is reacted with the compounds mentioned above to form NO_2. Some examples of these reactions are shown in equations 2.5 and 2.6.

$$NO + O \rightarrow NO_2 \tag{2.5}$$

$$NO + RO_2 \rightarrow NO_2 + RO \tag{2.6}$$

Oxides of nitrogen (NO_X) do not get converted to N_2, but rather, through the reactions shown above, HC is oxidized and NO is converted to NO_2. The presence of HC reduces the plasma energy required for NO to NO_2 conversion and greatly reduces acid formation. The presence of aldehydes and HC require an oxidation catalyst to be utilized downstream. (Hoard, 2001)

In addition to NO_X conversion, plasma catalysts can also be utilized for particulate removal. Since the plasma creates O and OH radicals and converts NO to NO_2, it can be expected that soot particles will also be oxidized provided they remain in the plasma for a sufficient period of time. To ensure this, a device, using a bed of catalyzed beads, mechanically/electrostaticly traps the soot particles in the plasma field. Laboratory experiments have shown that this greatly reduced the size of particles being released from the vehicle exhaust. (Hoard, 2001)

Plasma catalysts systems have shown high NO_X removal, as high as 80% when combined with a suitable oxidation catalysts, and high particulate removal rates. Additionally, they can function properly over a wide temperature range, 150 to 500 degrees Celsius. However, these systems have only been demonstrated in laboratory environments and are still much too large for practical use (Auto Emissions Magazine, Fall 1999). An additional drawback of these systems is the adverse effect on fuel economy, the large power consumption and need for additional HC's are expected to reduce fuel economy, however this, as of yet, has not been quantified. (Hoard, 2001)

2.3.6 Diesel Particulate Filters

Diesel particulate filters, or DPFs, are the main focus of this thesis. Particulate filters were first investigated in the 1970's and were characterized by wall flow trap element designs that force exhaust gases to flow through the porous walls of the filter element, depositing the solid matter on the walls. These early filters were actively thermally regenerated through the use of a heating system in order to maintain good performance and fuel economy. The complex regeneration system and sophisticated controls had a very high cost, and the entire unit was plagued with reliability issues.

The feasibility of these systems was largely in question until the introduction of catalyzed fuel and the mingling of catalytic material with the accumulated soot lowered the ignition temperature from the 600°C to as low as 300°C and below. This technological advancement made the development of passive regeneration systems possible (Khair, 1997).

The typical design of a passive regeneration system consists of an oxidation catalyst, often a proprietary platinum (Pt) unit, upstream of a wall flow filter. The

catalyst portion of the DPF oxidizes a portion of the NO present in the exhaust stream to form NO_2. The NO_2 is then utilized to fuel the combustion of the soot collected in the wall flow filter. It has been proven that NO_2 combusts soot at a much lower temperature than does O_2, thus allowing the filters to regenerate and completely destruct the soot within normal operating temperatures of the heavy-duty diesel exhaust stream (Allansson, et al., 2000). It should be noted that ash generated from the combustion of lube oil is not combusted by the DPF and needs to be periodically removed from the filter walls by back flushing with compressed air.

These systems are relatively compact and can be retrofitted into existing vehicles with very little modification to the vehicle. For this reason, DPFs are at the forefront of the after-treatment market. However, some DPF styles require the use of ultra-low sulfur fuel, less than 15 ppm in some cases.

This thesis will look at two specific styles of diesel particulate filters, the Engelhard DPX and the Johnson-Matthey CRT®. The Engelhard unit advertises reductions in particulate matter, soluble organic fractions, and CO and HC by 90%, 98%, and 90% respectively. This unit does not require the use of ultra-low sulfur diesel fuel or additives and operates at normal diesel operating temperatures. This diesel particulate filter system utilizes a catalyzed filter element in place of the oxidation catalysts. (Engelhard, 2002).

The Johnson-Matthey CRT® (Continuous Regenerating Technology) advertises reductions in PM, HC, and CO of greater than 90% and advertises NO_X reductions in the order of five to ten percent. This DPF requires a minimum exhaust temperature of at least 260° centigrade and an engine-out NO_X/PM ratio of greater than 20 for proper

operation. The CRT also requires the use of ultra-low sulfur diesel fuel. This diesel particulate filter system utilizes a platinum (Pt) based oxidation catalyst upstream of a wall flow filter element with a cell density of 200 cells/in^2. (Johnson-Matthey, 2001).

Chapter 3 – Experimental Procedures and Equipment

3.1 The Transportable Lab

All tests performed for this thesis were performed using the West Virginia University Transportable Heavy-Duty Vehicle Emissions Testing Laboratories, also known as the Translabs. This system was a complete in-vehicle engine emissions testing facility that could be set up in a location near the home base for operations of the fleet being tested.

Standard operating procedures for the WVU Translab called for a minimum of a four-man crew to be on site for testing, consisting of a field engineer, a gas operator, a safety monitor, and a vehicle diver.

Upon receipt of a vehicle, the Translab crew performed a safety inspection of the vehicle, which included inspection of the vehicle tires, engine and transmission fluid levels, and exhaust system, and recorded vehicle information, such as the vehicle identification number, tire size, engine model number, and engine identification number. After the vehicle had passed the inspections, it was installed on the chassis test bed.

As set forth in the Translab protocol, triplicate runs were performed for each emissions test. Additional repeat runs were performed if the coefficient of variation for CO_2 and NO_X emissions exceeded 5% or whenever deemed necessary by the field engineer. A minimum of three test runs were averaged for each regulated emissions result in order to alleviate variation in the data. Exceptions to this protocol were cold start tests; due to the time limitations involved with cold start testing, particularly the required 12 hour minimum period prior to the start of any cold start test as specified in

the CFR (40 CFR-PART 86), a single run was accepted for cold start runs if the field engineer viewed it as valid.

3.1.1 The Power Absorber Test Bed

The WVU Translab test bed allowed stationary simulation of a vehicle driving cycle. It consisted of two sets of rollers, one set for each drive axle, which allowed the tires to spin as the vehicle was held stationary with chains attached to the test bed, and a dynamometer unit, which monitored vehicle speed and affected loading.

The vehicle being tested was connected to the dynamometer unit directly through the drive axle using specially designed aluminum wheel hub adapters. To facilitate the hub adapters, the outside set of drive wheels were removed and the adapters bolted on in their place. To prevent tire and vehicle damage on single axle vehicles, hydraulic jacks were positioned on scales and used to support approximately 50% of the rear axle curb weight, the amount of weight traditionally carried by the outside set of tires. Figure 3.1 shows the hub adapters installed on a transit bus. Note the above-mentioned support jack in the lower left corner of the photograph.

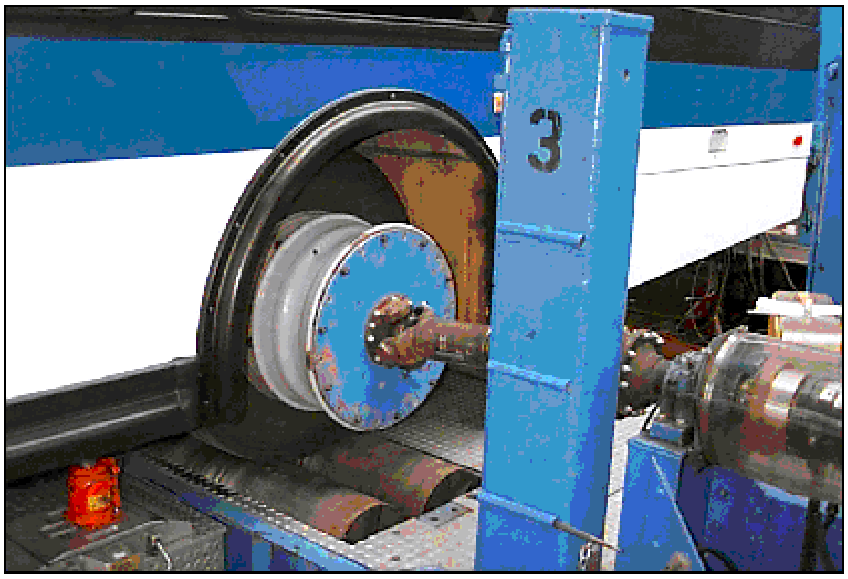

Figure 3.1: **Hub adapters connecting the vehicle drive axle to the dynamometer unit of the Translab test bed**.

The dynamometer unit consisted of speed and torque transducers, two power absorber units, and two sets of selectable flywheels. A Lebow torque and speed transducer was attached to each of the shafts connecting the hub adapters to the power absorber drivetrain. These transducers provided continuous speed and torque data to the computer and can be seen in the lower right corner of Figure 3.1.

The power absorber units were used to apply load to the vehicle during the test cycle in order to simulate road conditions and assist with braking. The power absorbers used were Mustang Dynamometer eddy current absorbers. They operate by applying a DC current to the stationary field coils of the absorber, thus creating a magnetic field. The iron rotors, which were connected to the drivetrain, rotated in this magnetic field generating eddy currents. These eddy currents produce a resultant force opposite to the direction of rotary motion. The Mustang Dynamometers can produced a maximum continuous load of 250 h.p. with a torque of 390 lb. ft. (Bata, et al., 1991).

The sets of selectable flywheels were used to simulate vehicle inertia. Using the flywheels, an inertial load equal to the approximate vehicle test weight was applied. The inertial load could be applied in 250-pound increments, to a maximum of 60,000 pounds, by engaging any number of the eight steel flywheel disks in one of the 256 different combinations. These disks were bearing mounted on a solid steel shaft and were engaged using one of the four driving rotors (two flywheel disks per driving rotor, one located on either side). The flywheel settings, and corresponding inertial load, were determined using the tire size and gross vehicle weight in order to compensate for rolling resistance and vehicle momentum respectively. This was done using the method of equivalent energy where: (Bata, et al., 1991)

$$KE_{Flywheels} = KE_{Vehicle} - KE_{Syetem} \tag{3.1}$$

$$\frac{1}{2} I_f \omega^2 = \frac{1}{2} m V^2 - \frac{1}{2} I_S \omega^2 \tag{3.2}$$

$$I_f = \frac{m}{\omega^2} V^2 - I_S \tag{3.3}$$

Where:

$I_f = mD^2 / 4 - I_S$

D = tire diameter

m = vehicle mass (from the vehicle test weight)

V = vehicle speed = $D\omega / 2$

ω = angular velocity of the tire

I_S = inertia of the system

The vehicle test weights were determined using one of two methods depending on the vehicle type. Vehicle test weights for transit buses were calculated by adding the vehicle curb weight and one half of the passenger load. The passenger load was determined by allowing 150 lbs. for each passenger and an additional 150 lbs. for the

driver. Vehicle test weights for all other vehicle types, including road tractors and refuse trucks, was determined to be 70% of the gross vehicle weight for vehicles under 60,000 lbs. GVWR. For vehicles over 60,000 lbs GVWR, 42,000 lbs (70% of 60,000 lbs.) was used for the test weight.

3.1.2 Analytical Trailer

The other major component of the Translab was the analytical trailer. The analytical trailer was the device that housed the dilution tunnel, instrumentation, and analyzers for the emissions measurement system. Figure 3.2 shows the analytical trailer, dilution tunnel, and exhaust pipe system utilized by Translab 1 and their relation to the test bed.

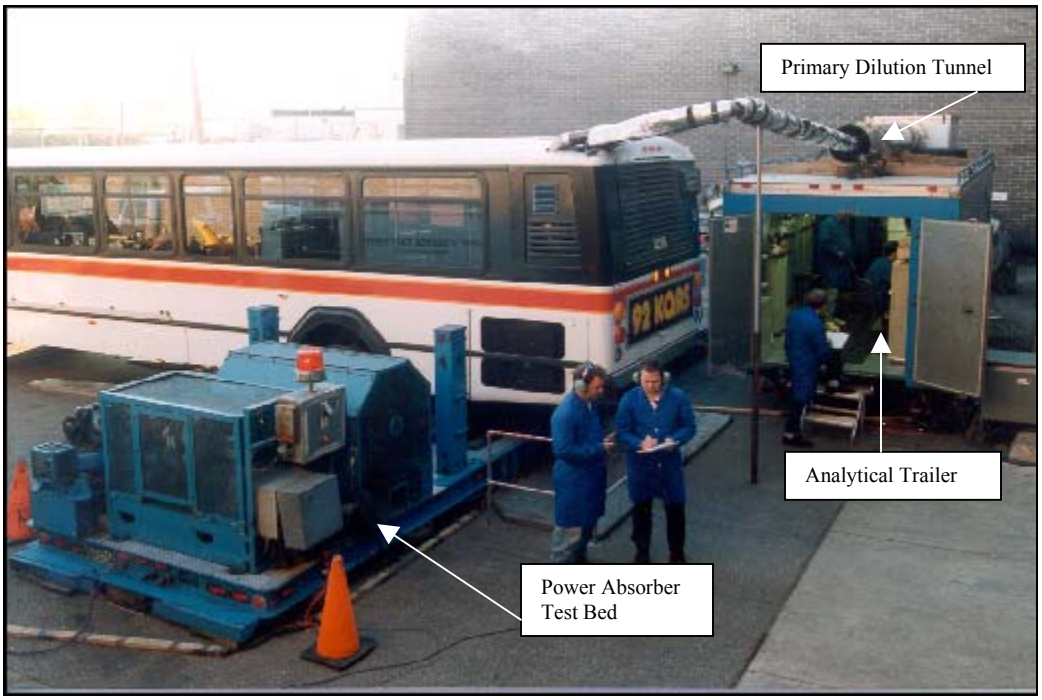

Figure 3.2: **Transit bus mounted on the test bed of Translab 1 connected to the analytical trailer for emissions testing**.

3.1.2.1 Dilution Tunnels

The Translab utilized a full-scale primary dilution tunnel for gaseous emissions analysis. It measured 20 feet in length and 18 inches in diameter and was constructed of stainless steel. This geometric configuration allowed for greater than ten diameters of mixing length.

One end on the dilution tunnel was connected to a large blower through a flexible two-ply neoprene-polyester duct. This blower was used to draw the mixture of exhaust gas and air through the dilution tunnel. The flow rate of this diluted gas was controlled by a critical flow venturi system (CFV) located at the inlet of the blower. The other end of the dilution tunnel was open to allow the inlet of ambient air for dilution and the connection to the vehicle exhaust system.

A stainless steel secondary dilution tunnel was utilized for particulate matter collection. This secondary dilution tunnel measured three feet in length and three inches in diameter and was located in the front of the analytical trailer. It was connected to a stainless steel 70-millimeter filter holder and a mass flow controller as specified in the CFR.

Three heated probes were used to extract exhaust samples from the dilution tunnel. These probes were located in the same section of the primary dilution tunnel as the secondary dilution tunnel, approximately 15 feet from the main tunnel inlet (Hall, 2002).

3.1.2.2 Gaseous Emission Analysis

Translab measured carbon dioxide, carbon monoxide, oxides of nitrogen (NO and NO_2), and hydrocarbons emissions with six independent analyzers. The analyzers were

connected to the data acquisition system via analog-to-digital converters. The data acquisition system recorded continuous data from each analyzer throughout each test run.

In addition to the continuous emission data collected, the Translab also collected bag samples of dilute exhaust and background air. These bag samples were used as an integrated measure of the exhaust and background air samples collected during the duration of the test run. They were collected in 30 inch by 30 inch Tedlar bags by pumping the respective sample into the bag from the primary dilution tunnel. The flow rates for the bag samples were monitored and controlled by the gas operator or the field engineer and were varied depending upon the length of the test cycle. After the conclusion of each test run, the bag samples were then pumped through the analyzers and the respective concentrations were measured and recorded by the data acquisition system. The collection bags were then evacuated via a pump.

Background air sample data were used to correct the integrated continuous data for atmospheric conditions. This correction was performed by applying equation 3.4.

$$[X_{mass}] = \sum_{i=1}^{n}\left[\frac{[X_e]_i}{10^6}\times(V_{mix})_i\times(density_X)\times\Delta T\right] - \frac{[X]_d}{10^6}\left(1-\frac{1}{DF}\right)\times V_{mix}\times density_X \quad (3.4)$$

where X represents the emissions species being evaluated, subscripts e, i, and d represent gaseous emission concentrations from the dilute bag, instantaneous values from the continuous data, and background air sample data values, respectively. V_{mix} is the total dilute exhaust volume in cubic feet per test phase corrected to standard conditions, $density_X$ is the density of the emission species being evaluated, and DF refers to the dilution factor discussed in section 3.1.2.4. (40 CFR-PART 86). Emission species whose mass was determined to be less than or equal to zero were reported as "Below Detectable Limits".

3.1.2.3 Gaseous Emission Analyzers

The WVU Translab operated six independent gaseous emission analyzers. Each analyzer was operated in the lowest range setting possible to give the best resolution in the data produced. The analyzers were recalibrated any time an operation range was changed, which coincided with the changing of the span gas concentration, or whenever deemed necessary by the field engineer. The analyzers were calibrated by running a known concentration of the appropriate span gas through a gas divider and injecting the resultant ratio of span gas and air into the analyzer being calibrated. The analyzers' output signals were recorded by the data acquisition system and compared with the known output signals for each concentration ratio. Necessary adjustments were made to the analyzers until agreement between the output signals was within acceptable limits.

Figure 3.3 shows the analyzer bench from Translab 1 that houses the low level carbon monoxide (LCO), high level carbon monoxide (HCO), carbon dioxide (CO_2), and NO_X (NO_X1 and NO_X2) analyzers and NO_X efficiency tester. The hydrocarbon (HC) analyzer is a free-standing unit and thus is not housed in this bench. Manufacturer information, model numbers, and ranges of operations for each analyzer are shown in Appendix A.

Figure 3.3: **Analyzer bench from WVU Translab 1.**

A. Hydrocarbon Analyzer

The total hydrocarbon (HC) measurements were made using a free-standing heated flame ionization detector (HFID). This highly sensitive detection method based the analysis on flame ionization of the hydrocarbon components of the diluted exhaust sample. This was accomplished by passing a regulated flow of the sample gas through a flame fueled by a regulated mixture of HC free air and a premixed fuel gas consisting of 40% hydrogen and 60% helium. The ionization process, which the hydrocarbon components of the exhaust sample undergo, created electrons and positive ions, which are collected by polarized electrodes. The collection of ions resulted in the flow of electrical current through the measuring circuitry in a rate proportional to the rate at which carbon atoms entered the burner, thus measuring the concentrations of hydrocarbons in the diluted exhaust sample (Evans, 2001; Hall, 2002).

In order to prevent condensation in the lines and equipment and the loss of high-molecular weight hydrocarbons, the HC sampling system was maintained at a temperature of 350°F.

B. Oxides of Nitrogen (NO_X) Analyzer

The WVU Translab utilized two NO/NO_X analyzers. These analyzers were used to determine the concentrations of either: (1) nitric oxide (NO) or (2) NO and nitrogen dioxide (NO_2) which when measured together were denoted as NO_X. One analyzer was always operated in NO_X mode and was labeled as NO_X1, while the other analyzer was toggled between operation modes and was labeled as NO_X2. To ensure appropriate agreement between the two NO/NO_X analyzers, they utilized the same sampling probe from the dilution tunnel.

These analyzers operated on the principle of chemiluminescent detection. In the NO mode of operation, sample NO from the diluted exhaust was converted to NO_2 through the process of gas-phase oxidation. In order to stimulate the oxidation process, molecular ozone was produced within the analyzer from air or oxygen supplied from an external source. A characteristic of this reaction was the elevation of a portion of the NO_2 molecules, approximately 10%, to an electronically excited state, followed by the immediate reversion to the non-excited state. This reversion was accompanied by the release of photons which impinge on the photomultiplier detector, generating a low-level DC electrical current which was then amplified into the measurement signal recorded by the data acquisition system.

In NO_X mode, the analyzers operated in the same fashion, except the sample was routed through a converter where the NO_2 present in the sample was dissociated to form NO. Instrument response was proportional to the total NO present, including both the amount of NO initially present and the amount of NO dissociated from the present NO_2.

In addition to the two NO/NO_X analyzers, each Translab was equipped with a NO_X efficiency tester. This piece of equipment was used to monitor how effectively the NO/NO_X analyzers were converting NO_2 into NO. The conversion efficiency was maintained at or above the 98% level (Evans, 2001; Hall, 2002; Rosemount, 1991)

All components of the NO_X sampling system were held at 235ºF to avoid water condensation in the lines and equipment.

C. Carbon Monoxide Analyzers

The WVU Translab utilized two carbon monoxide (CO) analyzers, one for low CO concentration levels, labeled as LCO, and one for high CO concentration levels, labeled HCO. Due to the wide range that CO can fluctuate during a test cycle, utilizing two analyzers allowed for better resolution of data produced. The two CO analyzers, along with the carbon dioxide analyzer, shared a single sample probe and heated line. In addition to maintaining the sampling system at 235ºF to prevent condensation, a Hankinson gas dryer was utilized to prevent moisture from entering the analyzers.

Both CO analyzers were Non-Dispersive Infrared (NDIR) analyzers. This system functioned on the principle of selective absorption. In this process, infrared energy of a particular wavelength was transmitted through the emission sample. The CO in the sample absorbed the energy with wavelength of 4.5 to 5 microns, while energy of different wavelengths was transmitted through the sample. This "charged" sample then flowed through one of two parallel optical cells. The other optical cell was a sealed reference cell installed by the manufacturer and tuned to the wavelength of CO. The analyzer passed an equal energy infrared beam through each optical cell, and the

difference in these two readings was the concentration of CO being measured from the diluted exhaust sample (Hall, 2002; Rosemount, 1991).

D. Carbon Dioxide Analyzer

The carbon dioxide (CO_2) analyzer utilized by the WVU Translab was of the same type as the CO analyzers, a NDIR. It shared sampling ports and heated lines and was also maintained at 235ºF.

This analyzer operated on the same principle as the CO analyzer, with the major differences being the reference cell and wavelength absorbed by the CO_2. CO_2 absorbs energy of wavelength measuring between 4 to 4.5 microns. As a result of this phenomenon, the reference cell was tuned to this wavelength rather than to the 4.5 to 5 wavelength for the CO analyzer (Evans, 2001; Hall, 2002).

3.1.2.4 Particulate Matter Collection

The primary method of particulate matter (PM) data collection was performed gravimetrically through the use of the secondary dilution tunnel. The secondary dilution tunnel provided cooling to the diluted exhaust mixture, in accordance with CFR 40, Part 86, Subpart N, to a maximum filter-face temperature 125ºF. The dilute exhaust was pulled across two Pallflex 70-mm fluorocarbon coated fiberglass filters, a primary filter and a backup filter, by a rotary vane pump. The flow rates of the dilute exhaust sample and the additional dilution air were controlled by two Sierra mass flow controllers (Evans, 2001).

An environmental chamber was used to pre-condition and post-condition the filters for a minimum of 12 hours prior to weighing. The environmental chamber was maintained at 50% ±5% relative humidity and 70ºF ±10ºF. The filters were conditioned

in glass petri dishes to minimize the likelihood of being contaminated by outside sources. After conditioning, the filters were weighted using a microbalance with a sensitivity of 0.01 μgrams.

Background PM samples were collected at the beginning and end of each testing day. This was performed to account for the amount of PM in the ambient air as well as to account for re-entrainment of PM from the dilution tunnel walls. These filters were treated as regular test filters with respect to pre- and post-conditioning. The background filter weights were used to correct the test particulate filter weights in accordance with CFR 40, Part 86, Subpart N using equation 3.5.

$$P_{mass} = \left(V_{mix} + V_{sf}\right) * \left[\frac{P_f}{V_{sf}} - \left(\frac{P_{bf}}{V_{bf}} * \left[1 - \left(\frac{1}{DF}\right)\right]\right)\right] \tag{3.5}$$

where P_{mass} was the mass of the particulate emitted during the test phase, V_{mix} was the total volume of dilute exhaust corrected to standard conditions, V_{sf} was the volume of sample removed from the primary dilution tunnel, P_f was the combined weight of PM collected during a test cycle on both the primary filter and backup filter, P_{bf} was the combined weight of PM collected on both background filters, V_{bf} was the volume of dilution air sampled during the background test, and DF was the dilution factor, calculated from equation 3.6.

$$DF = \frac{13.4}{\left[CO_{2e} + \left(HC_e + CO_e\right)10^{-4}\right]} \tag{3.6}$$

where the subscript "e" identified a gaseous emission concentration collected from the dilute sample bag (40 CFR-Part 86).

3.1.2.5 Fuel Economy Calculations

Fuel economy was calculated using a carbon-balance method. This method assumed that the total mass of carbon in the fuel was equal to the mass of carbon found in the exhaust. This method neglects the contributions of lubricating oil consumption to the exhaust carbon and the fuel carbon lost due to blowby, fuel seepage past the piston rings. These factors are minor and tend to counteract each other.

Using the total weight of hydrocarbons, carbon monoxide, and carbon dioxide collected during testing, the mass of carbon in the exhaust is given by equation 3.7.

$$G_S = \left[\frac{12.011}{12.011 + \alpha(1.008)}\right] HC_{mass} + 0.429 CO_{mass} + 0.273 CO_{2mass} \quad (3.7)$$

where α is the atomic hydrogen to carbon ratio of the fuel, assuming there is no sulfur, oxygen, or nitrogen present in the fuel, HC_{mass} is the total mass of hydrocarbons emitted in the exhaust, CO_{mass} and CO_{2mass} are the total masses of carbon monoxide and carbon dioxide emitted, respectively.

The mass of carbon in the exhaust was then converted to a fuel volume and consequently into a fuel economy in units of miles per gallon (MPG) using equation 3.8.

$$MPG = \left[\frac{gC/gal\ \ of\ \ fuel}{Gs}\right] (\text{Distance Traveled}) \quad (3.8)$$

Where gC/gal of fuel is the carbon weight fraction of the test fuel.

3.1.2.6 Data Acquisition System

The WVU Translab data acquisition system consisted of a main computer, reduction computer, vehicle operator video monitor, control and data acquisition hardware, and signal controlling devices. The main computer was used to control all

aspects of test execution, from the pre-test calibration of the analyzers and instrumentation to the collection of data recorded during a test cycle. This computer was pre-programmed with various driving schedules, which are discussed later in this thesis, which the vehicle operator followed during a test. The vehicle operator monitor was connected to the main computer and displayed all information that the field engineer monitored from inside the analytical trailer, including a real time trace of vehicle speed versus time that the driver was to follow.

The control and data acquisition system hardware included two digital dynamometer controllers, two signal-processing boards, and numerous signal-conditioning modules. The digital dynamometer controllers were Dyne Systems Co. Dyn-Loc IV units and were connected to the main computer in a closed loop system. The main computer sent signals to the dynamometer controllers responsible for applying load on the dynamometers, thus simulating road drag and aerodynamic losses.

All output signals from the analyzers and transducers were fed through the RTI-815 signal processing boards and Analog Devices 3B signal conditioning modules. The signal conditioning modules were used in the calibration process of the analyzers. The RTI-815 boards converted the output signals from the analyzers and transducers into ADC codes, which were recorded on the main computer and then sent to the reduction computer.

The reduction computer was used to perform all post-test analysis of the raw experimental data, which included data conversion from ADC codes to engineering units, continuous integration of the results, and graphical analysis of the test results. (Hall, 2002)

3.2 Special Equipment

During the data collection portion of this thesis, some special equipment was used. This equipment included a TEOM, Tapered Element Oscillating Microbalance, and a smoke opacity meter.

3.2.1 TEOM

The TEOM, Tapered Element Oscillating Microbalance, is a system that provides real-time data about the particulate mass concentrations in the diluted diesel exhaust. The TEOM system operates by passing exhaust gas through a hollow glass tube, which is allowed to oscillate at its natural frequency, and through a small filter element, which traps the PM from the exhaust gas. As the PM is deposited on the filter, the natural frequency of the system, hollow tube and filter assembly, changes. A computer records this frequency and changes it into a mass calculation using the formula found in equation 3.9.

$$M = K_0(F_1^{-2} - F_0^{-2}) \tag{3.9}$$

where M is the resultant mass in grams, F_1 is the current frequency, F_0 is the initial frequency, and K_0 is the calibration constant for tapered element (Okrent, 1998). The computer logged data as often as every 0.21 seconds. These data were computed and reported from the computer as mass concentration (mg/m^3), total mass (grams), and mass rate (g/s).

These data were of most concern relative to this thesis for the cold start test runs. These data were used to determine the cold start efficiencies of the DPFs for trapping particulate matter and, if possible, to determine the temperature at which the DPFs activate and begin to oxidize the PM.

3.2.1.1 TEOM Limitations

As the TEOM system is a very sensitive piece of equipment, there are certain limitations involved with its use. Sample flow rate, sample temperature, moisture content, and filter age all have significant effects on the confidence of the TEOM data.

The flow rate of the sample exhaust gas through the filter affects the agreement with conventional gravimetric particulate sampling measurements. As the flow rate is increased, the residence time for ultrafine PM and volatiles to become attached to the filter surfaces decreases due to the increased velocity. However as the flow rate is decreased, the positive-to-negative mass ratio decreased, lowering the accuracy or real-time particulate measurement. Through experimentation, a flow rate of 2 liters per minute was found to best compromise between conventional filtration agreement and real-time characteristics (Gilbert, 2002).

Lower sampling temperatures have proven to allow more volatile organic compounds to be trapped by the filter element, however increased temperatures have shown higher moisture rejection characteristics. A 40°C sampling temperature has shown to provide the optimum compromise between VOC and moisture rejection (Gilbert, 2002).

Moisture content can greatly affect the TEOM system data by giving an instantaneous false reading of particulate mass collected by the filter element. As the sampling mass is reported continuously, the filters cannot be post-conditioned, as are traditional particulate filters, to lesson the effects of moisture content.

It has been shown that aged filters more efficiently trap particulate matter than do new filters. New filters collect 40% less mass on the first test than on the third test.

When the first test with a new filter is disregarded, the 99% confidence in the TEOM data was ±4.3%. For comparison, conventional gravimetric mass measurement has a 99% confidence of 1.7% for PM data (Gilbert, 2002).

3.2.2 Smoke Opacity Meter

Another piece of special equipment that was used for a portion of the data collection stage of this thesis was a Telonic Berkeley Inc. Model 107 smoke opacity meter. The smoke opacity meter was used to measure the opacity of the exhaust gas and particulate mixture as well as determine the exhaust, or smoke, density. The smoke opacity meter measured contributions of particulate matter as well as contributions of white smoke to the opacity value. These data were used in evaluating the cold start performance of the DPF systems.

The smoke opacity meter functioned on the principle of attenuation of the intensity of a light beam by smoke aerosol absorption and scattering. The light beam utilized by the meter was generated by a green light emitting diode (LED) and a condensing lens. The light beam was projected through the center of the exhaust stream and detected by a photodiode. The output signals from the LED and the photodiode were sent through the ADC controllers and recorded by the main lab computer. The smoke opacity and smoke density were then determined from the light intensity reduction expressed in equation 3.10.

$$\frac{l}{l_0} = e^{-n\bar{a}QL} \tag{3.10}$$

where l_0 is the light intensity emitted by the LED, l is the light intensity detected by the photodiode, n is the number density of smoke particles, $\bar{a}$ is the average particle

projected area, $\bar{Q}$ is the average particle extinction coefficient, and L is the light beam path length within the smoke (the diameter of the exhaust pipe). The smoke opacity, N, is shown in equation 3.11 as a function of the light intensity reduction, and the smoke density, K, is shown in equation 3.12 as a function of the smoke opacity (Telonic Berkeley, 1999).

$$N = \left(1 - \frac{l}{l_0}\right) * 100 = opacity(\%) \tag{3.11}$$

$$K = \left(-\frac{1}{L}\right) * \ln\left(1 - \frac{N}{100}\right) = SmokeDensity(m^{-1}) \tag{3.12}$$

Chapter 4 - Test Vehicles, Driving Cycles, and Results

4.1 Cold Start DPF Performance

4.1.1 Test Vehicles

Seven vehicles were tested for cold start DPF performance evaluation. Table 4.1.1 summarizes the vehicles tested in this program. Six of these vehicles were 1999 Orion II transit buses taken from the Washington Metropolitan Area Transit Authority (WMATA) fleet. All of these vehicles were equipped with Cummins 6BT5.9 engines rated at 175 hp and were tested at 18,975 pounds. Of these six buses, two were equipped with oxidation catalysts and used as a baseline for DPF performance. The remaining four buses were equipped with DPFs, two with Engelhard DPXs and two with Johnson-Matthey CRTs.

The seventh vehicle in this study was a 1995 Mack tractor truck owned by West Virginia University. This truck was equipped with a Mack E7-400 V-MAC II six-cylinder engine rated at 400 hp. It was tested at a weight of 42,000 pounds using a standard muffler in place and then retested with an Engelhard DPX. It is noted that the Engelhard DPX utilized on the WVU Mack was not optimized for this application. It was a unit intended for a 435 hp Detroit Diesel Corporation engine, however the Mack engine was of similar displacement.

The WMATA buses were chosen for warm weather-cold start performance evaluation, while the WVU Mack tractor truck was chosen for cold weather-cold start evaluation. The average ambient temperatures during cold start test runs were 76°F and 34°F respectively.

Table 4.1.1: Vehicles Tested for Cold Start DPF Performance Evaluation.

fleet	number	vehicle	engine	aftertreatment	fuel
WMATA	3722	Orion II Transit Bus	Cummins 6BT5.9	Oxidation Catalyst	D1
WMATA	3723	Orion II Transit Bus	Cummins 6BT5.9	Oxidation Catalyst	D1
WMATA	3724	Orion II Transit Bus	Cummins 6BT5.9	Engelhard DPX	ULSD1
WMATA	3725	Orion II Transit Bus	Cummins 6BT5.9	Engelhard DPX	ULSD1
WMATA	3726	Orion II Transit Bus	Cummins 6BT5.9	Johnson Matthey CRT	ULSD1
WMATA	3727	Orion II Transit Bus	Cummins 6BT5.9	Johnson Matthey CRT	ULSD1
WVU	21017	Mack Tractor Truck	Mack E7-400 V-MAC II	Engelhard DPX	ECD1
				standard muffler	ECD1

4.1.2 Driving Schedules

All WMATA buses were tested using variations of the Central Business District cycle (CBD) found in the Society of Automotive Engineers Standards J1376: Fuel Economy Measurement Test (Engineering Type) for Trucks and Buses (SAE, 1997). The CBD cycle consisted of fourteen acceleration ramps each followed by brief steady state periods of 8.94 m/s (20 mph). Each steady state portion was followed by a deceleration ramp with approximately twice the slope as the previous acceleration ramp and a short idle period, resulting in a total test time of 900 seconds.

Each bus was subjected to a single cold start test run followed by at least three hot start runs. The cold start tests were performed using the ColdCBD test cycle. This test cycle was a continual loop of CBD cycles. The cold start tests were concluded when the field engineer determined that the exhaust temperature, carbon monoxide, and hydrocarbon emissions had sufficiently stabilized.

The hot start test runs were performed using the 3CBD driving cycle. This test cycle consisted of three CBD cycles run back-to-back, with the first sequence being a warm-up with no data collection. Due to the effectiveness of the DPFs, the CBD cycle length was tripled to increase the amount of PM collected on the filters to facilitate accurate gravimetric measurement. The 3CBD driving cycle is shown in Figure 4.1.1 as

driven during testing. Note that this figure shows only the portions of the cycle in which data are collected, there are an additional fourteen ramps at the beginning of the cycle, which are not shown, that comprise the warm-up sequence of the 3CBD driving cycle.

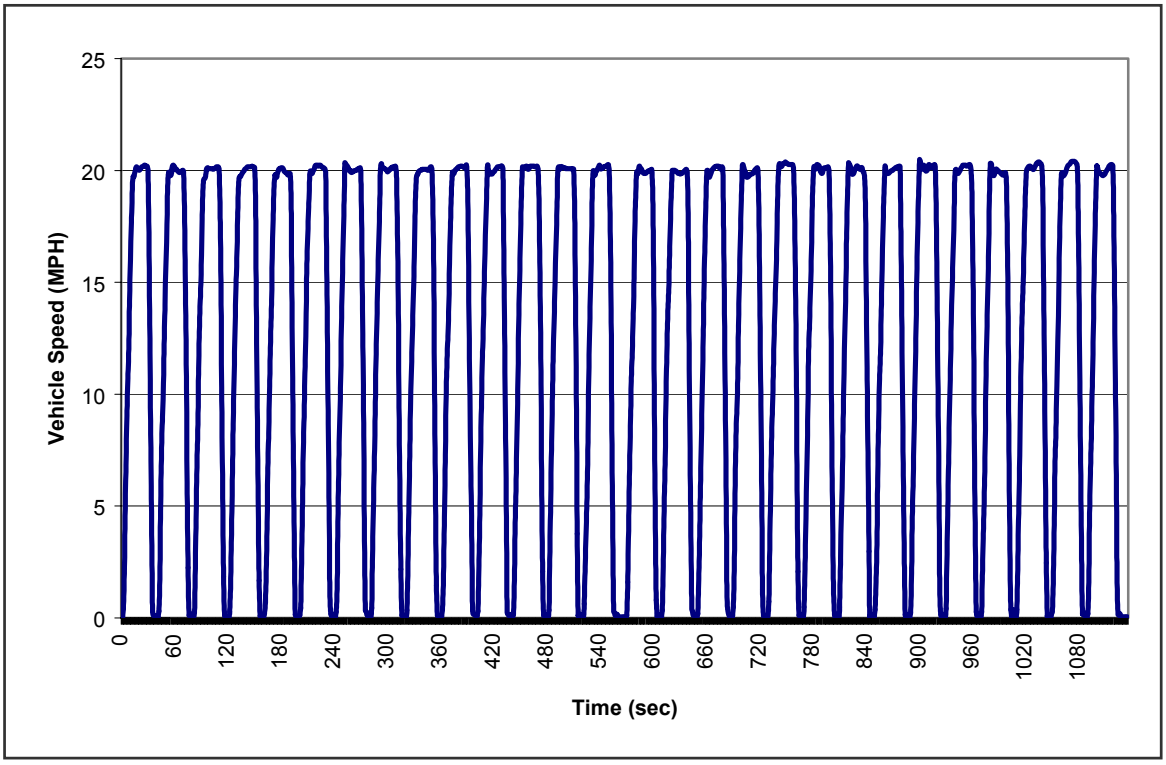

Figure 4.1.1: The 3CBD driving cycle utilized for hot start testing with WMATA transit buses as driven by WMATA bus 3722.

The WVU Mack tractor truck was tested with two separate driving schedules developed by West Virginia University, the WVU one peak cycle (denoted as WVU-1P) and the WVU 5 Mile truck route (denoted as 5miles). The main difference between a driving cycle and a driving route was the respective definition of test length. A cycle was a speed versus time schedule where the test concluded at a given time (in seconds) without regard to total distance traveled, whereas a route was a speed versus distance schedule that ended when a specified total distance was reached without regard to elapsed time.

A variation of the WVU 5 Mile route was used for all hot start test runs. The WVU 5 Mile route was developed to simulate both transient and steady state vehicle operations of a class 8 truck. It consisted of five acceleration ramps, each to a steady state speed of 8.94, 11.18, 13.41, 15.64, and 17.88 m/s (20, 25, 30, 35, and 40 mph) respectively. Each steady state period was followed by a deceleration and an idle period. The total distance covered in a single WVU 5 Mile test run was five miles (Clark, et al., 1994).

The variation of the WVU 5 Mile route that was used for hot start test runs was denoted as 2-5miles. This cycle repeated the WVU 5 Mile route two times continuously for a total distance traveled of 10 miles. This double schedule was utilized to ensure sufficient loading of the PM filters to facilitate accurate measurement. Figure 4.1.2 shows the vehicle speed versus time plot for a hot test run using the 2-5miles route.

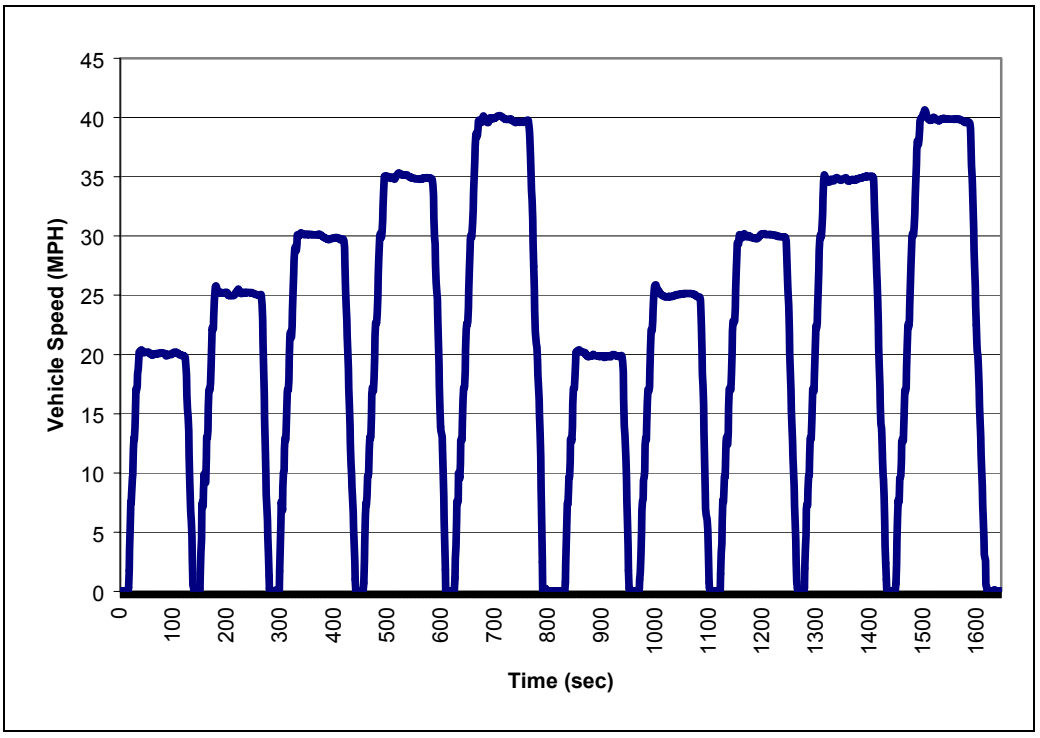

Figure 4.1.2: The 2-5miles driving route developed by West Virginia University as driven by the WVU Mack.

The WVU one-peak cycle was used for cold start test runs with the WVU Mack tractor truck. The WVU one-peak cycle utilized the first acceleration ramp and steady state speed of the 5-peak cycle in a repeated fashion much like the CBD cycle. The CBD cycle was determined to be inappropriate for large class 8 vehicles, such as the Mack tractor truck, due to their inability to meet the steep accelerations under heavy load conditions. The WVU one-peak offers much more realistic accelerations for these types of vehicles. Much like the ColdCBD cycle, the WVU one-peak repeated indefinitely until stopped by the field engineer when the exhaust temperature, carbon monoxide, and hydrocarbon emissions stabilized. Figure 4.1.3 shows a plot of the vehicle speed versus time for the WVU one-peak as driven during a cold start test run of the WVU Mack tractor truck.

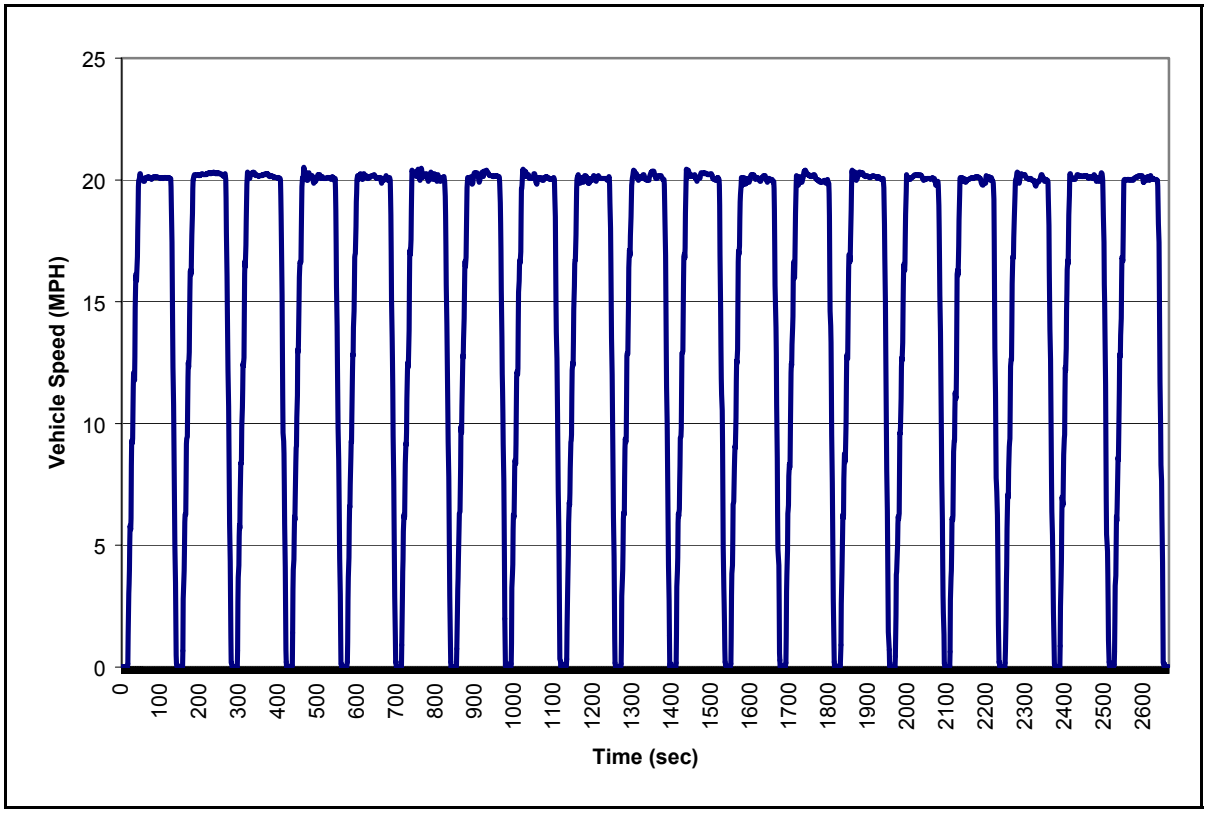

Figure 4.1.3: The WVU one-peak (WVU-1P) driving cycles as used for cold start testing on the Mack Tractor Truck.

4.1.3 Results

There were two areas of concern for the cold start DPF performance evaluation: general operational efficiency of the DPF under cold start conditions and determination of an approximate light-off temperature at which the emissions stabilize. In this section, continuous data, integrated data, and general observations are presented.

4.1.3.1 CO Emissions

Carbon monoxide emissions from the WMATA Orion II transit buses equipped with either the Engelhard DPX or the Johnson-Matthey CRT were reduced by 72.7% and 76.9%, respectively, when compared to the oxidation catalyst equipped vehicles. Figure 4.1.4 graphically demonstrates this reduction in a grams per mile basis (g/mile). In this figure, each bar represents the average of the integrated emissions data for each type of after-treatment device, with error bars showing the maximum and minimum values recorded.

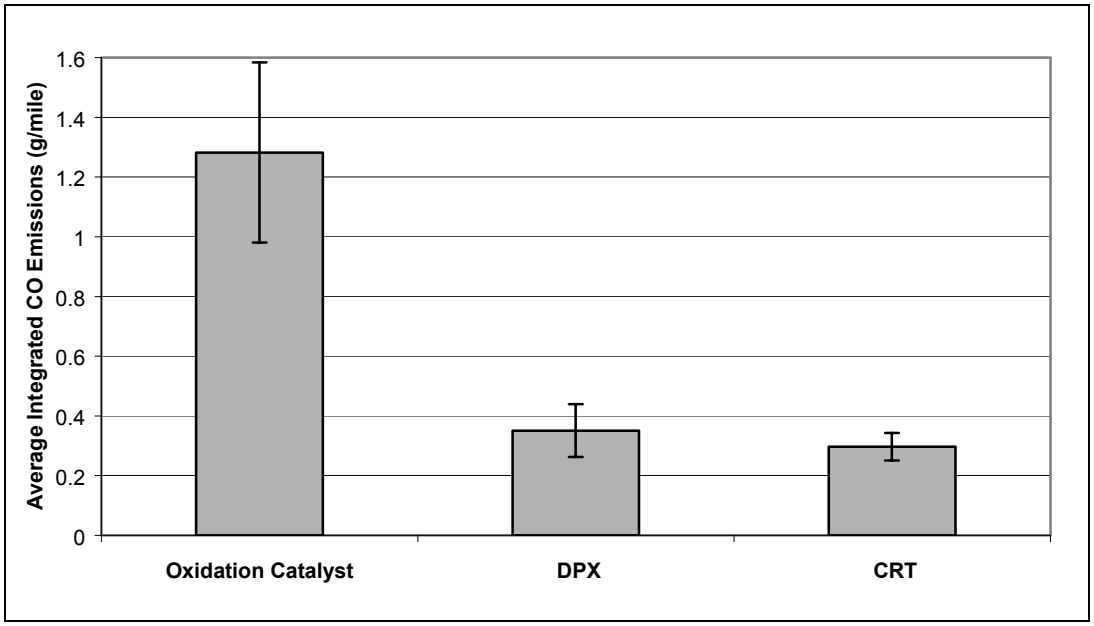

Figure 4.1.4: Average CO emissions recorded during cold start test runs from WMATA Orion II transit buses, with maximum and minimum values shown as error bars.

Figure 4.1.5 shows the continuous CO data collected from three of the six WMATA buses, one from each type of after-treatment tested. The plot was limited to three samples for clarity, however it should be noted that the other three vehicles tested produced similar results. Additionally, only the first one thousand seconds of each test run is shown to compensate for the varying test length and for additional clarity. From this figure, it can be seen that the particulate filter equipped vehicles released less CO and the emission concentration stabilized much faster.

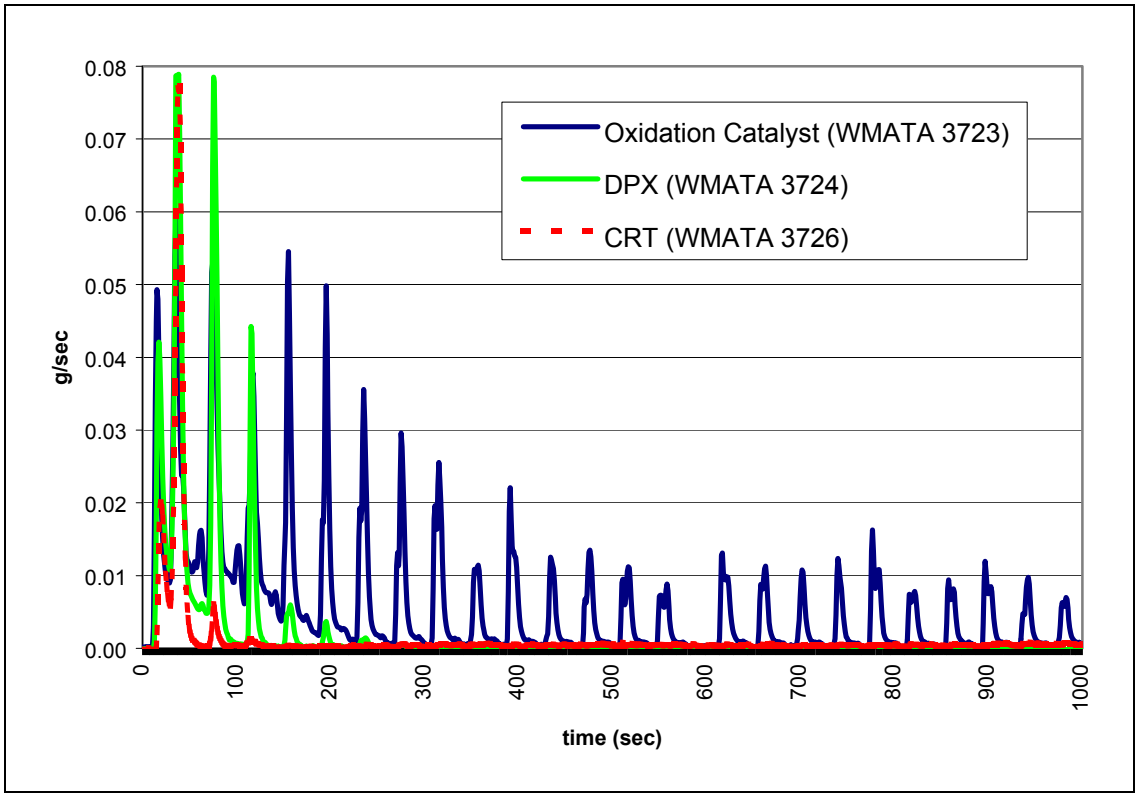

Figure 4.1.5: Continuous CO emissions data from three WMATA transit buses

The WVU Mack tractor truck experienced a 53% reduction in CO emissions when using the Engelhard DPX particulate filter. Similar to the WMATA vehicles, CO emissions, in addition to being lower in concentration, also stabilized much faster. Figure 4.1.6 demonstrates this phenomenon by showing the continuous CO emissions in units of parts per million (ppm) versus time for DPF equipped and non-equipped runs. Also

shown in this figure is the exhaust temperature, which was use in determination of DPF light-off temperature discussed in Chapter 5 – Conclusions.

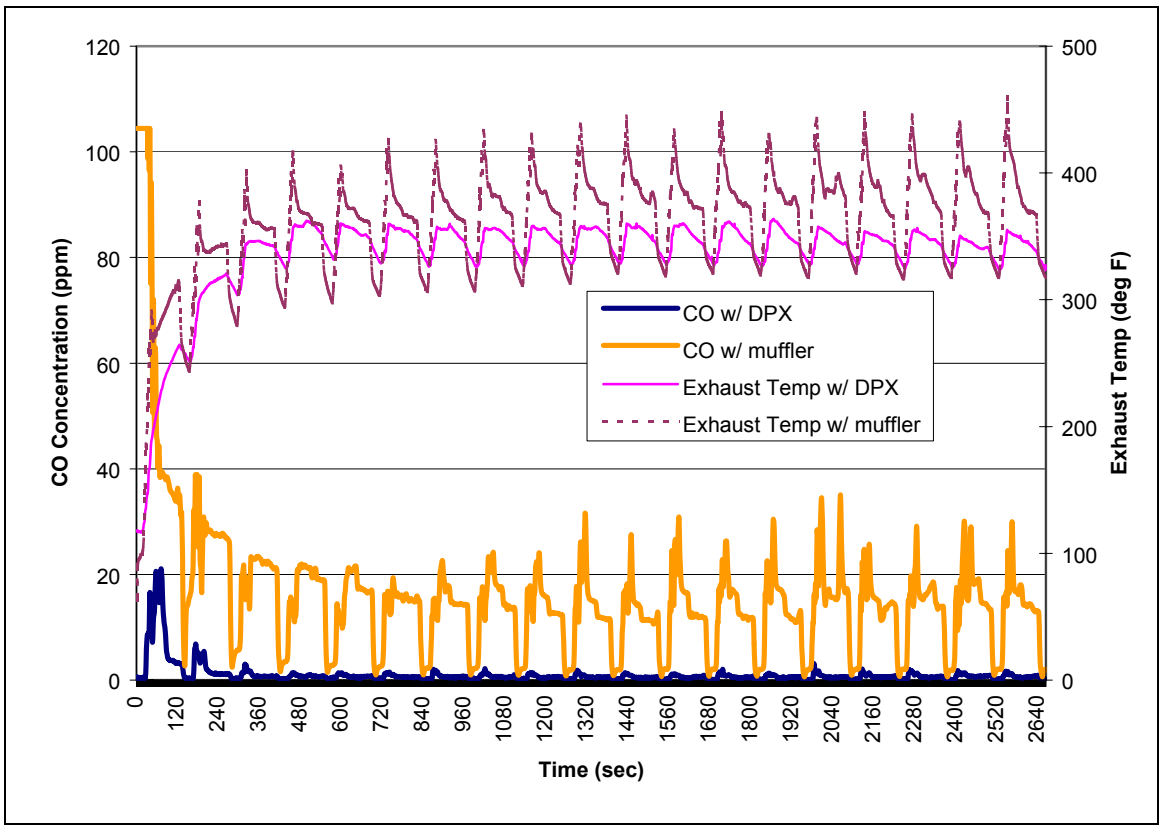

Figure 4.1.6: Continuous CO emissions taken from the WVU Mack tractor truck during cold-weather cold start testing.

4.1.3.2 HC Emissions

Hydrocarbon emissions from the WMATA transit buses equipped with DPFs were 83% and 86% lower for the Engelhard DPX and Johnson-Matthey CRT respectively when compared to the oxidation catalyst equipped vehicles. Figure 4.1.7 shows the average integrated HC emissions concentrations collected during warm-weather cold start test runs in units of grams/mile. Each bar in this figure represents the average HC emission levels recorded for each after-treatment device, with error bars showing the maximum and minimum values recorded. As the data from WMATA 3725 was below

detectable limits, no error bar is shown for the DPX column as only one value was available.

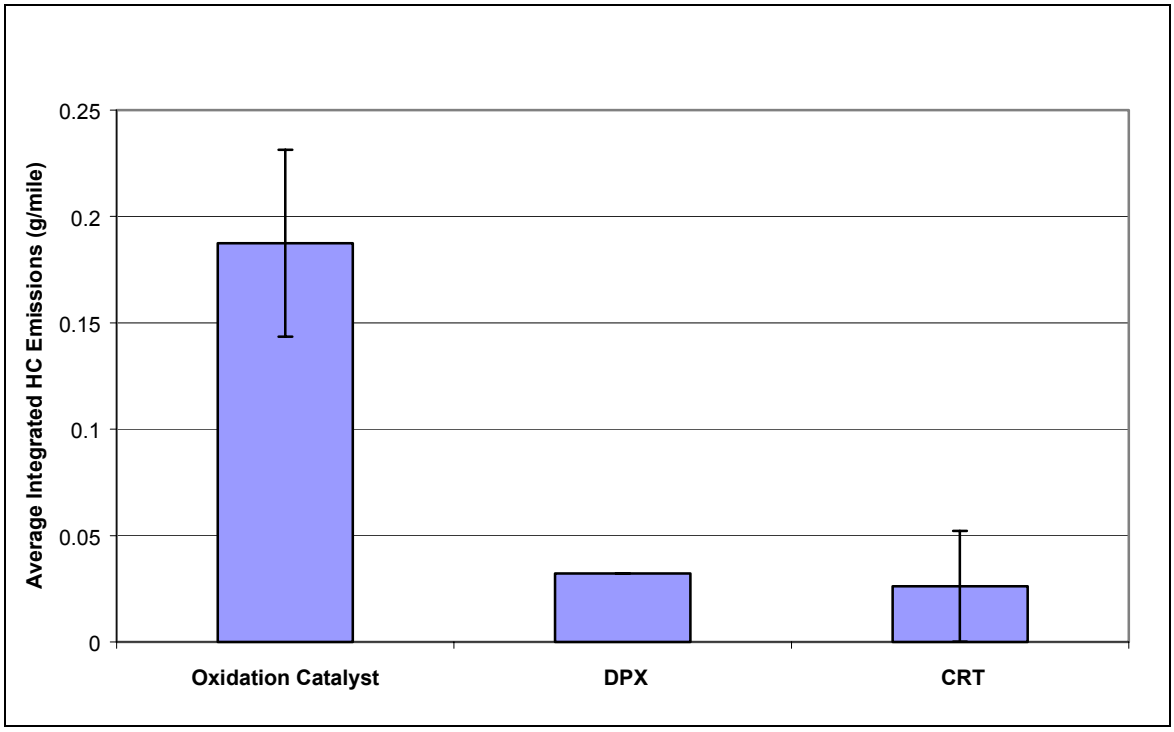

Figure 4.1.7: Average HC emissions collected during cold start testing of the WMATA transit buses.

Figure 4.1.8 shows the first one-thousand seconds of continuous HC data collected from three of the WMATA Orion II transit buses tested. This plot shows rapid decrease in HC emissions to near undetectable limits experienced in the particulate filter equipped vehicles. After approximately 400 seconds, the HC emissions dropped into the noise levels of the HC analyzer for both the DPX and CRT particulate filters.

The WVU Mack tractor truck experienced a 78% reduction in HC emissions when equipped with the Engelhard DPX particulate filter. This reduction is represented in Figure 4.1.9. This figure shows the continuous HC emissions and exhaust temperature for two cold start test runs, one run using the DPF and one using a standard muffler. From this plot, it can be seen that the DPX begins greatly reducing HC emissions at a

relatively low exhaust temperature, and emission levels stabilize after approximately 400 seconds.

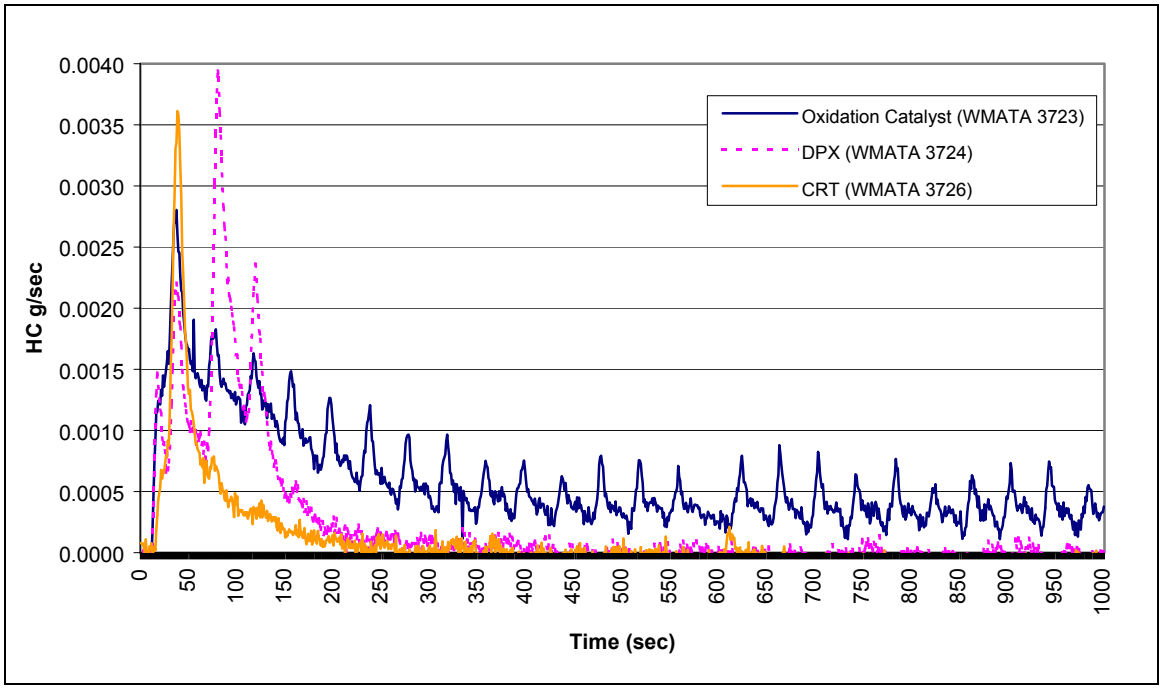

Figure 4.1.8: HC emissions from cold start testing of WMATA transit buses.

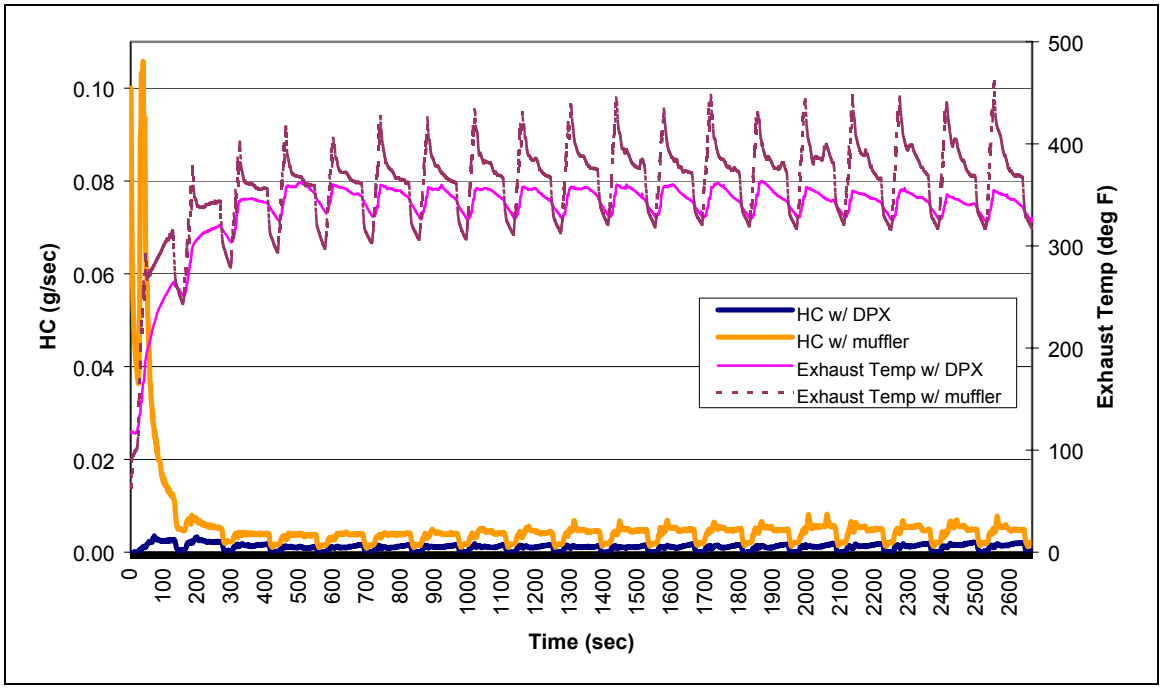

Figure 4.1.9: HC emissions from cold start testing of the WVU Mack tractor truck.

4.1.3.3 NO_X Emissions

As expected, no significant NO_X reductions were recorded in any of the seven vehicles tested in this program. However, NO emissions were reduced through conversion to NO_2 by the DPFs. On average, these reductions were 30% and 46% with the Engelhard DPX and Johnson-Matthey CRT, respectively. Figure 4.1.10 shows the average integrated NO_X and NO emissions measured from the WMATA buses. It should be noted that only total NO_X emissions were measured from the WVU Mack, thus it was not considered in determining NO/NO_X split characteristics. It was determined that NO-NO_2 conversion increased proportionally with the exhaust temperature until the particulate filter light-off temperature was reached and engine-out emissions production stabilized. An example of this phenomenon is shown in Figure 4.1.11. In this figure, the NO and NO_X emissions are shown from WMATA bus 3724 equipped with an Engelhard DPX relative to the post-filter exhaust temperature. Note that forth order trend lines were added to the raw data for clarity due to the overlap of the NO and NO_X data sets. Additionally, it was determined that engine-out emissions stabilized at approximately 500 seconds.

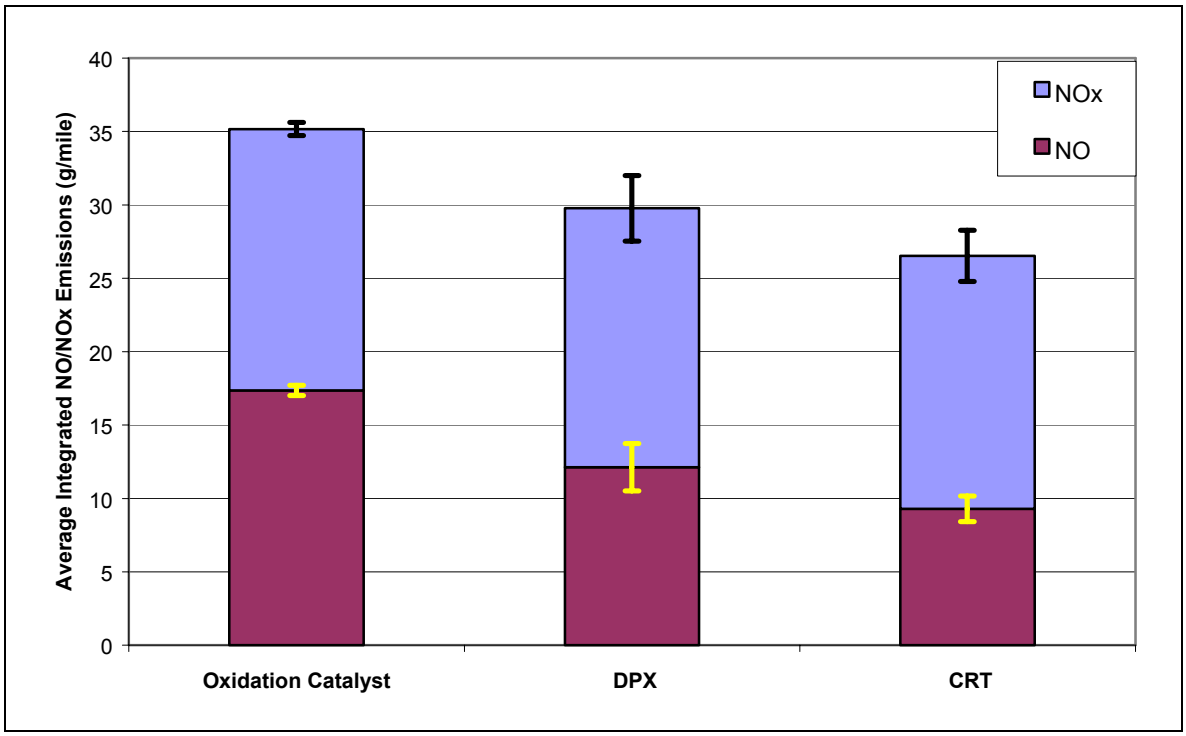

Figure 4.1.10: Average integrated NO and NO_X emissions in grams per mile collected from cold start testing of WMATA buses

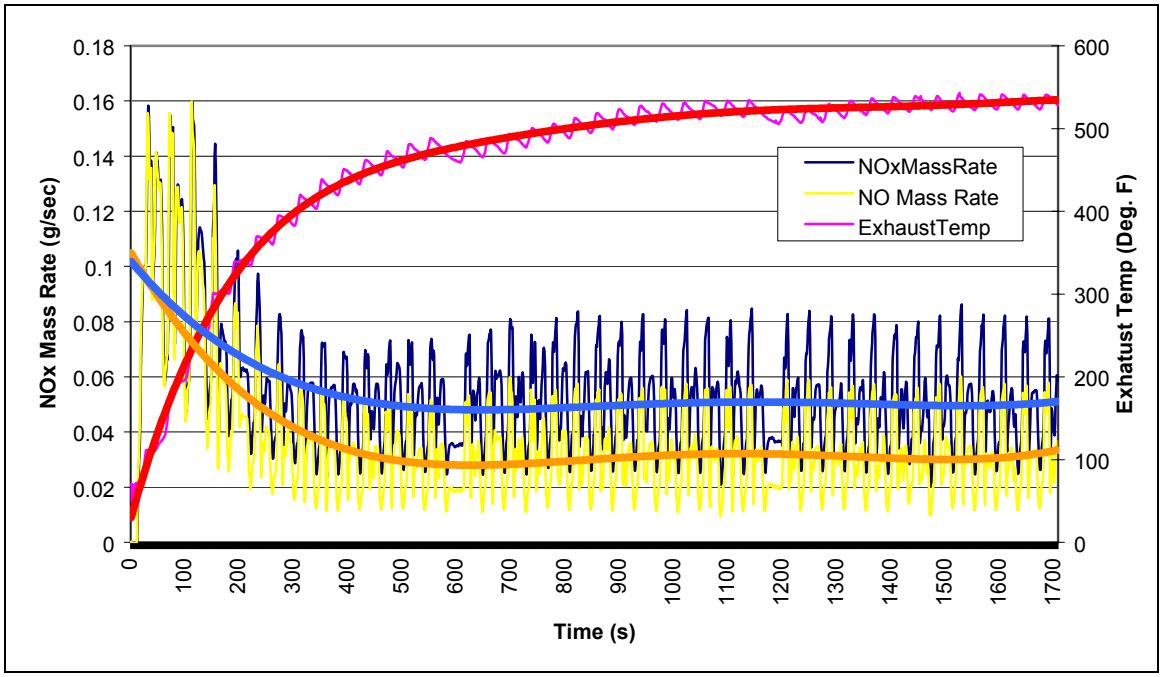

Figure 4.1.11: NO/NO_X split shown from WMATA bus 3724 using an Engelhard DPX

4.1.3.4 CO_2 Emissions / Fuel Economy

No significant changes were noticed in CO_2 emissions from any of the seven vehicles tested. Additionally, fuel economy was not significantly affected by the particulate filter retrofit. A maximum fuel economy increase of approximately seven percent was recorded from the WMATA fleet vehicles, however this was a vehicle-to-vehicle comparison and not a pre-to-post retrofit comparison, thus the fuel economy variation was attributed to other circumstances, such as possible variations in engine timing or air filter quality, and consequently disregarded. A fuel economy penalty is possible with the retrofitting of DPFs to existing vehicles as the exhaust backpressure may increase due to flow restrictions across the filter.

4.1.3.5 PM Emissions

The greatest emission reductions were witnessed in the particulate matter data where an order of magnitude reduction occurred for all vehicles in the program. PM concentrations from the WMATA buses went from an average of 0.052 g/mile with the oxidation catalysts to 0.0052 g/mile and 0.0037 g/mile with the Engelhard DPX and Johnson-Matthey CRT respectively. This figured to a 90% and 93% reduction, respectively. The WVU Mack data showed a reduction from 0.24 g/mile with the muffler to 0.021 g/mile with the DPF. This was a reduction of greater than 99%.

TEOM data for all vehicles showed a cycle-wide reduction in mass concentration, however the most important observation from this data was the lack of a spike in the data at engine start-up. This correlates to filter efficiency at low, or ambient, temperatures, i.e. the filters collect PM before reaching the particulate filter light-off temperature. Figure

4.1.12 shows the TEOM data for two cold-weather cold-start test runs using the WVU Mack, one with the DPF installed and one with a muffler in place.

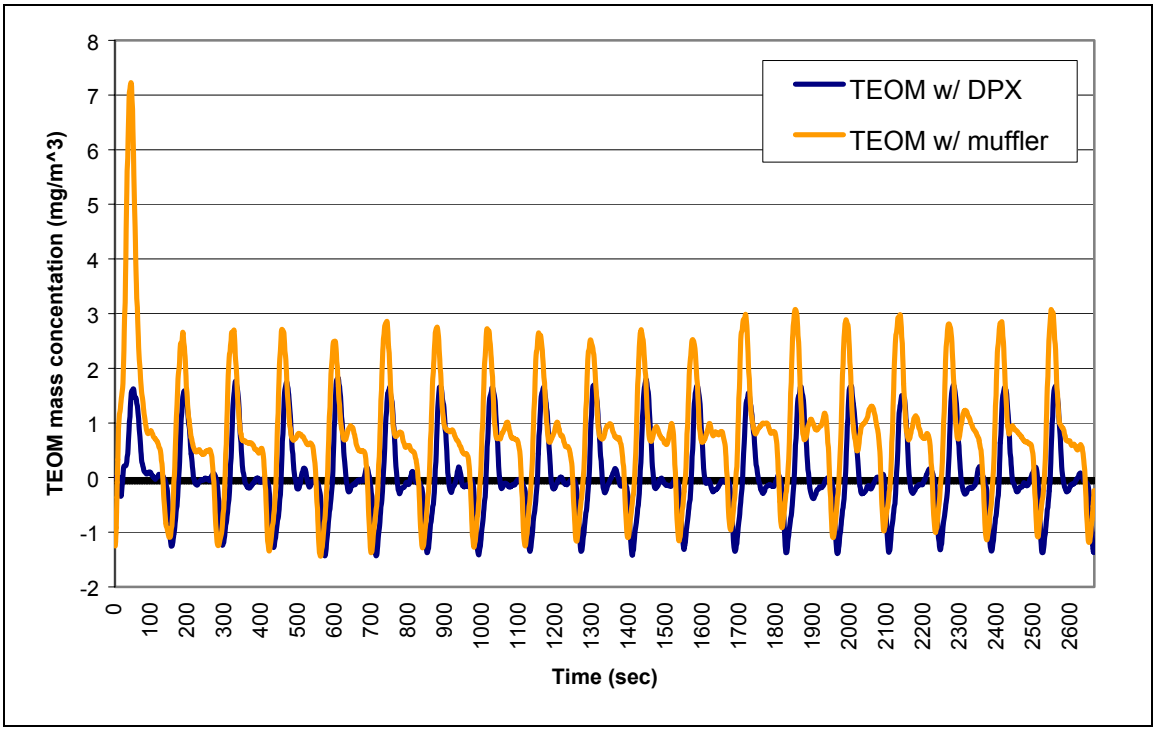

Figure 4.1.12: TEOM data from the WVU Mack tractor truck from cold-weather cold-start testing.

4.1.3.6 White Smoke Emissions

The particulate filters had little affect on reducing white smoke emissions. The continuous data showed a large "puff" of smoke emitted at initial engine start up on each cold start run, thus suggesting the particulate filters do not filter the white smoke constituents. However, it should be noted that inconsistencies, including electrical noise and analyzer drift, were found in the smoke opacity data for several test runs, thus voiding the opacity data collected from these runs. Additionally, opacity measurements were not taken during the testing of the WVU Mack tractor truck. Figure 4.1.13 shows the continuous data collected from a sample cold start test run from vehicle WMATA 3724. Shown on this figure are the smoke opacity, smoke density, and exhaust

temperature data from this run. The white smoke puff emitted at engine start up is visible as a spike in opacity seen on the left of the figure.

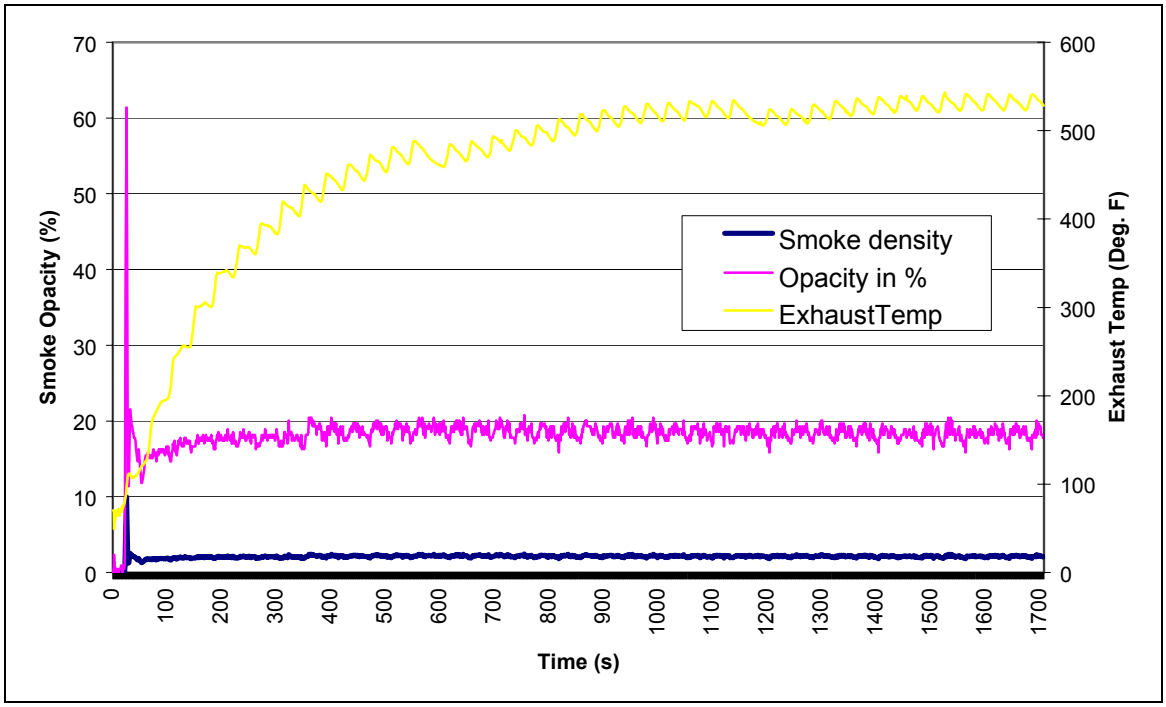

Figure 4.1.13: Smoke opacity, smoke density, and exhaust temperature data from WMATA bus 3724.

4.2 Long-Term Durability Evaluation of Ralph's Grocery Fleet Vehicles

To determine the aging characteristics and durability of the diesel particulate filters, a three-year, three-round study was performed in Riverside, California using trucks from the Ralph's Grocery Fleet based out of Riverside, California. The selected vehicles were originally tested in the spring and summer of 2000. The same vehicles were retested for round two in the spring of 2001. The final tests were performed in the spring of 2002.

4.2.1 Test Vehicles

Four vehicles were chosen for the long-term DPF durability evaluation. These vehicles were 1998 Sterling Class 8 tractor trucks taken from the Ralph's Grocery Fleet

in Riverside, California. Two vehicles were equipped with Engelhard DPXs and two with Johnson-Matthey CRTs. Each vehicle was equipped with a 12.7 liter Detroit Diesel Corporation Series 60 six-cylinder engine and a 10-speed manual transmission. Each truck had a gross vehicle weight of 80,000 pounds and was tested at 42,000 pounds.

It was predicted that the diesel particulate filter performance would degrade proportionally with the mileage accumulated between testing rounds. The mileage of each vehicle at the time of testing for each round is shown in Figure 4.2.1.

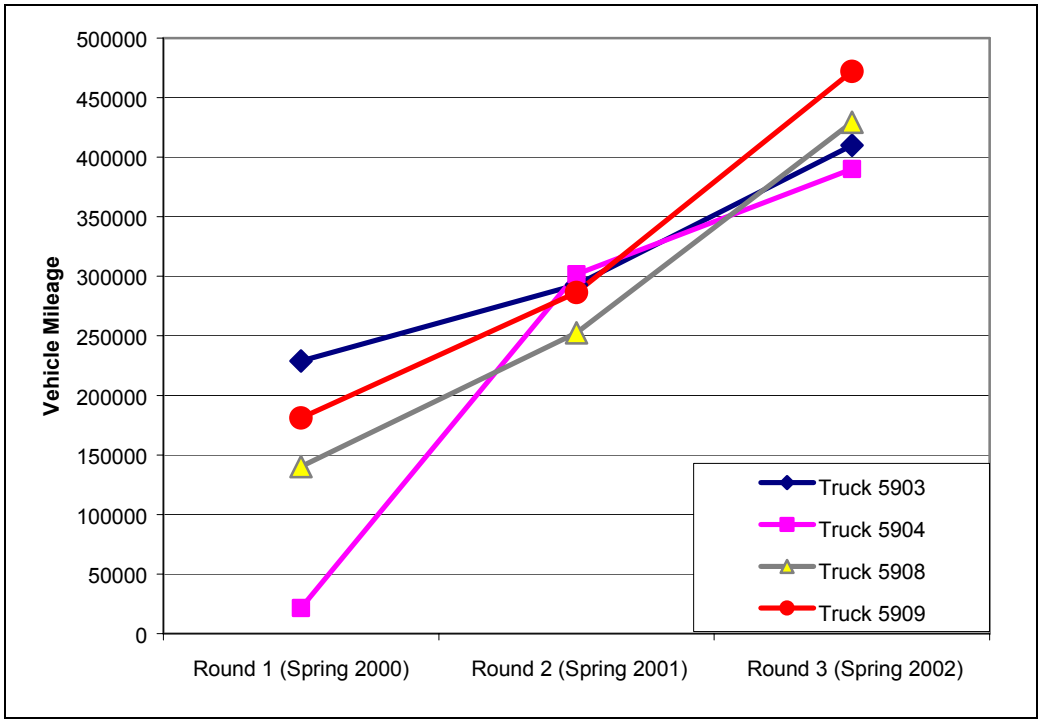

Figure 4.2.1: Vehicle mileage for durability study

4.2.1.1 Vehicle Fuels

As set forth in the original test matrix by Keith Vertin of NREL, National Renewable Energy Laboratory, three fuels were utilized during the course of this durability study. They included CARB Diesel, Emission Control Diesel (ECD), and Emission Control Diesel-1 (ECD1). Table 4.2.1 shows the test vehicles, DPFs, and the fuels utilized in

each round. It should be noted that in Table 4.2.1, CRT and DPX refer to the Johnson-Matthey CRT and Engelhard DPX respectively.

Table 4.2.1: Vehicle Test Matrix for Durability Study

	Round 1		Round 2		Round 3	
Vehicle ID Number	DPF	Fuel	DPF	Fuel	DPF	Fuel
5903			CRT	ECD		
	CRT	ECD	NONE	ECD	CRT	ECD1
	NONE	ECD	CRT	ECD1	NONE	CARB
	NONE	CARB	NONE	ECD1		
			NONE	CARB		
5904	CRT	ECD	CRT	ECD	CRT	ECD1
	NONE	ECD	CRT	ECD1	NONE	CARB
	NONE	CARB	NONE	ECD1		
			NONE	CARB		
5908	DPX	ECD	DPX	ECD	DPX	ECD1
			DPX	ECD1	NONE	CARB
5909	DPX	ECD	DPX	ECD	DPX	ECD1
					DPX	CARB

Table 4.2.2 shows the fuel characteristics for each of the fuels utilized in this study as reported by the US Department of Energy, Office of Transportable Technologies (USDOE, 2002). It has been shown that the use of ultra-low sulfur fuels, particularly ECD, can reduce all regulated engine out emissions when compared to engine out emissions produced from CARB fueled engines. In previous emission testing performed by West Virginia University for NREL, emissions reductions for regulated emissions ranged from a low of three percent for NO_X emissions to a maximum of thirteen percent for PM and HC emissions (LeTavec, et al., 2000). This is important to note, as CARB fuel was the only fuel used consistently in each round of testing for this evaluation.

Table 4.2.2: Fuel Properties for CARB, ECD, and ECD1 Diesel as Reported by the US Department of Energy Office of Transportable Technologies (USDOE, 2002)

Property	SI Units	CARB	ECD	ECD1
Density	kg/m^3	844.5	811.9	828.5
Distillation (Initial Boiling Point)	Deg. C	177.6	211.6	168.9
Cetane Number	unitless	54.1	64.7	51.3
Cetane Index	unitless	50.6	67.2	49.8
Carbon	mass %	85.8	84.7	87.01
Hydrogen	mass %	13.44	14.44	13.82
Sulfur	ppm	121.1	7.4	13.1
Olefins	volume %	3.4	2.5	3
Saturates	volume %	72.8	88	75.9
Total Aromatics	mass %	22.5	10.9	22.8
Ash	mass %	<0.001	<0.001	<0.001
Heat of Combustion, gross (HHV)	MJ/kg	45.74	46.42	45.96
Heat of Combustion, net (LHV)	MJ/kg	42.89	43.36	43.02
Flash Point	Deg. C	71.7	87.2	58.3
Cloud Point	Deg. C	-9	-3	-11

4.2.2 Driving Schedules

For consistency of test results between testing rounds, the same driving schedule was used for all testing throughout the study. The driving schedule utilized was the City-Suburban Heavy Vehicle Route, or CSHVR. This route was developed by West Virginia University in 1999 as a useful and realistic test schedule for truck emissions characterization. It has proved to be relatively insensitive to vehicle test weight, as it demands full power operation of the vehicle during acceleration ramps without regard to test weight (Clark, et al., 1999).

The CSHVR was developed from data logged from vehicles performing local deliveries in Akron, OH and Richmond, VA. This data was used to develop three speed versus time driving cycles, a Yard cycle, a Freeway cycle, and a City-Suburban cycle. The City-Suburban cycle was converted to a speed versus distance route, the CSHVR, in which the test vehicle performed numerous maximum accelerations throughout the test schedule. The resultant route covered a distance of 6.68 miles with a maximum speed of

43.8 mph (Clark, et al., 1999). Figure 4.2.2 shows the trace of the CSHVR route as driven by a test vehicle.

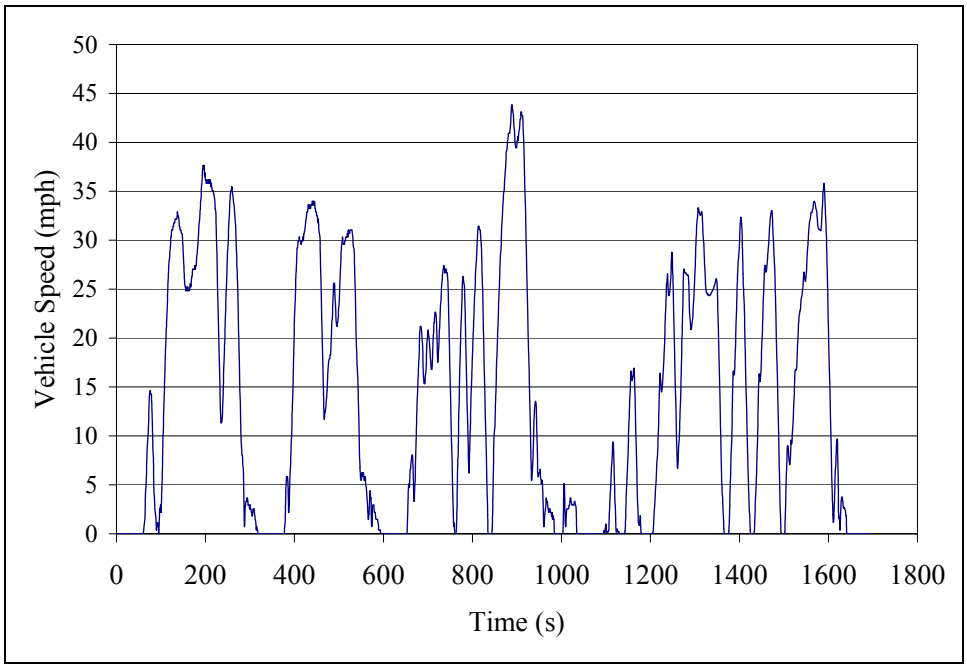

Figure 4.2.2: Scheduled speed vs. time for the CSHVR as driven by a test vehicle.

The CSHVR was used for all test runs performed in this study without DPFs installed, however, in order to facilitate sufficient particulate filter loading when using a DPF, the route distance was doubled to 13.4 miles by repeating the route sequence. This double length route was denoted as 2cshvr.

4.2.3 Results

The purpose of this evaluation was to determine the life cycle and durability of a diesel particulate filter. The data collected for this study is presented in this section in units of grams per mile (g/mile). The data is organized into three sets: emissions with DPFs installed, engine-out emissions using standard CARB fuel, and engine-out emissions using ultra-low sulfur fuels (ECD and ECD1). The engine-out emissions are presented in order to determine any existing trends or fluctuations in the round-to-round

data which may skew the approximation of DPF durability. The existence and possible causes of these fluctuations are discussed in a subsequent section of this thesis.

4.2.3.1 CO Emissions

CO emissions from test runs using the DPFs are shown in Figure 4.2.3. CO emissions were consistent for all vehicles in round one, however the Engelhard DPX equipped vehicles showed a significant increase in CO concentrations in rounds two and three compared to the Johnson-Matthey CRT equipped vehicles. Note that, as specified in the original test matrix, truck 5903 was not tested with ECD1 fuel in round 2.

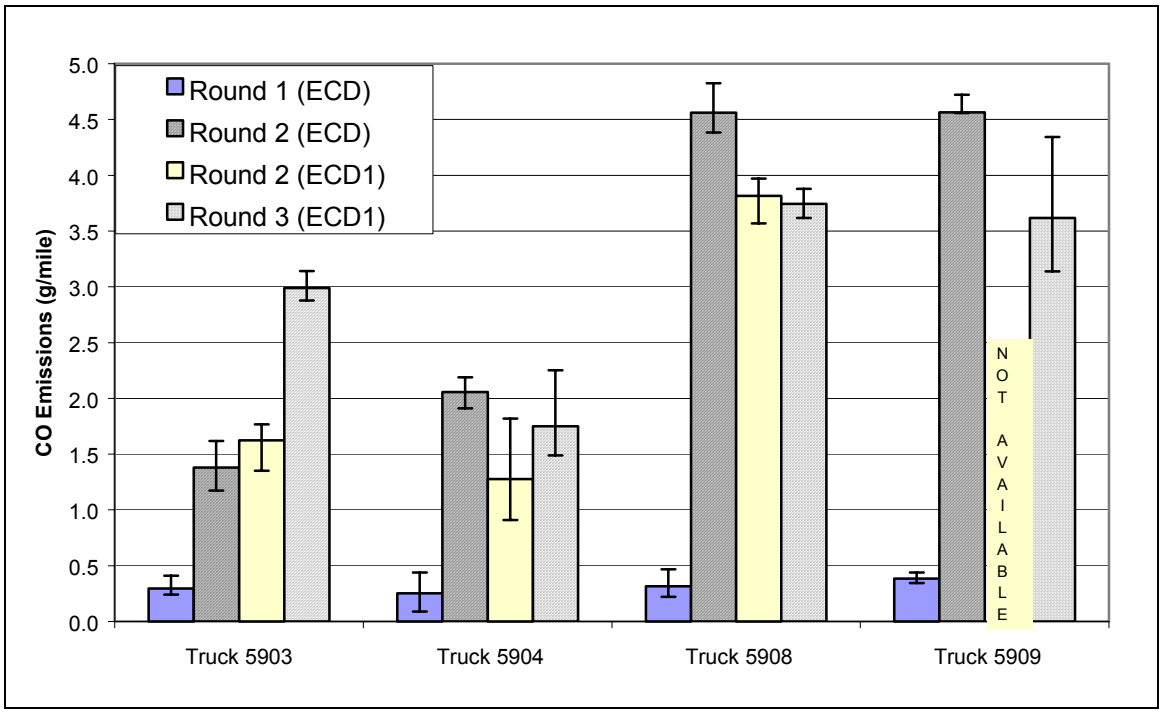

Figure 4.2.3: CO emissions from test runs using DPFs

CO emissions from test runs without DPFs installed are shown in Figures 4.2.4 and 4.2.5. Only trucks 5903 and 5904 were tested without particulate filters in each round of this study, additionally truck 5904 was only tested with ECD1 fuel in round 2 without a particulate filter. In round three, no vehicles were tested without a particulate filter running on ultra-low sulfur fuel. Trucks 5908 and 5909 were tested with CARB

fuel without a particulate filter installed in round three, however this data is not shown as there is no data to compare it to in the previous rounds of testing.

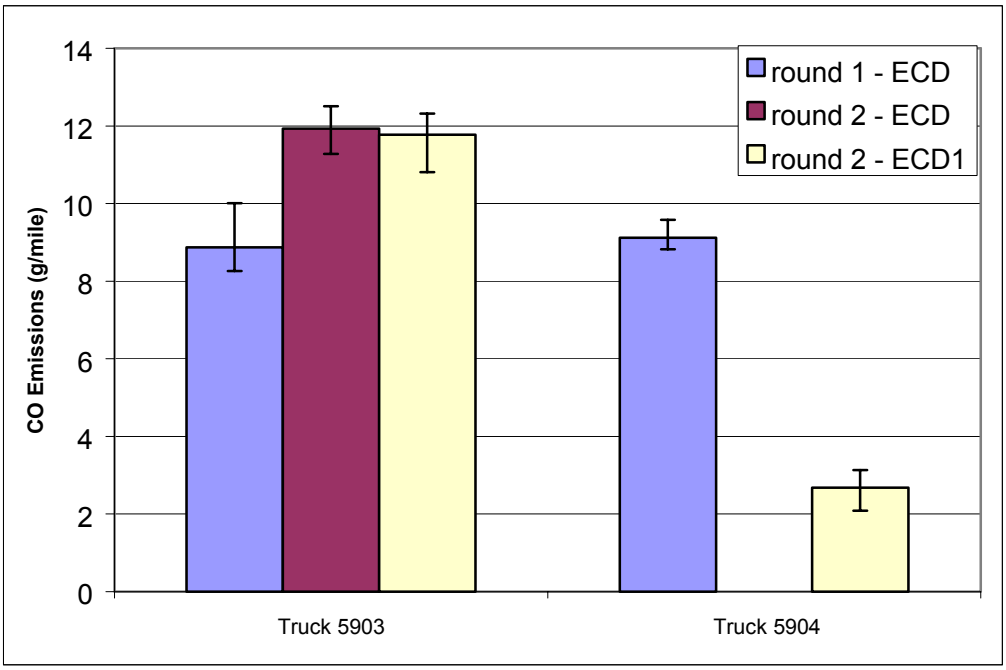

Figure 4.2.4: CO emissions from trucks 5903 and 5904 running on ultra-low sulfur fuel without the DPFs.

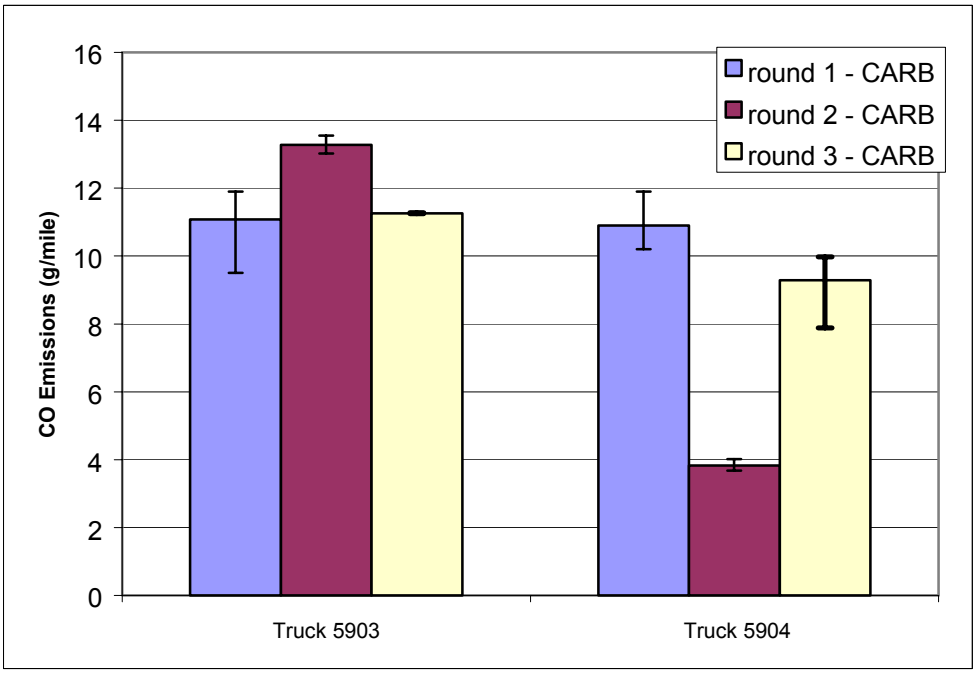

Figure 4.2.5: CO emissions from trucks 5903 and 5904 running on CARB fuel without the DPFs.

Round one yielded CO emissions reductions of greater than 90 percent for both DPF types. In round two, CO emissions reductions dropped to approximately 85 percent for the CRT and 62 percent for the DPX while the vehicles were fueled with ECD. While fueled with ECD1, reductions were 81 percent and 52 percent for the CRT and DPX respectively. Round three data showed reductions of approximately 74 percent and 57 percent for the CRT and DPX respectively, however these reductions were recorded with the filter equipped vehicles running on ECD1 fuel and the non-filter equipped vehicles using CARB fuel.

4.2.3.2 HC Emissions

HC emissions from test runs utilizing the DPFs are shown in Figure 4.2.6. HC emissions from round one were below detectable limits for all of the trucks tested. Additionally, truck 5903 equipped with a Johnson-Matthey CRT released below detectable limits of HC throughout all rounds of testing. Round three data for truck 5908 was declared "not reportable" due to inconsistencies within that data.

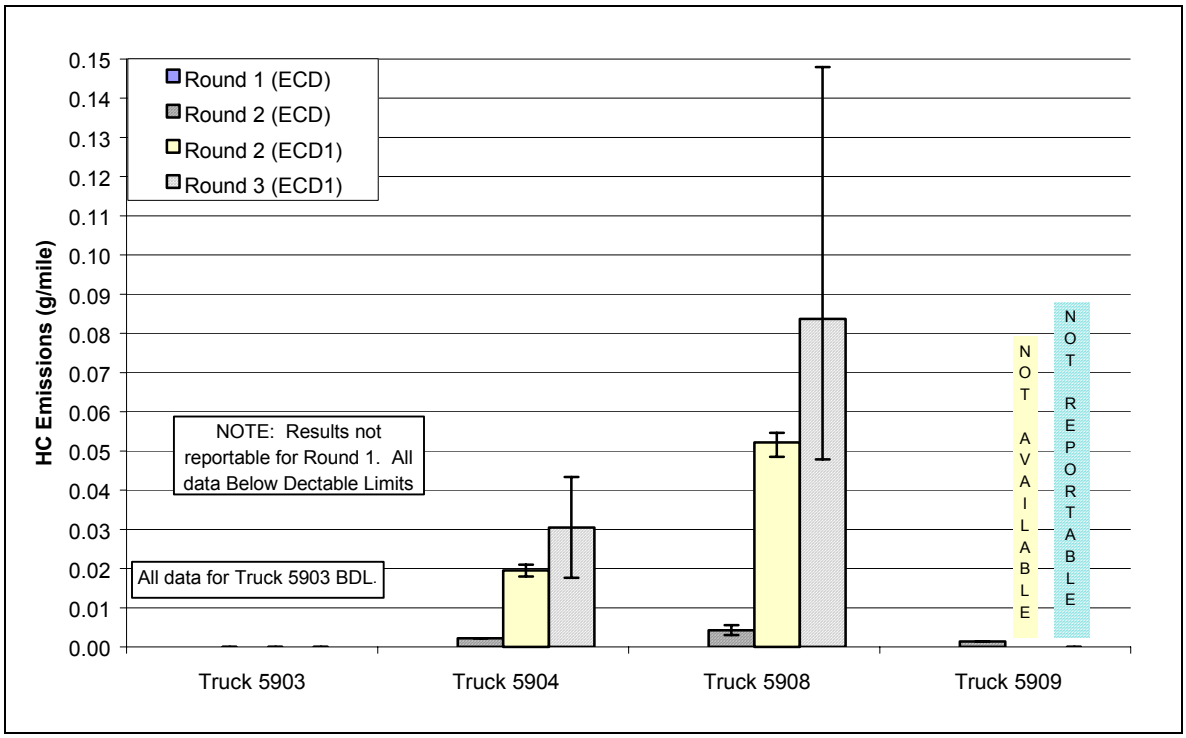

Figure 4.2.6: HC emissions from test runs utilizing the DPFs.

Figure 4.2.7 shows the engine-out emissions of Trucks 5903 and 5904 when fueled with ECD and ECD1 fuels. Engine out emissions of the same trucks when fueled with CARB fuel are shown in Figure 4.2.8.

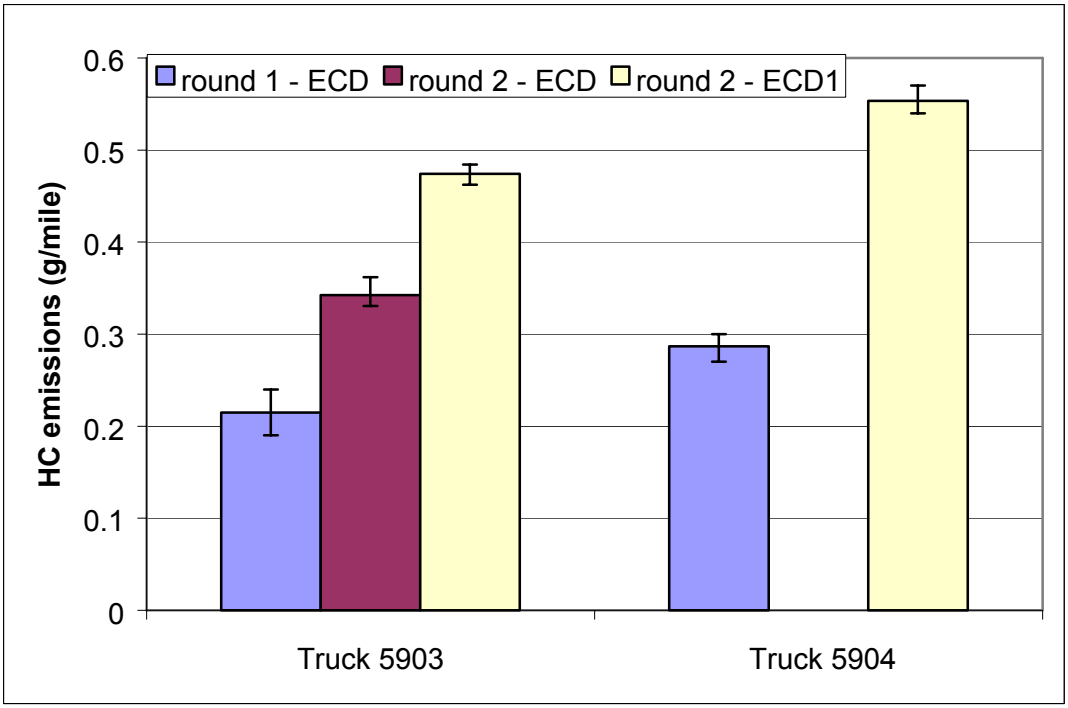

Figure 4.2.7: HC emissions from trucks 5903 and 5904 running on ultra-low sulfur fuel without the DPFs.

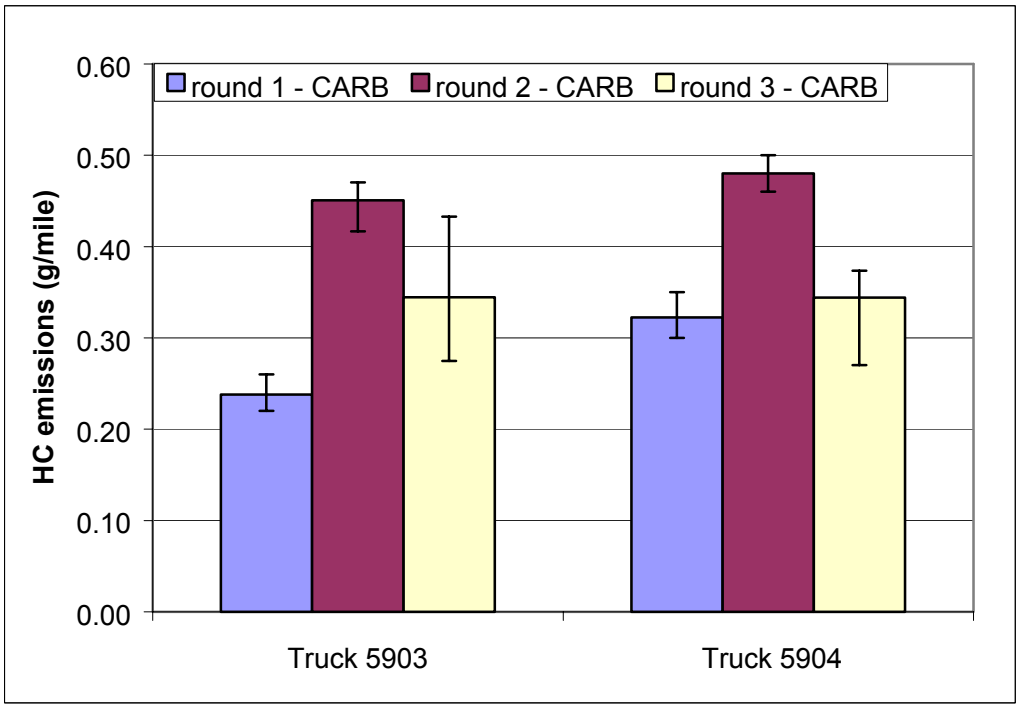

Figure 4.2.8: HC emissions from trucks 5903 and 5904 running on CARB fuel without DPFs.

Round one test data yielded HC emission reductions greater than 99 percent for all vehicles tested. While testing with ECD fuel in round two, reduction levels remained approximately 99 percent for both DPF types, however with the ECD1 fuel, reduction levels dropped to 98 percent and 89 percent for the CRT and DPX respectively. Round three HC emission reductions were approximately 95 percent and 75 percent for the CRT and DPX respectively, however these reductions were achieved with respect to engine-out emissions data from CARB fuel rather than ECD1.

4.2.3.3 NOx Emissions

NOx emissions from round one tests using DPFs are shown in Figure 4.2.9. Only NOx data was recorded in this round of testing, thus a determination of the NO/NOx split could not be made. Figures 4.2.10 and 4.2.11 show the NO/NOx emissions from DPF equipped test runs from round two and round three respectively. Round two demonstrated an approximate 27 percent average conversion rate from NO to NO_2, while round three showed only a 24 percent conversion rate.

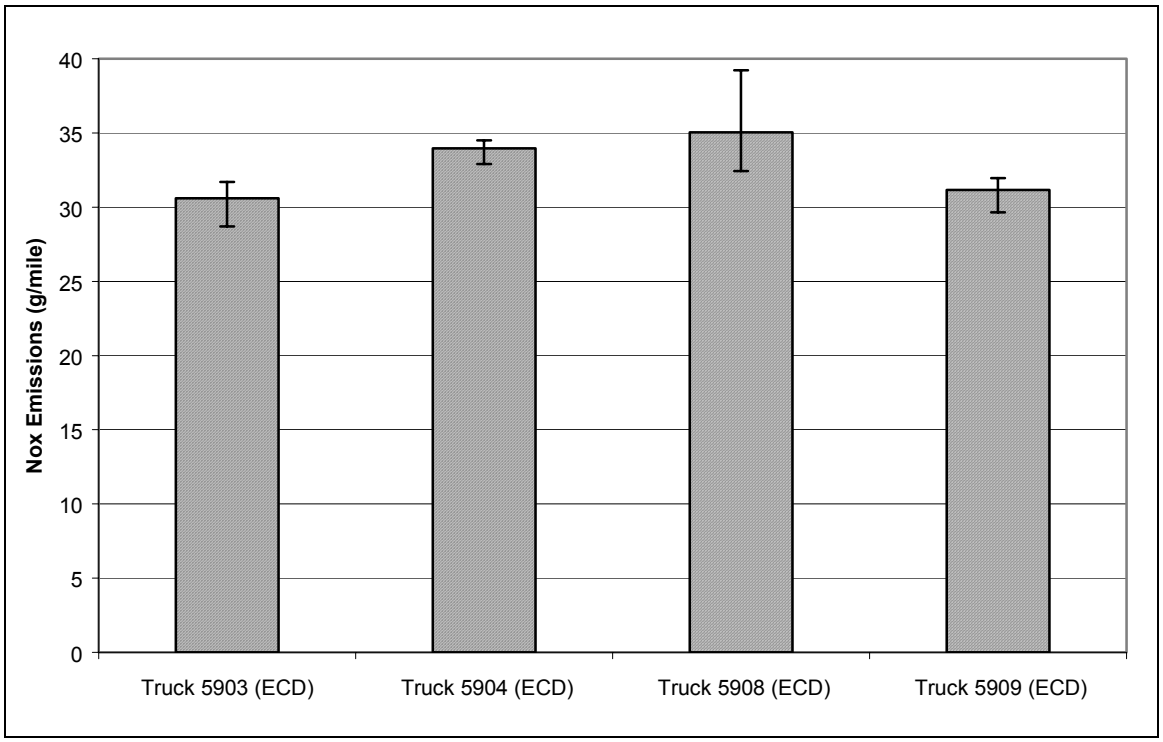

Figure 4.2.9: Round one NOx emissions using particulate filters.

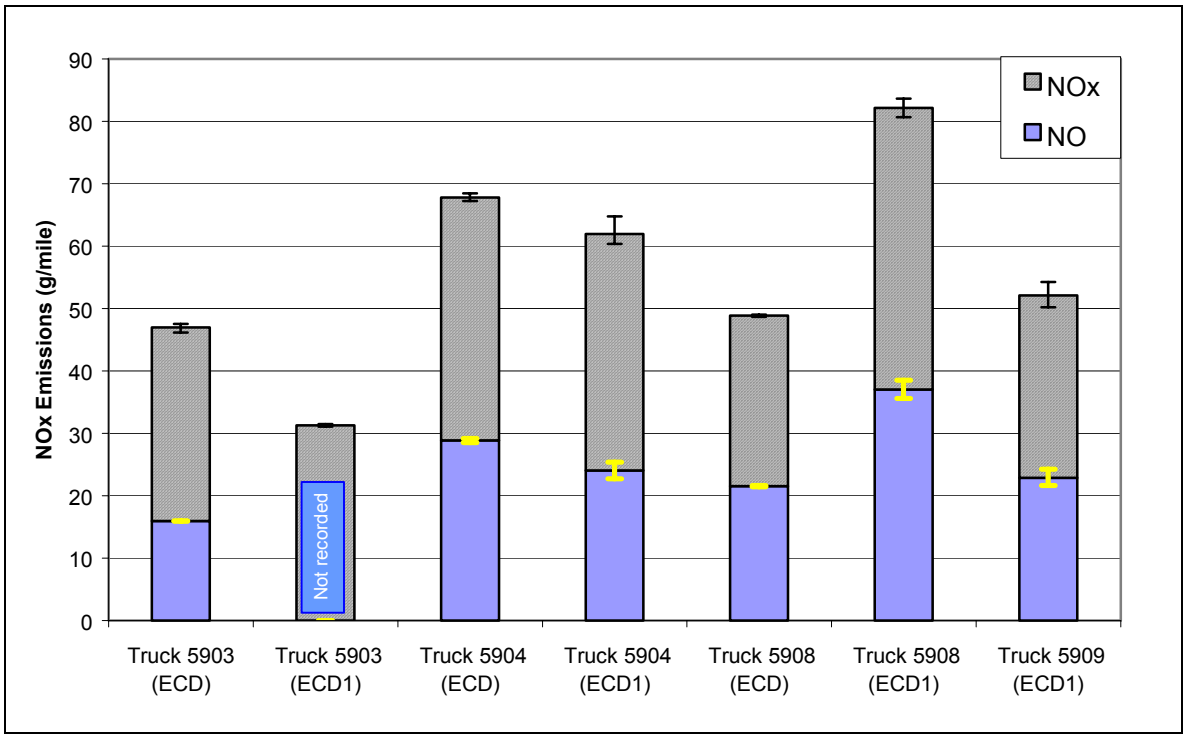

Figure 4.2.10: Round two NO and NOx emissions using particulate filters.

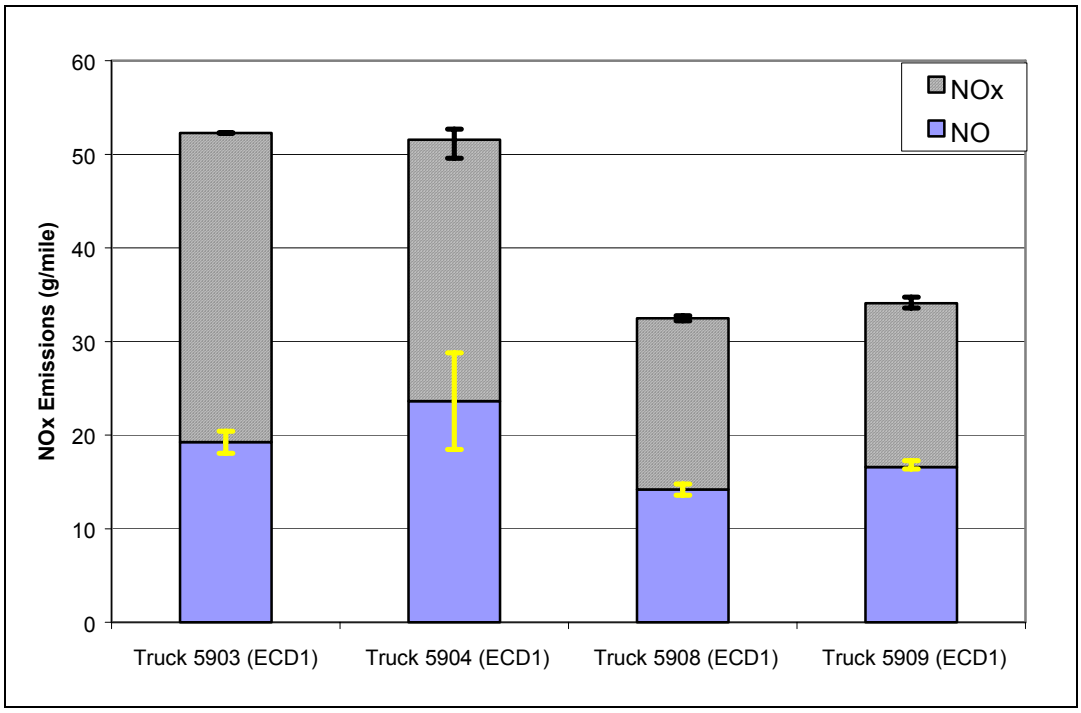

Figure 4.2.11: Round three NO and NOx emissions using particulate filters.

NOx emissions from test runs not using DPFs are shown in Figures 4.2.12 and 4.2.13 for ECD/ECD1 fueled runs and CARB fueled runs respectively. As NO is not converted to NO_2 without the presence of a catalyst, NO emissions were not reported for these runs in any round of testing.

As expected, there were no significant reductions in NOx concentrations in any of the rounds of testing. However, NO concentrations were lowered by approximately 27 percent and 24 percent, in rounds two and three, respectively.

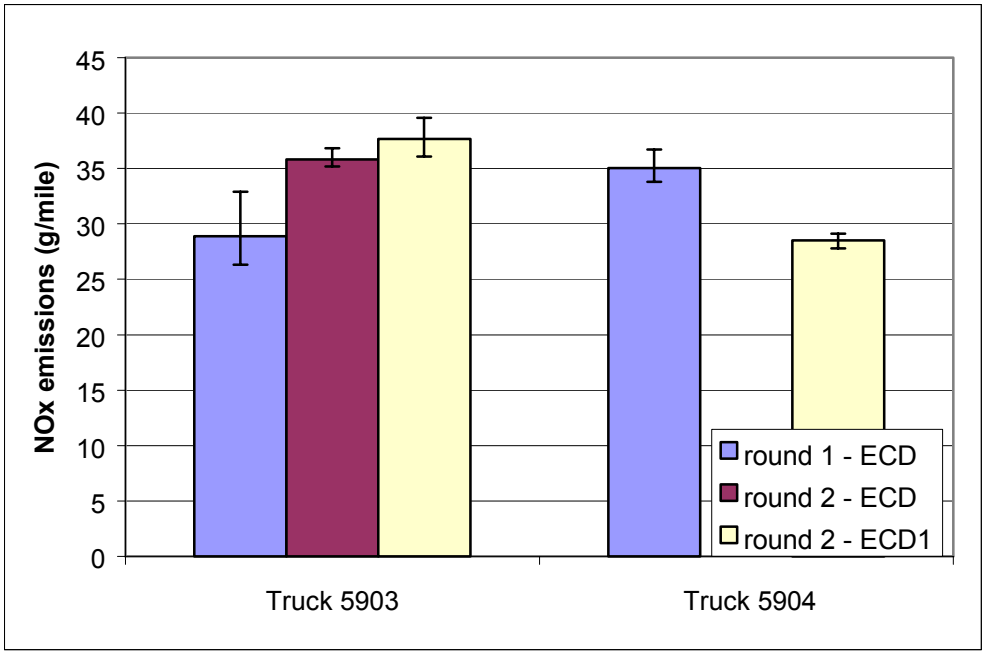

Figure 4.2.12: Total NOx emissions from ECD/ECD1 fueled test runs without DPFs.

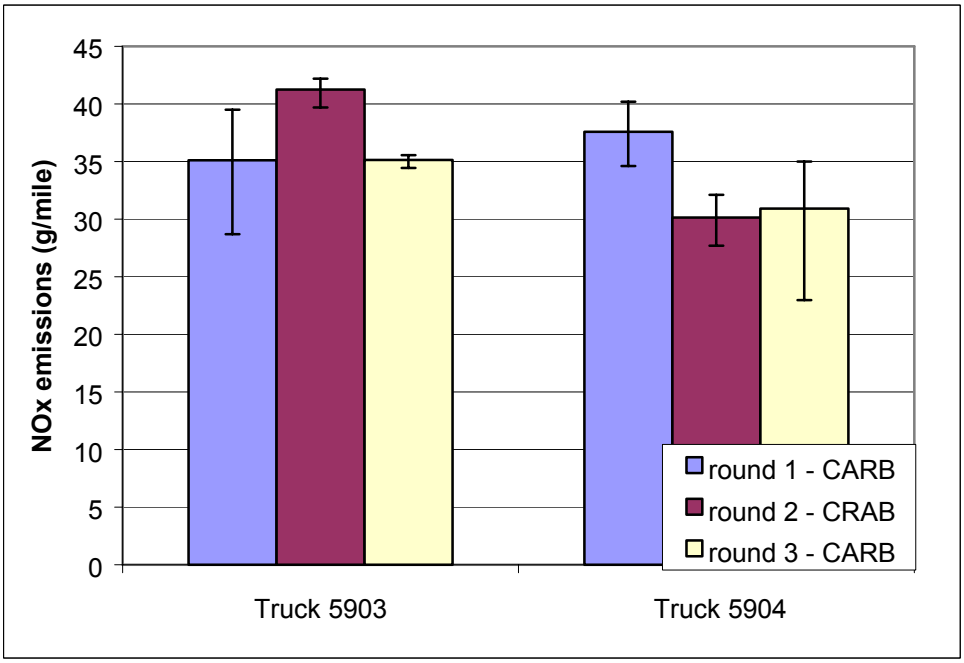

Figure 4.2.13: Total NOx emissions from CARB fueled test runs without DPFs.

4.2.3.4 CO_2 Emissions / Fuel Economy

Figure 4.2.14 shows the CO_2 emissions released during testing with DPFs installed. The calculated values for the fuel economy for these tests are shown in Figure 4.2.15 in units of miles per gallon (MPG). Variations in the fuel economy from round to round were generally slight, with truck 5908 seeing the largest variation between rounds one and two, a twelve percent decrease.

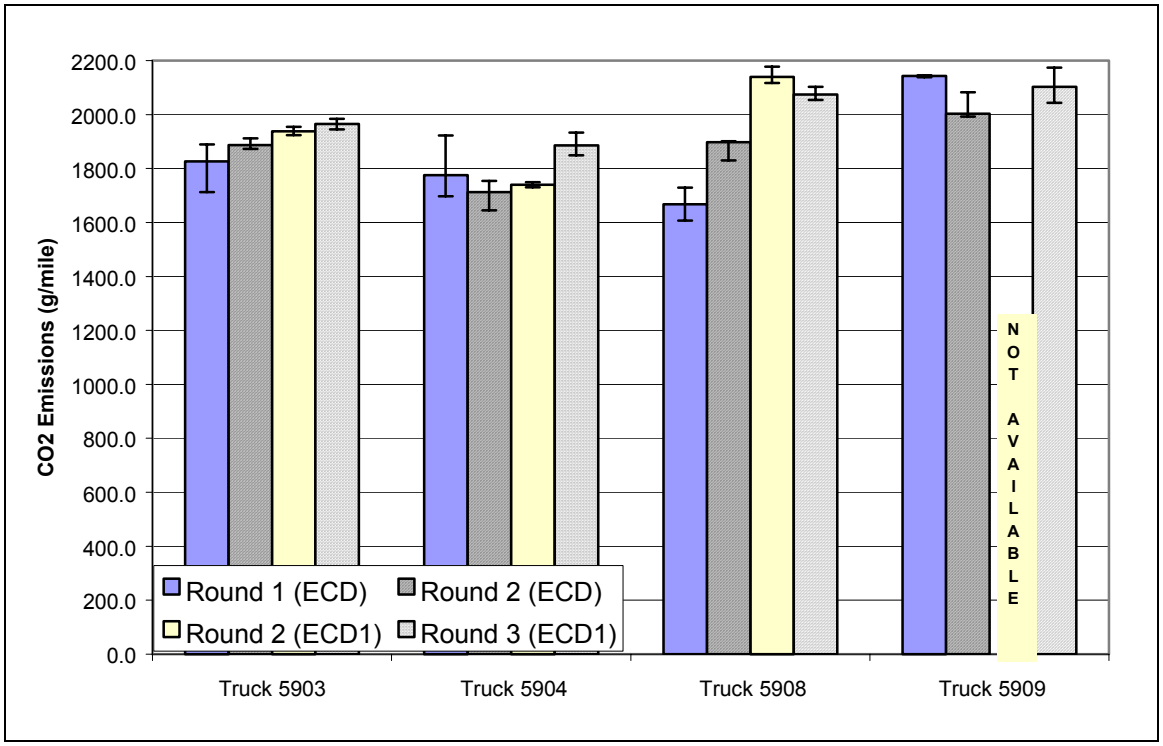

Figure 4.2.14: CO_2 emissions from test runs with DPFs installed.

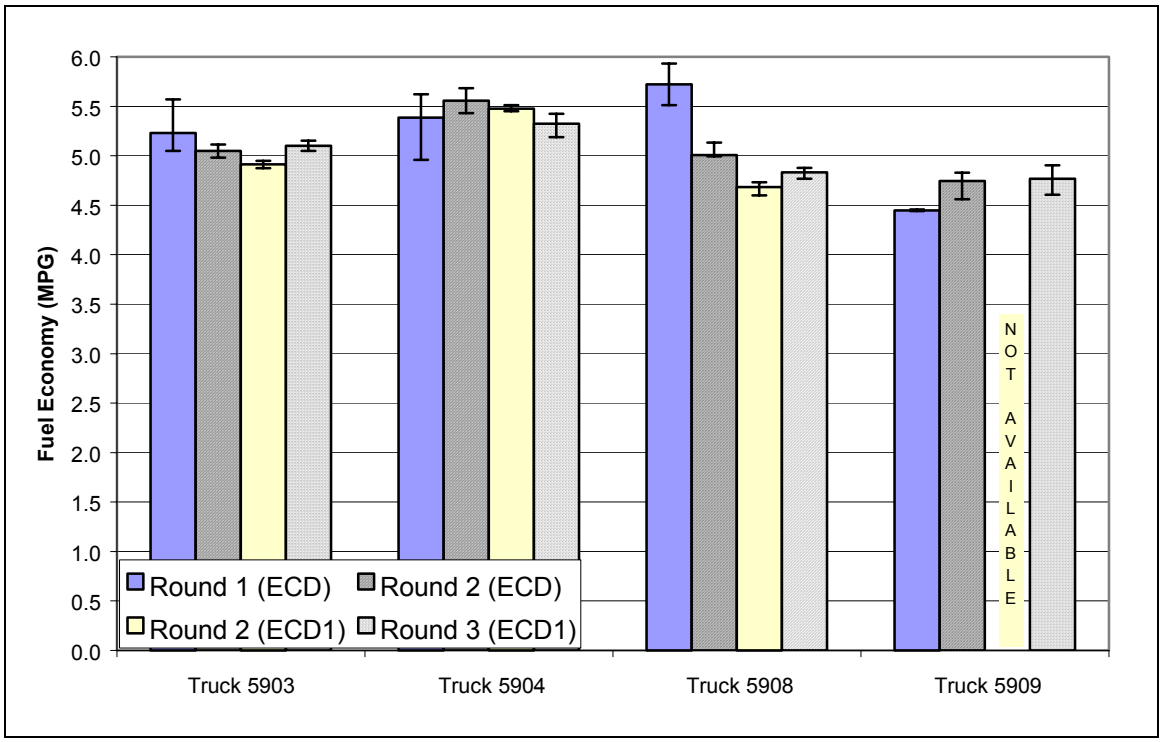

Figure 4.2.15: Fuel economy from test runs with DPFs installed.

CO_2 emissions and fuel economy values for non-DPF equipped runs using ECD and ECD1 fuel are shown in Figure 4.2.16. Figure 4.2.17 shows similar plots of data collected for non-DPF runs using CARB fuel.

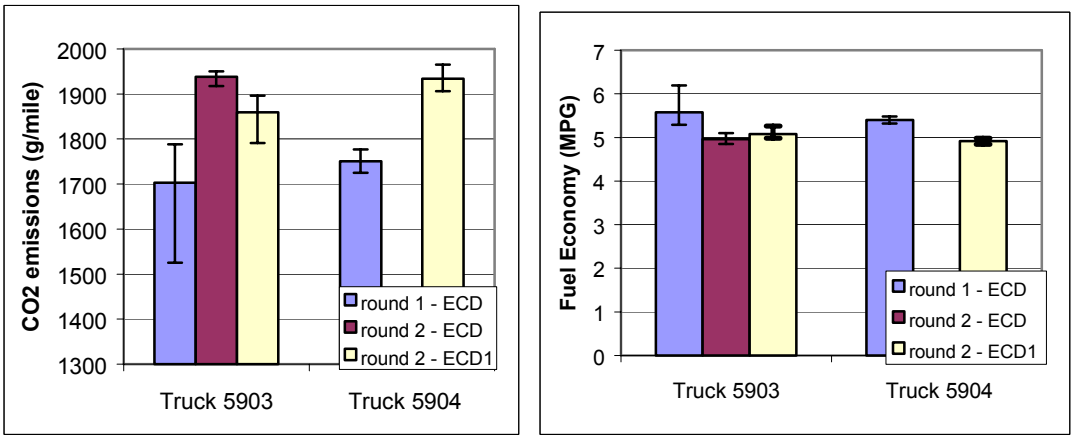

Figure 4.2.16: CO_2 emissions (left) and fuel economy (right) for non-DPF test runs using ECD/ECD1 fuel.

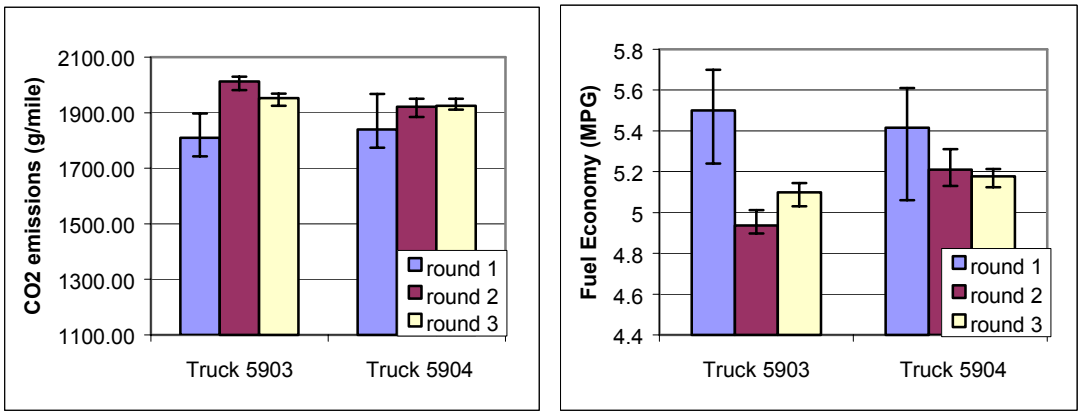

Figure 4.2.17: CO_2 emissions (left) and fuel economy (right) for non-DPF test runs using CARB fuel.

No significant changes in CO_2 emissions were recorded in this evaluation. With the exception of the CRT equipped vehicles tested in round two, all CO_2 data was slightly higher for DPF equipped test runs, averaging five percent, with an extreme outlier of 10.8 percent recorded from DPX equipped vehicles in round three. This is attributed to the increased exhaust backpressure typically caused by particulate filters. CRT equipped vehicles demonstrated a slight reduction, less than seven percent, in CO_2 emissions in round two. This suggests a vehicle and/or DPF maintenance issue which will be discussed in a subsequent section of this chapter.

As expected, fuel economy fluctuated only a few percent between testing rounds. In most cases, the fuel economy fluctuated less than 0.3-MPG between testing rounds. The exception to this, however, was truck 5908, which showed a 0.7-MPG reduction in fuel economy between rounds one and two. This non-typical fluctuation suggests a buildup of ash on the filter surface within the DPF, the significance of which is discussed a later portion of this chapter.

4.2.3.5 PM Emissions

Figure 4.2.18 shows the PM emissions from particulate filter equipped test runs. In round one, filter efficiencies were so high that neither truck 5903 or 5908 released a detectable amount of particulate matter. This continued for truck 5903 in round two when fueled with ECD fuel. PM emissions increased for all vehicles when fueled with ECD1 fuel in round two. This increase was attributed to the higher quantities of sulfur and total aromatics in the ECD1 fuel compared to the ECD fuel as shown in Table 4.2.2. Note that, as stated in the original test matrix, truck 5909 was not tested in round two with ECD1 fuel.

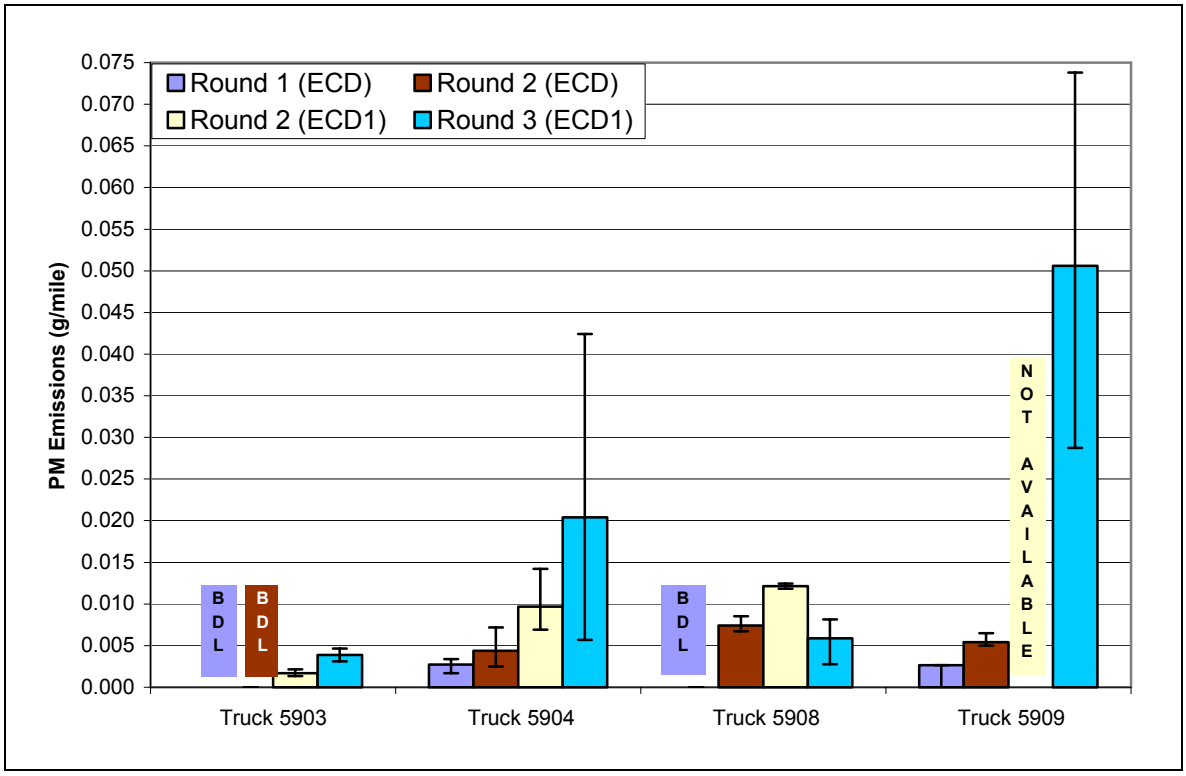

Figure 4.2.18: PM emissions from DPF-equipped test runs.

Figures 4.2.19 and 4.2.20 show the engine-out PM emissions from non-DPF test runs fueled with ECD/ECD1 fuel and CARB fuel respectively. As stated earlier, truck

5904 was not tested in round two with ECD fuel, and only CARB fuel was used in round three when testing without DPFs installed.

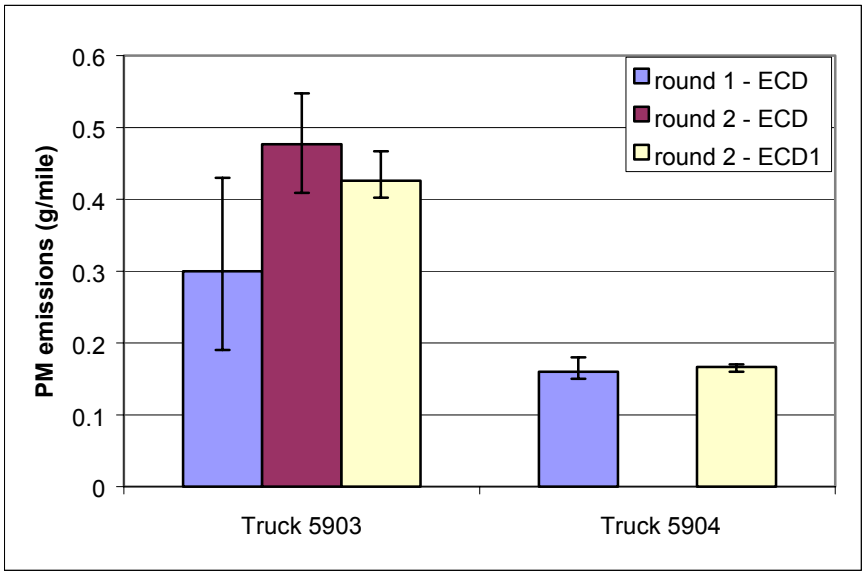

Figure 4.2.19: Engine-out PM emissions from non-DPF test runs using ECD/ECD1 fuel.

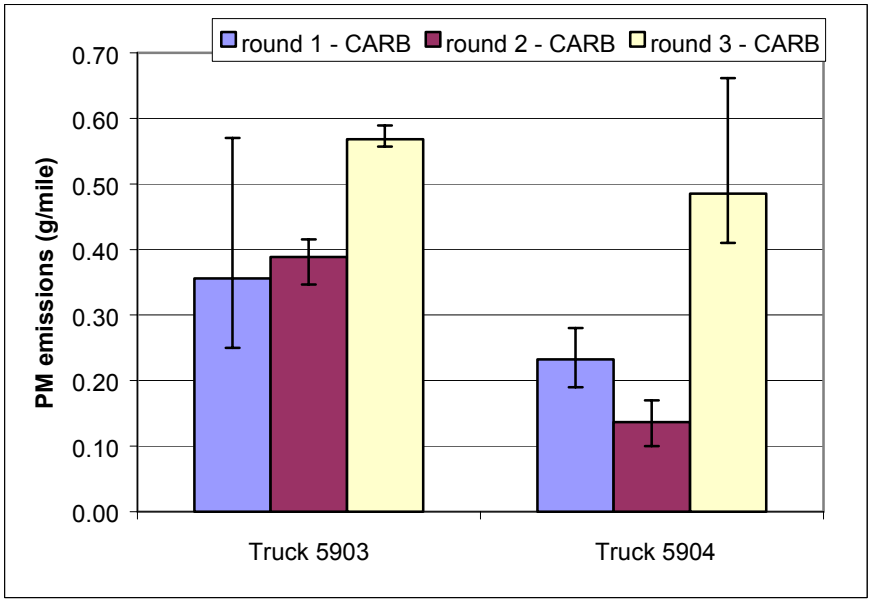

Figure 4.2.20: Engine-out PM emissions from non-DPF test runs using CARB fuel.

As predicted, particulate matter emissions were greatly reduced through out all rounds of testing. Round one showed reductions greater than 99 percent for both DPF

types tested. Results were similar in round two when testing with ECD fuel, however reductions dropped slightly to 98 percent and 96 percent for the CRT and DPX respectively when testing with ECD1 fuel; again this was attributed to the higher concentrations of sulfur and total aromatics in this fuel. Round three tests produced reductions of 97 percent and 95 percent for the CRT and DPX respectively, however the round three calculations were performed using engine-out PM levels from CARB fuel and filtered PM levels from ECD1 fuel.

4.2.4 Limitations of Study

As with any experimentally acquired data, both human and mechanical errors can skew or corrupt the data. Accordingly, there are three pertinent issues that affect the validity of this study: the vehicle and DPF maintenance, number of vehicles tested, and a lack of consistency in vehicle configuration between rounds.

4.2.4.1 Vehicle and DPF Maintenance

During any type of long-term study, all possible sources of variance need to be monitored. At times, this can be a very daunting task, especially when some of these sources are out of the control of the researchers. Such was the case with vehicle and particulate filter maintenance. The vehicle maintenance records were not made available to the researchers at the time of the study. Vehicle maintenance, especially engine modifications, tuning, and controls, can have a large effect on engine-out emissions. Without access to these records, the emissions data cannot be normalized to account for possible fluctuations caused by maintenance operations performed on the test vehicles.

Similarly, DPF maintenance can affect emissions concentrations. Although the DPFs studied in this evaluation were passive regeneration units, maintenance was still

required at periodic intervals. Most significant to the scope of this study was the active removal of ash from the filter surfaces inside the particulate filter. Ash does not react with the catalysts within the filters and thus may build up within the filter causing diminished flow and increased exhaust backpressure. The increased exhaust backpressure has a detrimental effect to CO_2 emissions and consequently a similar effect on fuel economy. Maintenance records showed the removal of ash from the particulate filters just prior to the round three testing, however ash was not removed prior to the first two rounds of testing, making round to round comparisons more difficult.

4.2.4.2 Test Vehicles

Although four test vehicles are adequate for most studies, such a limited number of vehicles may have a negative effect on the results of a long-term study of this nature. By limiting the number of vehicles in such a fashion, the demands on the testing facility become much greater. Fluctuations in data become more apparent and have an increased effect on the results as the data is averaged over a small number of vehicles. Even relatively minor fluctuations, such as driver variance, can have a dramatic effect on the outcome of the test results.

4.2.4.3 Test Consistency

A large problem with the data presented was the lack of consistent information between testing rounds. Although the original test matrix was followed, multi-variable changes occurred at numerous points in the study. The most prominent of these changes was the fuel change / DPF removal in round three. By only testing the vehicles with a different fuel when the DPF was removed, namely CARB fuel rather than ECD or ECD1 as in the previous rounds, there was no consistent baseline from which to compare the

three rounds. An attempt to estimate the engine-out emissions from ECD or ECD1 fuel for round three proved to be infeasible due to fluctuations and inconsistencies in the data, as described above.

4.3 General Performance Evaluation and Manufacturer Comparison

The objective of this study was to determine and compare the general performance characteristics of two styles of diesel particulate filter, the Johnson-Matthey CRT and the Engelhard DPX. All vehicles in this study were tested using driving schedules representative of the actual duty of the vehicle. Additionally, all vehicles were tested solely on ultra-low sulfur diesel fuels used by the respective fleets.

4.3.1 Test Vehicles

For the general performance evaluation and product comparison ten, vehicles were chosen from three fleets, including the Westchester County Transit Authority (WCTA), Washington Metropolitan Area Transit Authority (WMATA), and the New York City Department of Sanitation (NYCDOS).

4.3.1.1 Westchester County Transit Authority (WCTA)

Two transit buses were selected from the WCTA fleet. They included a 1996 Orion bus with an 8.5L six cylinder Detroit Diesel Series 50 engine rated at 272 horsepower and a Neoplan articulated transit bus with a 12.7L six cylinder Detroit Diesel Series 60 engine rated at 450 horsepower.

Test weights were determined by adding one half of the passenger load (assuming 150 pounds per passenger plus 150 pounds for the driver) to the vehicle curb weight. The

Orion bus was tested at 29,650 pounds, while the Neoplan bus was tested at 55,700 pounds.

Each bus from this fleet was tested with the Engelhard DPX, Johnson-Matthey CRT, and a standard muffler.

4.3.1.2 Washington Metropolitan Area Transit Authority (WMATA)

Four transit buses were tested from the WMATA fleet for general performance evaluation and product comparison. Two 1995 Ikarus buses equipped with 11L Cummins M11-330E engines rated at 330 horsepower were tested. Bus number 5203 was equipped with a Johnson-Matthey CRT, while bus number 5229 was equipped with an Engelhard DPX.

The other two buses from this fleet were Orion Transit buses equipped with 5.9L Cummins 6BT5.9 engines rated at 175 horsepower. Bus number 3724 was equipped with an Engelhard DPX, and bus number 3726 was equipped with a Johnson-Matthey CRT.

The Ikarus buses were tested at 51,900 pounds, while the Orion buses were tested at 18,975 pounds. The test weights were obtained in the same fashion as with the WCTA buses.

4.3.1.3 New York City Department of Sanitation (NYCDOS)

The New York City Department of Sanitation supplied four vehicles for evaluation. They were all 1997 Heil Crane Carrier Corporation refuse trucks equipped with 10.8L Cummins M11 engines rated at 280 horsepower. Trucks 25CF042 and 25CF043 were equipped with Johnson-Matthey CRT particulate filters, while trucks 25CF044 and 25CF045 were equipped with Engelhard DPX units.

The trucks were tested at approximately 65 percent of their gross vehicle weight of 65,098 pounds. The resulting test weight was 42,000 pounds.

Each vehicle in this evaluation was tested while running on ultra-low sulfur diesel fuel already in service at the respective fleets. Table 4.3.1 summarizes the vehicle information pertinent to this evaluation.

Table 4.3.1: Vehicle Information from General Performance Evaluation

Fleet	Number	Vehicle Type	Engine Manufacturer	Engine Model	Test Weight	Aftertreatment	Test Cycle
WCTA	479	Orion Transit Bus	Detroit Diesel	Series 50	34675	Engelhard	2BEELINE
						Johnson-Matthey	2BEELINE
						standard Muffler	BEELINE
WCTA	568	Neoplan Art. Transit Bus	Detroit Diesel	Series 60	55700	Engelhard	2BEELINE
						Johnson-Matthey	2BEELINE
						standard Muffler	BEELINE
WMATA	5203	Ikarus Transit Bus	Cummins	M11-E330E	51900	Johnson-Matthey	2WMATA
						standard Muffler	WMATA
WMATA	5229	Ikarus Transit Bus	Cummins	M11-E330E	51900	Engelhard	2WMATA
						standard Muffler	WMATA
WMATA	3724	Orion Transit Bus	Cummins	6BT5.9	18975	Engelhard	2WMATA
						standard Muffler	WMATA
WMATA	3726	Orion Transit Bus	Cummins	6BT5.9	18975	Johnson-Matthey	2WMATA
						standard Muffler	WMATA
NYCDOS	25CF042	Refuse Truck	Cummins	M11	42000	Johnson-Matthey	NYGTC3X
						standard Muffler	NYGTC3X
NYCDOS	25CF043	Refuse Truck	Cummins	M11	42000	Johnson-Matthey	OCRTC2X
						standard Muffler	OCRTC2X
NYCDOS	25CF044	Refuse Truck	Cummins	M11	42000	Engelhard	OCRTC2X
						standard Muffler	OCRTC2X
NYCDOS	25CF045	Refuse Truck	Cummins	M11	42000	Engelhard	NYGTC3X
						standard Muffler	NYGTC3X

4.3.2 Driving Schedules

As shown in Table 4.3.1, six driving schedules were used in this test matrix. Of these six driving schedules, four were unique cycles and two were extended length cycles. The unique driving cycles were BEELINE, WMATA, NYGTC3X, and OCRTC2X. The two extended length cycles were 2BEELINE and 2WMATA. Each cycle was developed by WVU in order to simulate the specific use of each vehicle being tested.

4.3.2.1 BEELINE / 2BEELINE Cycle

The BEELINE Cycle was developed specifically for the Westchester County Transit Authority. The 2BEELINE Cycle is a double length BEELINE cycle developed to facilitate sufficient particulate filter loading for microbalance measurement when testing with a diesel particulate filter.

The cycle was developed from data logged from continuous operation over an eight-day period of two buses in Westchester County, NY. Both Engine Control Module (ECM) and global positioning system (GPS) data were logged, however only ECM data was used in the development of the driving cycle. The continuous data was divided into "microtrips" on a speed basis. A microtrip is defined as a period of vehicle operation, beginning when vehicle speed exceeds 0.5 mph and ending when vehicle speed returns to less than 0.5 mph, with an included period of idle at the conclusion of vehicle motion.

A total of 2,257 microtrips resulted from the continuous data. Using a random number generator, microtrips were selected and joined in a string as a possible driving cycle with greater than 1,700 seconds. Using this process, 120,000 candidate strings were developed. The root mean square (RMS) was calculated for each string using equation (4.3.1), and the string with the lowest RMS, excluding any string with discontinuities in the microtrip data or excessively steep acceleration or deceleration ramps, was selected as the driving cycle (Wayne, 2002).

$$RMS = \sqrt{\left[\left(\frac{A-A'}{A}\right)^2 + \left(\frac{B-B'}{B}\right)^2 + \left(\frac{C-C'}{C}\right)^2 + \left(\frac{D-D'}{D}\right)^2 + \left(\frac{E-E'}{E}\right)^2\right]} \quad (4.3.1)$$

A – Kinetic Energy No Idle (mph^2) for database
A′ - Kinetic Energy No Idle (mph^2) for candidate cycle
B – Average Vehicle Speed No Idle (mph) for database
B′ – Average Vehicle Speed No Idle (mph) for candidate cycle

C – Standard Deviation of Speed No Idle (mph) for database
C′ - Standard Deviation of Speed No Idle (mph) for candidate cycle
D – Average Vehicle Speed with Idle (mph) for database
D′ – Average Vehicle Speed with Idle (mph) for candidate cycle
E – Percentage Time Idle (%) for database
E′ – Percentage Time Idle (%) for candidate cycle

The resulting BEELINE Cycle has an RMS value of 0.49%, a total time of 1701 seconds, and a distance of 6.81 miles. Figure 4.3.1 shows the BEELINE cycle trace.

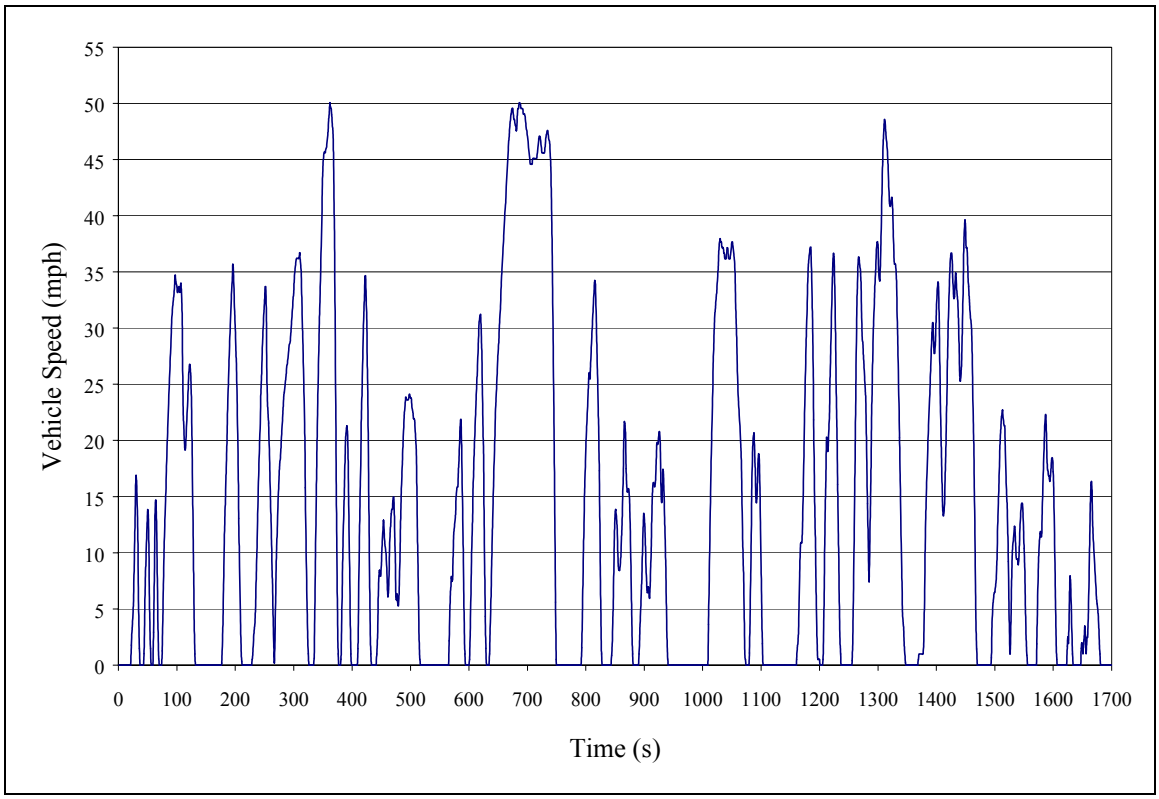

Figure 4.3.1: BEELINE cycle driving cycle developed for WCTA.

4.3.2.2 WMATA / 2WMATA Cycle

The WMATA cycle was developed specifically for the Washington Metropolitan Transit Authority. The 2WMATA cycle is a double length cycle developed to facilitate sufficient particulate filter loading for microbalance measurement when testing with a diesel particulate filter.

The WMATA cycle was developed in a similar fashion to the BEELINE cycle. Vehicle speed data was logged via a GPS from several transit buses in and around the Washington D.C. area. This data was divided into microtrips, randomly selected into candidate strings, and the resulting RMS values calculated using the same criteria used for the BEELINE cycle. The selected candidate string had an RMS value of 0.8896.

The selected candidate string was converted into a cycle through the addition of idle periods at the beginning and end of the cycle as well as between the microtrips comprising the candidate string. The idle operation within the cycle represented the percentage of idle operation within the database. The included idle times at the beginning and end of the cycle were set at 20 seconds each in order to allow for equipment response and measurement of all emissions from the driving cycle. The WMATA cycle is shown in Figure 4.3.2.

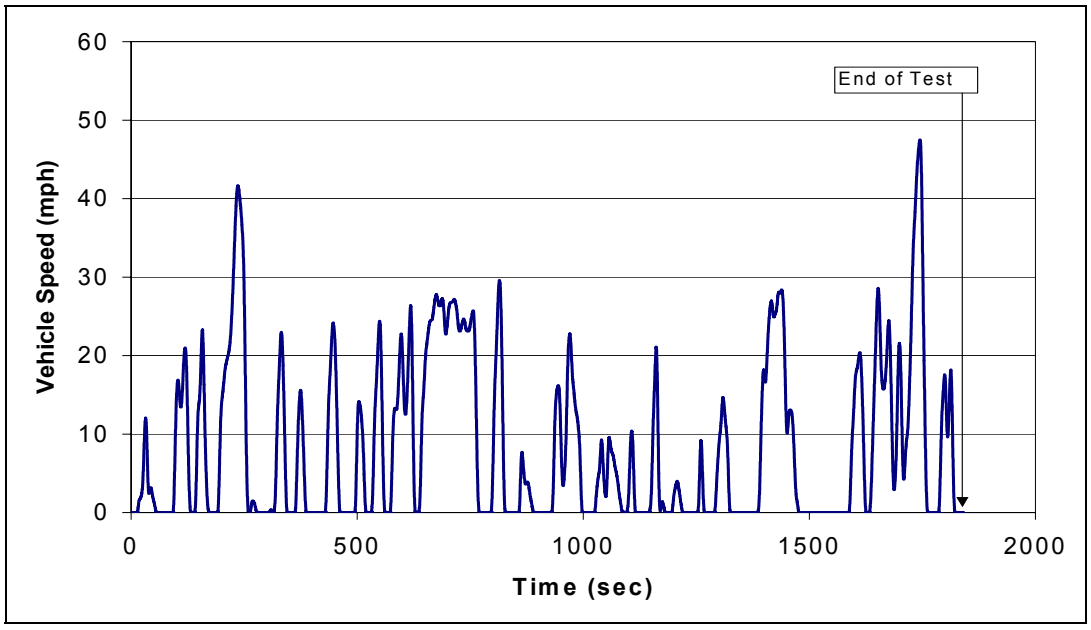

Figure 4.3.2: WMATA cycle developed for the Washington Metropolitan Area Transit Authority.

4.3.2.3 NYGTC3X Cycle

The NYGTC3X cycle is a derivative of the NYGTC cycle that was developed for the New York Department of Sanitation. Data was acquired by following refuse haulers in Morgantown, WV and New York City. Additionally, some supplementary data was acquired from a Detroit Diesel powered truck in New York City using a vehicle speed and pedal position data logger. Using this data it was determined that drivers seldom use full power when traveling form pickup point to pickup point, the average vehicle speed and distances traveled are low, and compaction cycles should be included in the cycle. The resulting driving cycle incorporated three compactions, one acceleration to 20 mph, three accelerations to 12.5 mph, and four accelerations to 5.5 mph. The distance traveled was 0.38 miles with a majority of time spent idling. Three warm-up ramps were included at the beginning of the cycle in order to insure the aftertreatment devices had sufficiently reached operating temperature prior to data collection (Wayne, 2002).

The NYGTC3X cycle was developed to facilitate sufficient particulate filter loading for microbalance measurement when testing with a diesel particulate filter. This modified cycle used three NYGTC cycles repeated sequentially. The cycle possessed three sets of three compactions, for a total of nine. The warm-up ramps were only included at the beginning of the first NYGTC cycle, and the total distance traveled was 1.14 miles. Figure 4.3.3 shows the NYGTC3X cycle as driven on the test bed. Note, the warm-up ramps were not shown on this figure as no data was recorded during that time.

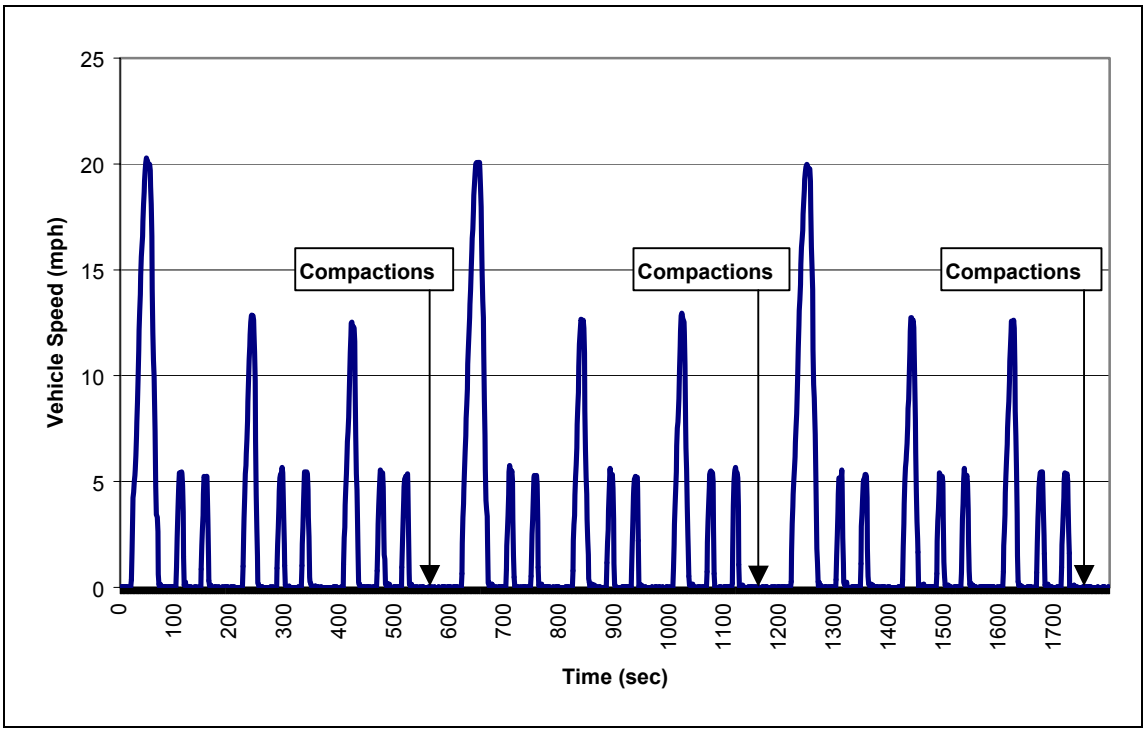

Figure 4.3.3: NYGTC3X cycle developed for the NY Department of Sanitation.

4.3.2.4 OCRTC2X Cycle

The OCRTC2X cycle was a derivative of the OCRTC cycle, which represents sanitation truck operation in Orange County, CA, however it was applied to the NYCDOS vehicles for sake of comparison. The OCRTC cycle, Orange County Refuse Truck Cycle, was developed from GPS data collected in February 2000. The continuous data was divided into microtrips, randomly selected into candidate strings, and the RMS values calculated as they were with the BEELINE and WMATA cycles.

The resulting cycle contained less overall idle time and higher maximum speeds than the NYGTC cycle. No warm-up ramps were included in this cycle.

The OCRTC2X cycle was developed to facilitate sufficient particulate filter loading for microbalance measurement when testing with a diesel particulate filter. It was composed of two OCRTC cycles run continually with an overall distance of 5.2 miles.

Four compaction cycles were included at 300 seconds, 1050 seconds, 1460 seconds, and 2200 seconds. Figure 4.3.4 shows the OCRTC2X as driven on the test bed (Wayne, 2002).

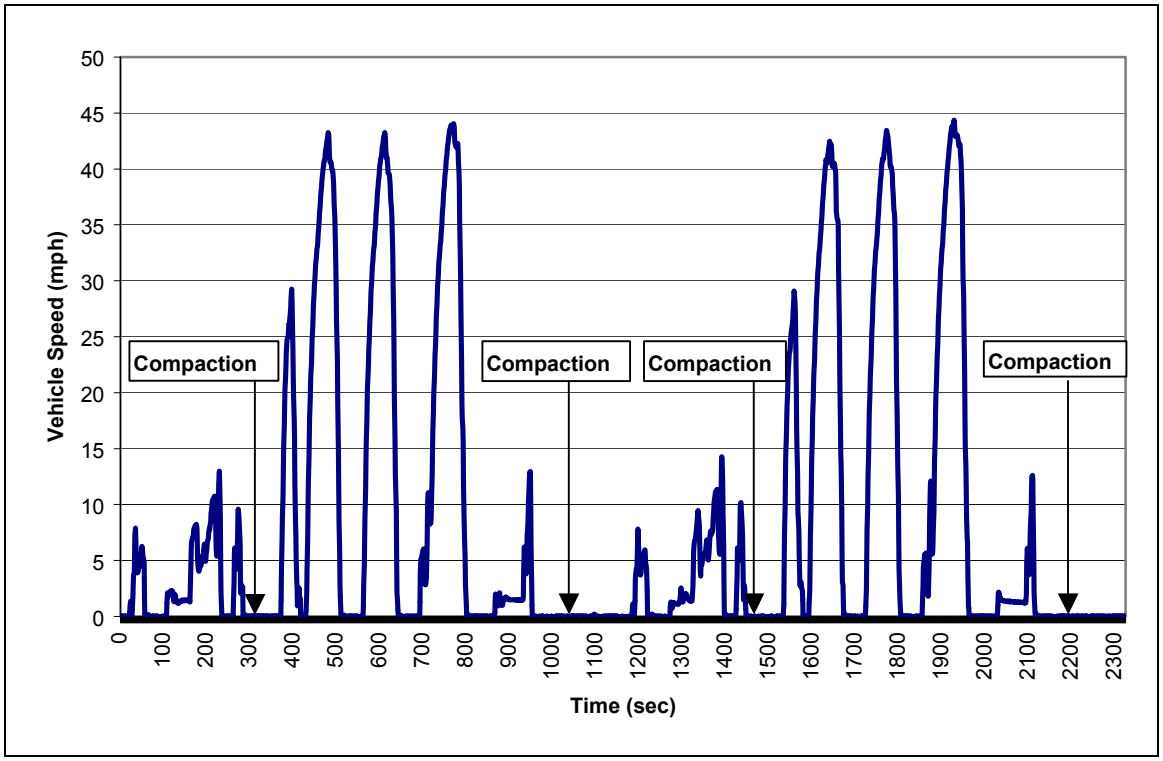

Figure 4.3.4: OCRTC2X developed for the Orange County Department of Sanitation and applied to the NYCDOS vehicles.

4.3.3 Results

It is known that comparisons of vehicle emissions collected using different driving schedules cannot be directly compared. However, as the purpose of this study is not to compare emission outputs but rather to compare DPF effectiveness under real-world simulations, this stipulation is being overlooked for the purposes of this study. In an effort to alleviate any discrepancies, all reported emissions reductions are averages taken from all vehicles tested.

4.3.3.1 CO Emissions

CO emissions were greatly reduced for all vehicles tested. The Engelhard DPX equipped vehicles showed reductions of 85 percent on average, while the Johnson-Matthey CRT equipped vehicles demonstrated reductions of approximately 84 percent on average.

Figure 4.3.5 shows the CO emissions for DPX equipped vehicles, and Figure 4.3.6 shows the CO emissions from CRT equipped vehicles. In both figures, each bar represents the average of three test runs performed on each vehicle with the respective aftertreatment, an Engelhard DPX, a Johnson-Matthey CRT, or a standard muffler.

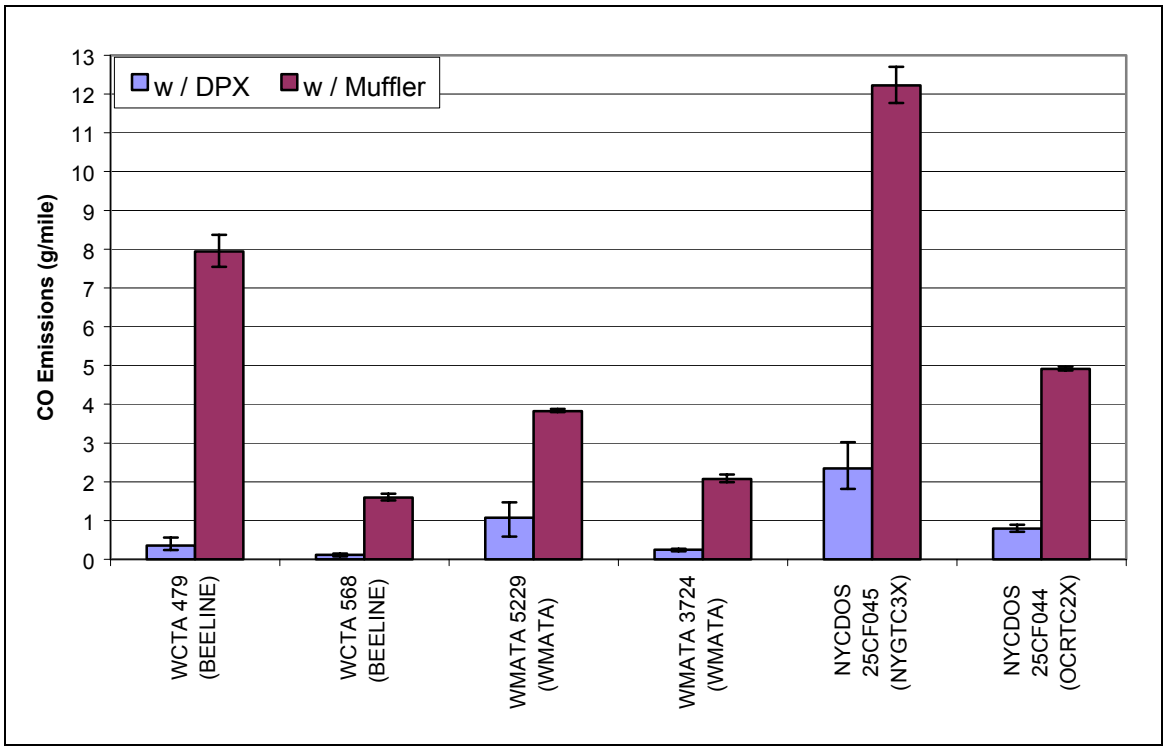

Figure 4.3.5: CO emissions from Engelhard DPX equipped vehicles.

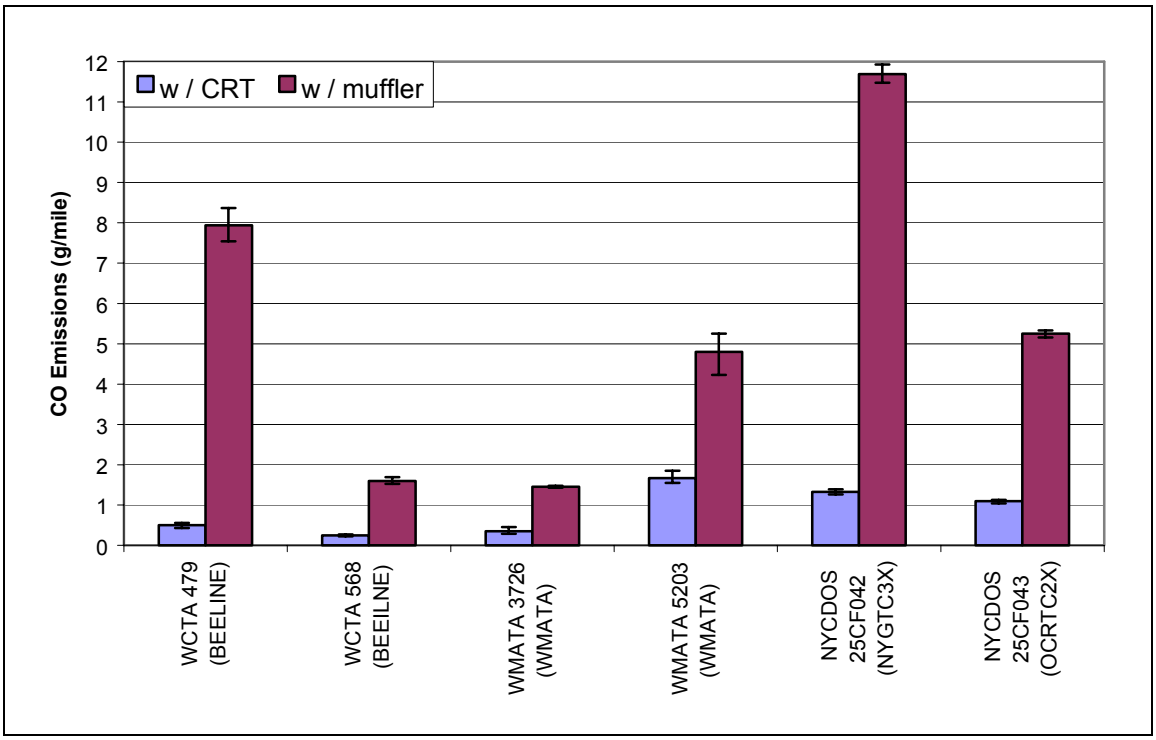

Figure 4.3.6: CO emissions from Johnson-Matthey CRT equipped vehicles.

4.3.3.2 HC Emissions

HC emission outputs were reduced by 76 percent and 81 percent for the DPX and CRT equipped vehicles, respectively, relative to the untreated exhaust. Four of the test vehicles achieved below detectable limit HC concentrations when testing with the diesel particulate filters. WCTA buses 479 and 568 produced below detectable limit HC emission concentrations when testing with both DPF types. Truck NYCDOS 25CF044 produced HC levels below detectable limits with the Engelhard DPX in use, while WMATA bus 3726 produced below detectable limit levels with the Johnson-Matthey CRT in place.

Figures 4.3.7 and 4.3.8 show the HC emissions for the DPX and CRT equipped vehicles respectively. Each bar in these figures represents the average HC emissions

produced during three valid test runs performed on each vehicle with the respective aftertreatment.

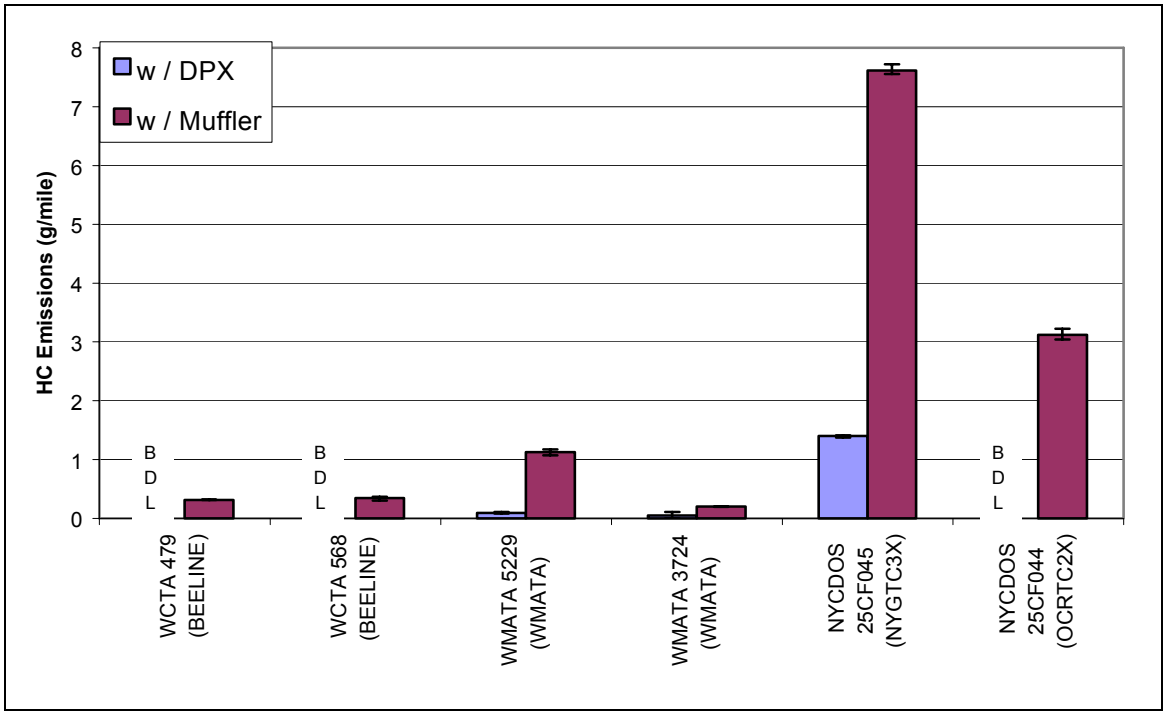

Figure 4.3.7: HC emissions from DPX equipped vehicles.

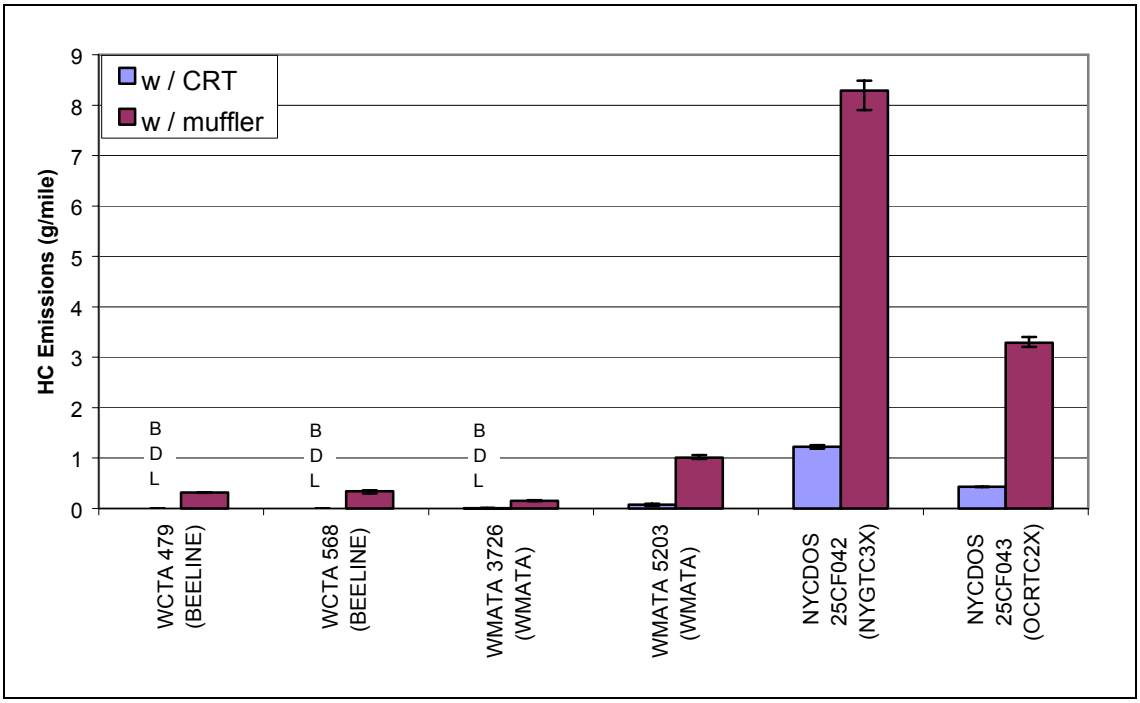

Figure 4.3.8: HC emissions from CRT equipped vehicles.

4.3.3.3 NOx and NO Emissions

As expected there was no significant change in NO_X emissions when testing with either the Engelhard DPX or the Johnson-Matthey CRT. There was less than one percent variance in emissions with the particulate filters compared to emissions with the standard mufflers.

When testing with catalyzed particulate filters, NO emissions are of greater concern than NO_X emissions. NO is converted to NO_2 by the catalyst inside the diesel particulate filter. By using two NO_X analyzers, the NO/NO_X fraction can be quantified. However, due to a failure of one of the chemiluminescent NO_X analyzers during testing, this was only accomplished for the WCTA fleet vehicles.

Through conversion to NO_2, the particulate filters reduced NO concentrations by 38.5 percent and 42 percent for the DPX and CRT, respectively, for the WCTA vehicles tested. Figure 4.3.9 graphically shows this reduction. In this figure, each bar represents the average NO or NO_X concentration recorded by the analyzers over three valid test runs.

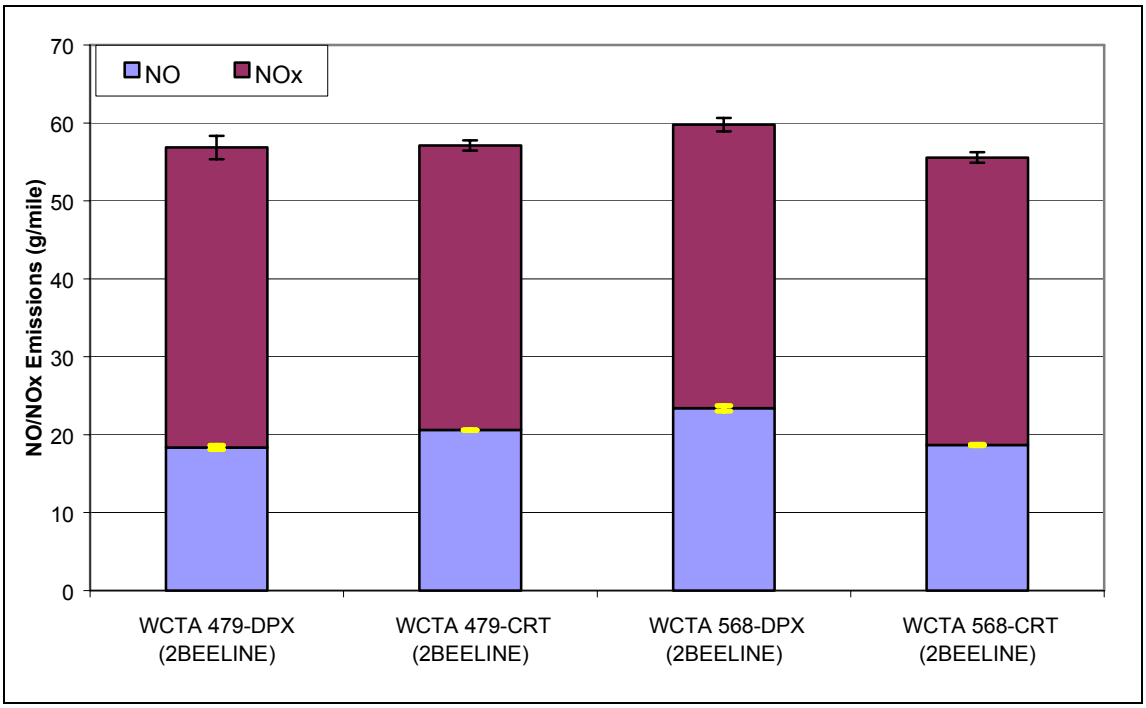

Figure 4.3.9: NO and NO_X emissions from the WCTA fleet vehicles tested.

4.3.3.4 CO_2 Emissions / Fuel Economy

On average carbon dioxide emissions increased slightly when testing with the particulate filters. This increase is attributed to an increase in exhaust backpressure associated with the addition of a diesel particulate filter into the exhaust stream. The average variance was an approximate 2.6 percent increase for the DPX equipped vehicles and approximate two percent increase for the CRT equipped vehicles. It should be noted, however, that the CO_2 measurement accuracy, approximately ±2%, could also account for the variance between filter equipped tests and tests using the standard muffler.

The increased backpressure discussed above also had a parasitic effect on the fuel economy of filter equipped vehicles. Average fuel economy dropped by 1.4 percent for Engelhard DPX equipped vehicles and 4.4 percent for Johnson-Matthey CRT equipped vehicles. Figures 4.3.10 and 4.3.11 show the calculated fuel economy for DPX and CRT equipped tests respectively.

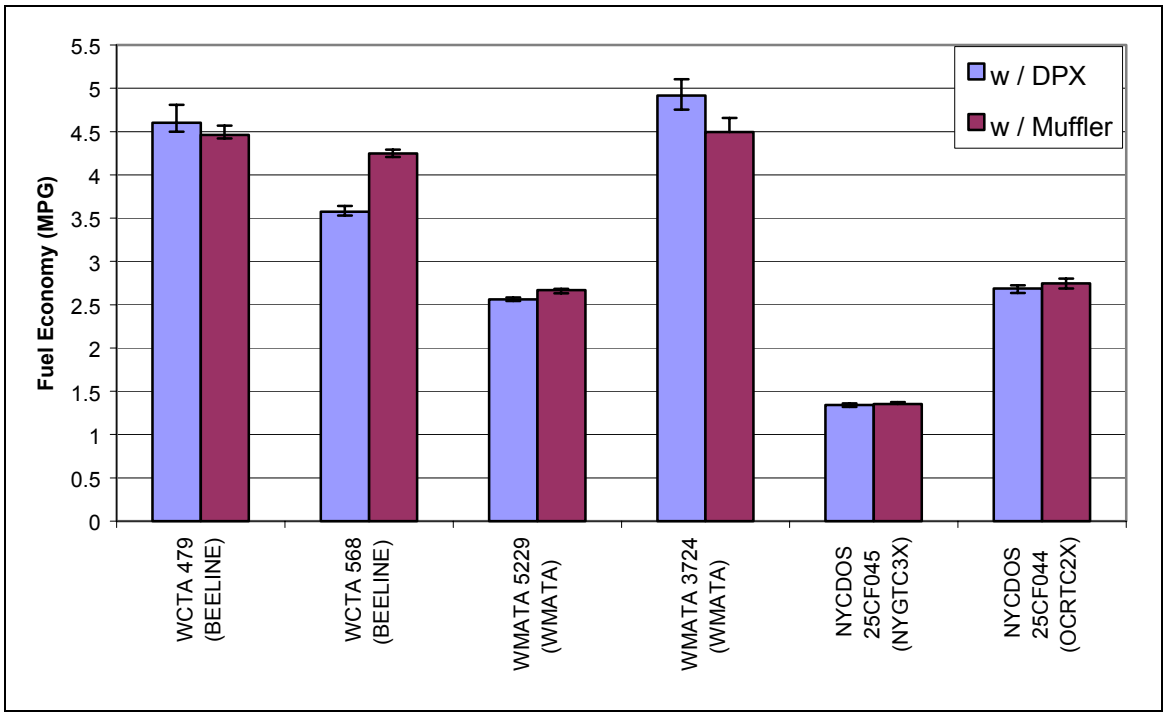

Figure 4.3.10: Fuel economy from Engelhard DPX equipped vehicles.

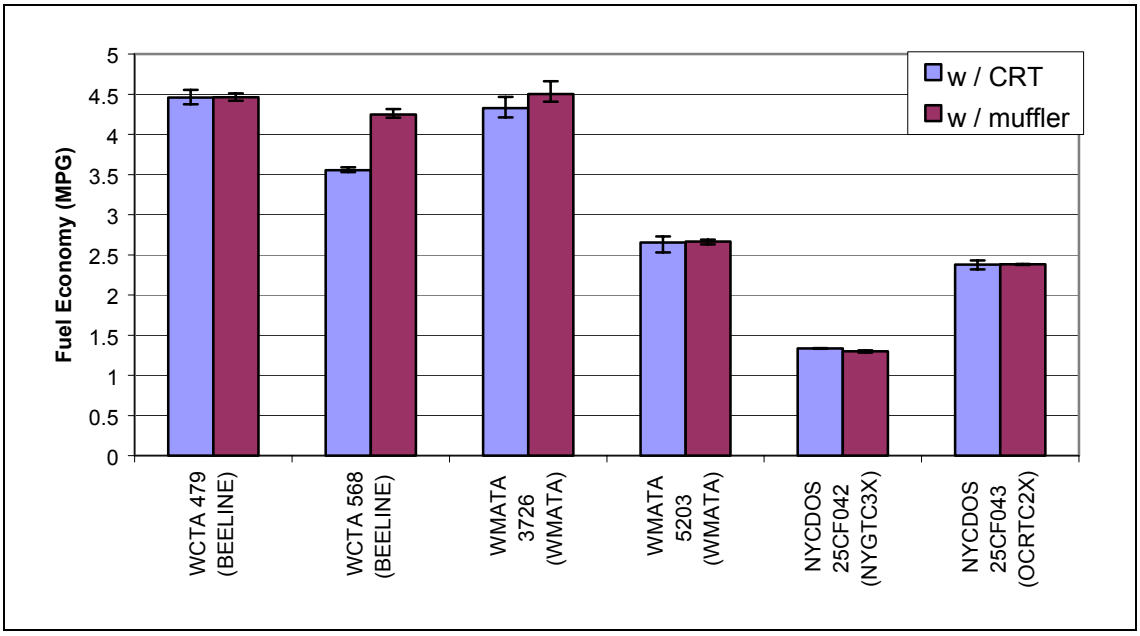

Figure 4.3.11: Fuel economy from Johnson-Matthey CRT equipped vehicles.

4.3.3.5 PM Emissions

As expected, the greatest emission reduction witnessed was from the particulate matter emissions. The Engelhard DPX equipped vehicles underwent an order of magnitude reduction going from an average emissions of 0.84 g/mile with the standard muffler to 0.053 g/mile with the DPX. This was an approximate 94 percent reduction. The Johnson-Matthey CRT proved slightly less efficient, with only an 82 percent reduction.

Figure 4.3.12 shows the average PM emissions produced from DPX equipped vehicles, while Figure 4.3.13 shows the average PM emissions produced from CRT equipped vehicles. Each bar in these figures represents the average of three test runs performed with each vehicle/aftertreatment configuration.

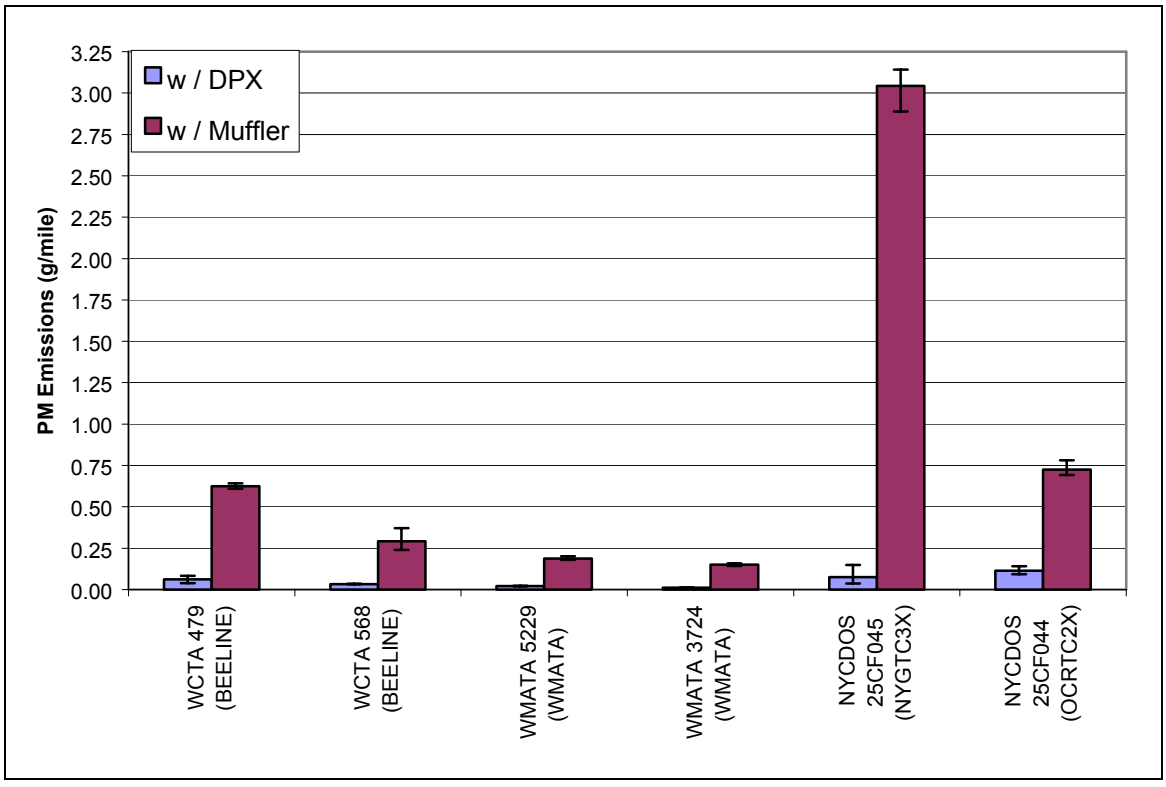

Figure 4.3.12: PM emissions from Engelhard DPX equipped vehicles.

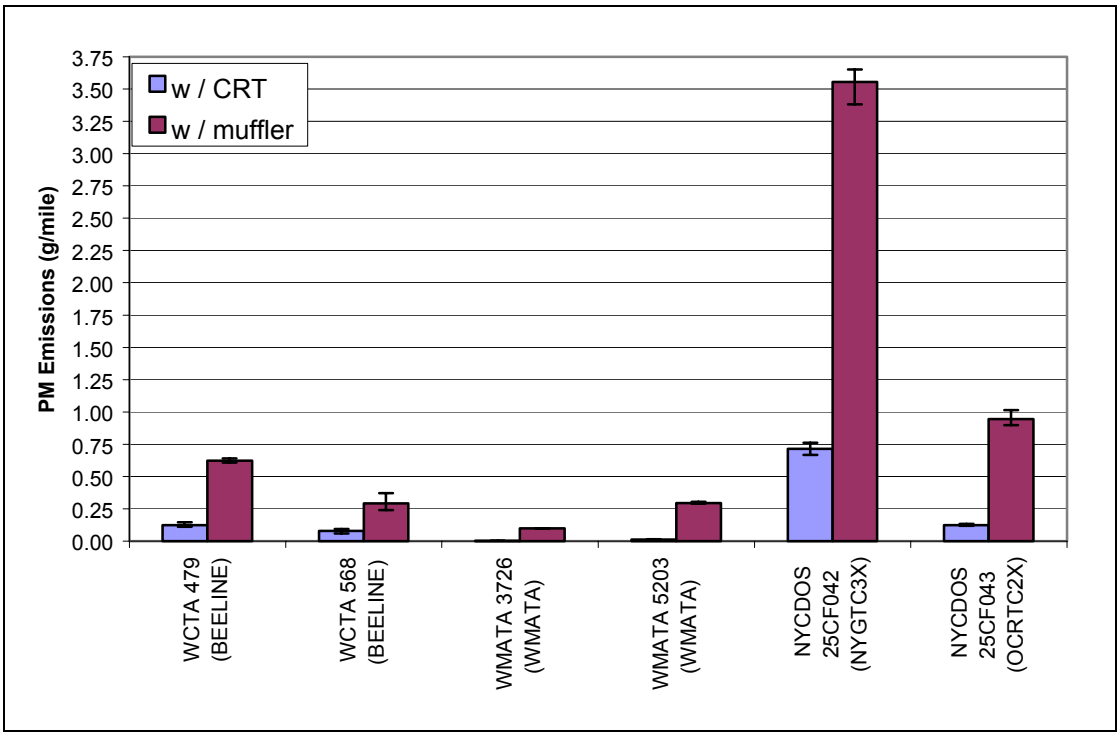

Figure 4.3.13: PM emissions from Johnson-Matthey CRT equipped vehicles.

Chapter 5 – Conclusions

5.1 Cold Start DPF Performance

Under cold start conditions, the diesel particulate filters proved to be very effective in reducing particulate matter from the exhaust stream, with reduction levels averaging greater than 90% for all DPFs tested. In the valid TEOM data collected, there was little variance in mass concentration data, suggesting that both the Engelhard DPX and the Johnson-Matthey CRT successfully filter particulate matter prior to the catalyst reaching its light-off temperature.

Based on gaseous emission stabilization, the light-off temperature was determined to be dependent on the post-filter exhaust temperature rather than the pre-filter exhaust temperature, regardless of the fact that the pre-filter temperature stabilized much faster. Gaseous emissions concentrations, including CO, HC, NO/NO_X, stabilized when the post-filter exhaust temperature reached between 400°F and 450°F for the Engelhard DPX under warm-weather cold start testing and between 330°F and 350°F under cold-weather cold start testing. The Johnson-Matthey CRT showed emissions stabilization between 375°F and 450°F under warm-weather cold start testing. The CRT was not tested under cold-weather conditions. After the catalyst light-off temperature was reached, the post-trap exhaust temperature continued to climb to as high as 550°F before stabilizing.

Based on the smoke meter data, neither particulate filter type tested had a significant impact on reducing white smoke emissions.

Average integrated carbon monoxide emissions were reduced by 72.7% for warm-weather cold start tests and 53% for cold-weather cold start tests using the Engelhard DPX. The Johnson-Matthey CRT reduced CO emissions by 76.9% during

warm-weather cold start tests. Hydrocarbon emissions were reduced by 83% and 78% by the DPX during warm-weather and cold-weather cold start testing respectively. HC emissions were reduced by 86% using the Johnson-Matthey CRT. No significant reductions were recorded for NO_X or CO_2 emissions from any of the DPFs tested, however NO emissions were reduced by 30% and 46% by the DPX and CRT respectively for warm-weather cold start testing. The NO/NO_X fraction was not calculated for the cold-weather cold start testing performed on the WVU Mack tractor truck.

5.2 Long-Term Durability Evaluation

The three-year evaluation of diesel particulate filter performance showed a slight degeneration in filter efficiency as accumulated mileage increased. This degeneration is most evident in the carbon monoxide, hydrocarbon, and particulate matter emissions.

CO emissions were most severely affected by the mileage increase. Round one CO reductions were greater than 90% for both the Engelhard DPX and Johnson-Matthey CRT; however in round two, average CO reductions decreased to 62% for the DPX and 85% for the CRT. Reductions again dropped in round three to only a 57% reduction from the DPX and 74% from the CRT.

HC emission reductions remained fairly constant between rounds one and two, with reductions of approximately 99% for both DPF types. However, when the fuel type was changed from ECD to ECD1, the reduction levels fell to 89% for the DPX while remaining at 98% for the CRT. In round three, the HC emission reductions gained from the DPX fell to 75% while the CRTs reductions averaged 95%.

Particulate matter emissions also remained steady from round one to round two, with reductions of greater then 99% for both DPF types while using the ECD fuel. However, in round three, the PM emissions reductions dropped to 95% and 97% for the Engelhard DPX and Johnson-Matthey CRT respectively.

Although the experimental data showed a trend toward diesel particulate filter degeneration relative to accumulated mileage, a definitive life span could not be determined for either the Engelhard unit or the Johnson-Matthey unit because of the discrepancies described in the previous chapter, including the use of multiple fuel types during testing and the lack of vehicle maintenance records.

5.3 General Performance Evaluation and Manufacturer Comparison

The general performance evaluation and product comparison showed some strengths and weakness of both the Engelhard DPX and Johnson CRT diesel particulate filters, although the two styles are very comparable.

Average carbon monoxide emission reductions were nearly identical for the two units, with an 85% reduction from the DPX and an 84% reduction from the CRT. Additionally, carbon dioxide emission variances were nearly identical, with an increase in CO_2 emissions of 2.6% and 2% for the DPX and CRT respectively.

Differences in hydrocarbon emission reductions from the two DPF styles were slightly more evident. The Engelhard DPX reduced HC emissions by 76% while the Johnson-Matthey CRT reduced HC emissions by 81%.

The greatest difference discovered between the two DPF types was in the area of particulate matter reductions. On average, the Johnson-Matthey CRT reduced PM emissions by 82% while the Engelhard DPX reduced PM emissions by 94%.

Both the Engelhard DPX and the Johnson-Matthey CRT are very effective aftertreatment devices. As this study has shown, there exists a slight trade-off between HC reduction and PM reduction between the two units.

References:

1. Allansson, R., Cooper, B., thoss, J., Uusimäki, A., Walker, A., Warren, J. (2000). *European Experience of High Mileage Durability of Continuously Regenerating Diesel Particulate Filter Technology* (SAE 2000-01-0480).
2. Auto Emissions Magazine, Number 14. "21st Century Diesel: A Clean Future." Fall 1999.
3. Bata, R., Clark, N., Gautam, M., Howell, A., Long, T., Loth, J., Lyons, D., Palmer, M., Rapp, B., Smith, J., Wang, W. (1991). *The First Transportable Heavy Duty Vehicle Emissions Testing Laboratory* (SAE 912668).
4. Browning, L. H. (1997). *Technologies and Costs for On-Road Heavy-Duty Engines Meeting 2004 Emissions Standards* (SAE 973256).
5. Chandler, K., Coburn, T., LeTavec, C., Uihlein, J., Vertin, K., Chatterjee, S., Hallstrom, K., Wayne, S., Clark, N., Gautam, M., Thompson, G., Lyons, D. (2002). *Year-Long Evaluation of Trucks and Buses Equipped with Passive Diesel Particulate Filters* (SAE 2002-01-0433).
6. Chernich, D. J., Jacobs, P. E., Kowalski, J. D. (1991). *A Comparison of Heavy-Duty Diesel Truck Engine Smoke Opacities at High Altitude and at Sea Level* (SAE 911671).
7. Clark, N., McKain, D., Messer, T., Lyons, D. (1994). *Chassis Test Cycles for Assessing Emissions from Heavy Duty Trucks* (SAE 941946).
8. Clark, N., Daley, J., nine, R., Atkinson, C. (1999). *Application of the New City-Suburban Heavy Vehicle Route (CSHVR) to Truck Emissions Characterization.* (SAE 1999-01-1467).
9. Code of Federal Regulations, Title 40, Part 86, Subpart N – Emissions Regulations for New Otto-Cycle and Diesel Heavy-Duty Engines; 86.132-90 Vehicle Preconditioning, 2002.
10. Engelhard. "Engelhard-DPX™ Catalytic Particulate Filters Overview." 2001. Engelhard . 05 Sept. 2002. <www.engelhard.com>.
11. Evans, J. C. (2001). *Influence of Fuel Sulfur Content on Emissions From Diesel Engines Equipped With Oxidation Catalysts*. M.S. Thesis, Department of Mechanical and Aerospace Engineering, West Virginia University, Morgantown, WV.
12. Gilbert, M. (2002). *Investigation into the Use of a Tapered Element Oscillating Microbalance for Real-Time Particulate Measurement*. M.S. Thesis, Department of Mechanical and Aerospace Engineering, West Virginia University, Morgantown, WV.
13. Hall, T. S. (2002). *Effects of Vehicle Weight Class and Model Year on Vehicle Contribution to Atmospheric Pollutant Inventories.* M.S. Thesis, Department of Mechanical and Aerospace Engineering, West Virginia University, Morgantown, WV.
14. Hammerle, R.H., Ketcher, D., Horrocks, R., Lepperhoff, G., Hűthwohl, G., Lűers, B. (1995). *Emissions from Diesel Vehicles with and without Lean NO_X and Oxidation Catalysts and Particulate Traps* (SAE 952391).
15. Heywood, John B., Internal Combustion Engine Fundamentals. McGraw-Hill, Inc., New York, NY. 1988.

16. Hoard, J. (2001). *Plasma-Catalysis for Diesel Exhaust Treatment: Current State of the Art* (SAE 2001-01-0185).
17. Johnson, J. V. (2002). *Diesel Emissions Control: 2001 in Review* (SAE 2002-01-0285).
18. Johnson Matthey. "CRT." 2001. Johnson Matthey Catalytic Systems Division. 05 Sept. 2002. <www.jmcsd.com>.
19. Khair, M.K. (1997). *Technical and Synergistic Approaches Towards the Twenty-First Century Diesel Engine* (SAE 972687).
20. Khair, M., McKinnon, D. L. (1999). *Performance Evaluation of Advanced Emissions Control Technologies for Diesel Heavy-Duty Engines* (SAE 1999-01-3564).
21. Kilcarr, Sean. "Diesel Engines Will Remain the Predominant Power Source for Commercial Trucks." Clean Air: Trucking's Contribution 10 Dec. 2001. <cleanair.fleetowner.com/ar/fleet_diesel_engines_remain/index.htm>.
22. LeTavec, C., Uihlein, J., Segal, J., Vertin, K. (2000). *EC-Diesel Technology Validation Program Interim Report* (SAE 2000-01-1854).
23. Mori, K., Jyoutaki, H., Kawai, K., Sakai, K. (2000). *New Quiescent Combustion System for Heavy-Duty Diesel Engines to Overcome Exhaust Emissions and Fuel Consumption Trade-Off* (SAE 2000-01-1811).
24. Okrent, D. A. (1998). *Optimization of a Third Generation TEOM® Monitor for Measuring Diesel Particulate in Real-Time* (SAE 980409).
25. Richards, R.R., Sibley, J.E. (1988). *Diesel Engine Emissions Control for the 1990's* (SAE 880346).
26. Rosemount Analytical Model 402 Hydrocarbon Analyzer Instruction Manual 015-082132, Rosemount Analytical Inc., LaHabra, California. 1991.
27. Rosemount Analytical Model 868 NDIR Analyzer Instruction Manual 015-748003, Rosemount Analytical Inc., LaHabra, California. 1991.
28. Rosemount Analytical Model 955 NO/NO_X Analyzer Instruction Manual 015-555479, Rosemount Analytical Inc., LaHabra, California. 1991.
29. SAE (1997). *Fuel Economy Measurement Test (Engineering Type) for Trucks and Buses.* Society of Automotive Engineers Standards J1376.
30. Su, T.F., Chang, C., Reitz, R., Farrell, P., Pierpont, A., Tow, T. (1995). *Effects of Injection Pressure and Nozzle Geometry on Spray SMD and D.I. Emissions* (SAE 952360).
31. Tanin, K.V., Wickman, D., Montgomery, D., Das, S., Reitz, R. (1999). *The Influence of Boost Pressure on Emissions and Fuel Consumption of a Heavy-Duty Single-Cylinder D.I. Diesel Engine* (SAE 1999-01-0840).
32. Telonic Berkeley Inc., Telonic Berkeley Model 107 Smoke Opacity Meter User's Manual. (January 7, 1999).
33. USDOE, (2002). United States Department of Energy, Office of Transportation Technologies. *Advanced Petroleum-Based Fuels, Fuel Properties Database*. <www.ott.doe.gov/fuelprops/>
34. Wayne, S., Nine, R. (2002). *Cummins Engine DPF Demonstration Program: Final Data Report.* Department of Mechanical and Aerospace Engineering, West Virginia University, Morgantown, WV.

35. Wayne, S., Nine, R., Clark, N., Schiavone, J. (2002). *Development of the Bee-Line Dynamometer Driving Schedule*. Department of Mechanical and Aerospace Engineering, West Virginia University, Morgantown, WV.
36. Yassine, M.K., Tagomori, M., Henein, N., Bryzik, W. (1996). *White Smoke Emissions Under Cold Starting of Diesel Engines*. (SAE 960249).
37. Zelenka, P., Kriegler, W., Herzog, P., Cartellieri, W. (1990). *Ways Toward the Clean Heavy-Duty Diesel* (SAE 900602).
38. 2002 Health Assessment Document for Diesel Exhaust. USEPA EPA/600/8-90/057F. 01 May 2002. U.S. Environmental Protection Agency, Washington, DC.

Appendix A

Analyzer Information

Lab 1 Analyzers

Analyzer	Abbreviation	Manufacturer	Model	Ranges	Repeatability / Precision
High Level Carbon Monoxide	HCO	Beckman Industrial	Model 868	0-1000 ppm 0-5000 ppm	Not Available
Low Level Carbon Monoxide	LCO	Horiba	AIA-210 LE	0-25 ppm 0-50 ppm 0-100 ppm 0-200 ppm	0.2% Full Scale
Carbon Dioxide	CO2	California Analytical Instruments	Model 300	3% 9.84% 14.79%	1% Full Scale
Oxide of Nitrogen Analyzer	NOx1	California Analytical Instruments	Model 400-HCLD	0-3000 ppm	0.5% Full Scale
Oxide of Nitrogen Analyzer	NOx2	California Analytical Instruments	Model 400-HCLD	0-3000 ppm	0.5% Full Scale
Hydrocarbon	HC	Rosemount Analytical	Model 402	1-5000 ppm	1% FullScale

Lab 2 Analyzers

Analyzer	Abbreviation	Manufacturer	Model	Ranges	Repeatability / Precision
High Level Carbon Monoxide	HCO	Rosemount Analytical	Model 880A	0-500 ppm 0-5000 ppm	1% Full Scale
Low Level Carbon Monoxide	LCO	Horiba	AIA-210 LE	0-25 ppm 0-50 ppm 0-100 ppm 0-200 ppm	0.2% Full Scale
Carbon Dioxide	CO2	Horiba	AIA-210 LE	3% 5% 6% 16%	0.2% Full Scale
Oxide of Nitrogen Analyzer	NOx1	Rosemount Analytical	Model 955	0-10 ppm 0-25 ppm 0-100 ppm 0-250 ppm 0-1000 ppm 0-2500 ppm 0-10000 ppm	5% Full Scale
Oxide of Nitrogen Analyzer	NOx2	Rosemount Analytical	Model 955	0-10 ppm 0-25 ppm 0-100 ppm 0-250 ppm 0-1000 ppm 0-2500 ppm 0-10000 ppm	5% Full Scale
Hydrocarbon	HC	Rosemount Analytical	Model 402	1-5000 ppm	1% Full Scale

Appendix B

Cold Start Data Summary

Test ID	Test Run ID	WVU Ref No.	Vehicle Type	Vehicle Number	Particulate Filter	Fuel	Driving Schedule	CO	NOx	NO	HC	PM	CO2	Miles	MPG	BTU
								(g/mile)	(g/mile)	(g/mile)	(g/mile)	(g/mile)	(g/mile)			
3812	2	WMATA-3722-D1-ColdCBD	Transit Bus	3722	None	D1	ColdCBD	0.9808207	18.258068	17.70788	0.2313664	0.0661875	1939.6193	3.3833411	4.9647522	25378.91
3814	2	WMATA-3723-D1-ColdCBD	Transit Bus	3723	None	D1	ColdCBD	1.5835181	17.353994	17.016823	0.1435002	0.0452666	1798.3119	5.4920621	5.3523922	23540.875
							AVERAGE	1.2821694	17.806031	17.362351	0.1874333	0.055737	1868.9656	4.4377016	5.1585722	24459.893
3817	2	WMATA-3724-ULSD1-ColdCBD	Transit Bus	3724	DPX	ULSD1	ColdCBD	0.4388592	15.392447	10.521631	0.032207	0.0027946	1812.4905	6.0707431	5.446178	23453.512
3823	1	WMATA-3725-ULSD1-ColdCBD	Transit Bus	3725	DPX	ULSD1	ColdCBD	0.2621583	19.866693	13.746644	e	0.0076202	1758.4413	6.0646024	5.6146839	22746.822
							AVERAGE	0.3505087	17.62957	12.134138	0.032207	0.0052074	1785.4659	6.0776727	5.5305309	23101.167
3824	2	WMATA-3726-ULSD1-ColdCBD	Transit Bus	3726	CRT	ULSD1	ColdCBD	0.2503033	18.987528	10.162495	0.0001113	0.0024564	1875.1769	6.1045737	5.2653089	24259.166
3826	2	WMATA-3727-ULSD1-ColdCBD	Transit Bus	3727	CRT	ULSD1	ColdCBD	0.3428077	15.49309	8.4091158	0.0521297	0.0050456	1722.4391	7.2504916	5.7310719	22267.629
							AVERAGE	0.2965555	17.240309	9.2858052	0.0261205	0.003751	1798.808	6.6775327	5.4981904	23273.397
3760	1	WVU-21017-CECD1-WVU-1P	Tractor Truck	21017	DPX	ECD1	WVU-1P	3.7368507	30.084562	29.534397	2.2429991	0.0416308	1925.3623	7.6013498	5.2026925	24952.85
3761	1	WVU-21017-CECD1-WVU-1P	Tractor Truck	21017	DPX	ECD1	WVU-1P	1.9122905	18.629768	18.53912	0.2677911	0.0014746	1730.0942	11.126739	5.7974563	22392.809
							AVERAGE	2.8245706	24.357165	24.036758	1.2553951	0.0215527	1827.7283	9.3650446	5.5000894	23672.829
3764	1	WVU-21017-CECD1-WVU-1P	Tractor Truck	21017	None	ECD1	WVU-1P	4.2903352	23.09654	23.074806	1.3185741	0.2633255	1872.4095	11.159514	5.3468914	24279.902
3765	1	WVU-21017-CECD1-WVU-1P	Tractor Truck	21017	None	ECD1	WVU-1P	3.8317795	17.190697	15.184056	1.1336472	0.2175973	1648.741	11.127871	6.0719404	21380.645
							AVERAGE	4.0610573	20.143619	19.129431	1.2261106	0.2404614	1760.5753	11.143692	5.7094159	22830.273

Appendix C

Durability Study Data Summary

ROUND 1

Test ID	Test Run ID	WVU Ref No.	Vehicle Type	Vehicle Number	Particulate Filter	Fuel	Driving Schedule	CO (g/mile)	NOx (g/mile)	NO (g/mile)	HC (g/mile)	PM (g/mile)	CO2 (g/mile)	Miles	MPG	BTU
1482	1	RA GRO-5903-ECD-2cshvr	Tractor Truck	5903	CRT	ECD	2CSHVR	0.41	28.7	N/A	e	e	1879	13.45	5.07	24870
1482	2	RA GRO-5903-ECD-2cshvr	Tractor Truck	5903	CRT	ECD	2CSHVR	0.24	31.4	N/A	e	e	1712	13.44	5.57	22658
1482	3	RA GRO-5903-ECD-2cshvr	Tractor Truck	5903	CRT	ECD	2CSHVR	0.24	31.7	N/A	e	e	1889	13.44	5.05	25001
							AVERAGE	0.2966667	30.6		BDL	BDL	1826.6667	13.443333	5.23	24176.333
1483	1	RA GRO-5903-ECD-CSHVR	Tractor Truck	5903	none	ECD	CSHVR	10.01	26.3	N/A	0.19	0.43	1525	6.72	6.19	20394
1483	3	RA GRO-5903-ECD-CSHVR	Tractor Truck	5903	none	ECD	CSHVR	8.96	26.3	N/A	0.22	0.33	1788	6.72	5.29	23853
1483	4	RA GRO-5903-ECD-CSHVR	Tractor Truck	5903	none	ECD	CSHVR	8.26	30	N/A	0.21	0.25	1731	6.72	5.47	23077
1483	5	RA GRO-5903-ECD-CSHVR	Tractor Truck	5903	none	ECD	CSHVR	8.26	32.9	N/A	0.24	0.19	1767	6.72	5.36	23559
							AVERAGE	8.8725	28.875		0.215	0.3	1702.75	6.72	5.5775	22720.75
1484	1	RA GRO-5903-CARB-CSHVR	Tractor Truck	5903	none	CARB	CSHVR	11.9	28.7	N/A	0.23	0.57	1816	6.72	5.47	23713
1484	2	RA GRO-5903-CARB-CSHVR	Tractor Truck	5903	none	CARB	CSHVR	11.3	31.2	N/A	0.26	0.42	1825	6.72	5.45	23816
1484	3	RA GRO-5903-CARB-CSHVR	Tractor Truck	5903	none	CARB	CSHVR	9.5	37.7	N/A	0.22	0.27	1766	6.72	5.64	23016
1484	4	RA GRO-5903-CARB-CSHVR	Tractor Truck	5903	none	CARB	CSHVR	11.5	38.4	N/A	0.23	0.27	1897	6.72	5.24	24758
1484	5	RA GRO-5903-CARB-CSHVR	Tractor Truck	5903	none	CARB	CSHVR	11.2	39.5	N/A	0.25	0.25	1743	6.72	5.7	22757
							AVERAGE	11.08	35.1		0.239	0.356	1809.4	6.72	5.5	23612
1487	2	RA GRO-5904-ECD-2cshvr	Tractor Truck	5904	CRT	ECD	2CSHVR	0.44	34.5	N/A	e	0.0031	1707	13.45	5.58	22601
1487	3	RA GRO-5904-ECD-2cshvr	Tractor Truck	5904	CRT	ECD	2CSHVR	0.09	34.5	N/A	e	0.0034	1697	13.44	5.62	22452
1487	4	RA GRO-5904-ECD-2cshvr	Tractor Truck	5904	CRT	ECD	2CSHVR	0.23	32.9	N/A	e	0.0017	1923	13.45	4.96	25446
							AVERAGE	0.2533333	33.966667		BDL	0.0027333	1775.6667	13.446667	5.3666667	23499.667
1488	1	RA GRO-5904-ECD-CSHVR	Tractor Truck	5904	none	ECD	CSHVR	9.58	36.7	N/A	0.27	0.15	1777	6.72	5.32	23710
1488	2	RA GRO-5904-ECD-CSHVR	Tractor Truck	5904	none	ECD	CSHVR	8.96	34.6	N/A	0.29	0.18	1750	6.72	5.4	23349
1488	3	RA GRO-5904-ECD-CSHVR	Tractor Truck	5904	none	ECD	CSHVR	8.82	33.8	N/A	0.3	0.15	1725	6.72	5.48	23005
							AVERAGE	9.12	35.033333		0.2866667	0.16	1750.6667	6.72	5.4	23354.667
1490	1	RA GRO-5904-CARB-CSHVR	Tractor Truck	5904	none	CARB	CSHVR	11.1	40.2	N/A	0.34	0.23	1821	6.72	5.46	23771
1490	2	RA GRO-5904-CARB-CSHVR	Tractor Truck	5904	none	CARB	CSHVR	11.9	34.6	N/A	0.3	0.28	1797	6.72	5.53	23479
1490	3	RA GRO-5904-CARB-CSHVR	Tractor Truck	5904	none	CARB	CSHVR	10.4	37.2	N/A	0.3	0.23	1774	6.72	5.61	23147
1490	4	RA GRO-5904-CARB-CSHVR	Tractor Truck	5904	none	CARB	CSHVR	10.2	38.3	N/A	0.35	0.19	1967	6.72	5.06	25643
							AVERAGE	10.9	37.575		0.3225	0.2325	1839.75	6.72	5.415	24010
1491	1	RA GRO-5904-CARB-CSHVR	Tractor Truck	5904	none	CARB	CSHVR	8.49	28.5	N/A	0.4	0.31	1674	6.72	5.95	21816
1491	2	RA GRO-5904-CARB-CSHVR	Tractor Truck	5904	none	CARB	CSHVR	8.61	33.4	N/A	0.37	0.24	1698	6.72	5.87	22125
							AVERAGE	8.55	30.95		0.385	0.275	1686	6.72	5.91	21970.5
1415	1	RA GRO-5908-ECD-2CSHVR-DPX	Tractor Truck	5908	DPX	ECD	2CSHVR	0.4677845	32.432449	N/A	e	e	1606.5976	13.44388	5.9320621	21270.344
1415	2	RA GRO-5908-ECD-2CSHVR-DPX	Tractor Truck	5908	DPX	ECD	2CSHVR	0.2581736	33.489796	N/A	e	e	1729.3677	13.44151	5.5121665	22890.637
1415	3	RA GRO-5908-ECD-2CSHVR-DPX	Tractor Truck	5908	DPX	ECD	2CSHVR	0.2218893	39.219471	N/A	e	e	1667.3876	13.44267	5.7172103	22069.68
							AVERAGE	0.3159491	35.047239		BDL	BDL	1667.7843	13.442687	5.7204796	22076.887
1442	1	RA GRO-5909-ECD-2CSHVR-DPX	Tractor Truck	5909	DPX	ECD	2CSHVR	0.342903	29.647787	N/A	e	0	2138.6492	13.445374	4.4572048	28308.549
1442	2	RA GRO-5909-ECD-2CSHVR-DPX	Tractor Truck	5909	DPX	ECD	2CSHVR	0.4388813	31.885643	N/A	e	0	2144.3262	13.447791	4.4450951	28385.67
1442	3	RA GRO-5909-ECD-2CSHVR-DPX	Tractor Truck	5909	DPX	ECD	2CSHVR	0.3736746	31.95944	N/A	e	0.0026439	2145.9856	13.446181	4.4418707	28406.275
							AVERAGE	0.3650853	31.16429		BDL	0.0026439	2142.967	13.446449	4.4480569	28366.831

ROUND 2

Test ID	Test Run ID	WVU Ref No.	Vehicle Type	Vehicle Number	Particulate Filter	Fuel	Driving Schedule	CO (g/mile)	NOx (g/mile)	NO (g/mile)	HC (g/mile)	PM (g/mile)	CO2 (g/mile)	Miles	MPG	BTU
1571	2	RA GRO-5903-ECD-2cshvr	Tractor Truck	5903	CRT	CECD1	2cshvr	1.7556393	31.480185	33.236107	#	0.0013267	1935.7368	13.4481	4.9186981	25651.477
1571	3	RA GRO-5903-ECD-2cshvr	Tractor Truck	5903	CRT	CECD1	2cshvr	1.3518047	31.363692	33.424946	#	0.0015701	1954.2341	13.446785	4.8739243	25888.174
1571	4	RA GRO-5903-ECD-2cshvr	Tractor Truck	5903	CRT	CECD1	2cshvr	1.7570486	31.058146	35.354916	#	0.0021548	1924.0784	13.442973	4.9484682	25498.193
							AVERAGE	1.6248309	31.300741	34.338656	BDL	0.0016872	1938.0164	13.445953	4.9137635	25679.281
1573	1	RA GRO-5903-ECD-2cshvr	Tractor Truck	5903	CRT	ECD	2cshvr	1.3458741	31.590487	32.475163	#	#	1874.249	13.448292	5.0815291	24830.516
1573	2	RA GRO-5903-ECD-2cshvr	Tractor Truck	5903	CRT	ECD	2cshvr	1.1746941	30.190668	15.95142	#	#	1874.9905	13.442917	5.0802498	24836.771
1573	3	RA GRO-5903-ECD-2cshvr	Tractor Truck	5903	CRT	ECD	2cshvr	1.6177349	31.319618	15.94956	#	#	1911.2965	13.449759	4.9820265	25326.432
							AVERAGE	1.3794343	31.033658	21.458714	BDL	BDL	1886.8453	13.446989	5.0479358	24997.907
1574	1	RA GRO-5903-ECD-CSHVR	Tractor Truck	5903	None	ECD	CSHVR	12.008365	36.812469	37.012867	0.3305433	0.5474	1950.2098	6.7230144	5.0999808	25455.391
1574	2	RA GRO-5903-ECD-CSHVR	Tractor Truck	5903	None	ECD	CSHVR	12.511749	35.416133	33.758148	0.3620268	0.4735332	1946.8552	6.7209225	4.8465727	26023.535
1574	6	RA GRO-5903-ECD-CSHVR	Tractor Truck	5903	None	ECD	CSHVR	11.276808	35.189869	33.620518	0.3343801	0.4089918	1917.3605	6.719482	4.9273376	25607.541
							AVERAGE	11.932314	35.806824	34.797178	0.3423167	0.4766417	1938.1418	6.7211429	4.9586304	25695.489
1575	1	RA GRO-5903-CECD1-CSHVR	Tractor Truck	5903	None	CECD1	CSHVR	12.198536	37.359364	36.324593	0.4758224	0.4086195	1869.915	6.7251768	4.9904904	25383.486
1575	2	RA GRO-5903-CECD1-CSHVR	Tractor Truck	5903	None	CECD1	CSHVR	12.318127	39.576266	36.364626	0.4843076	0.4021347	1791.4169	6.7211022	5.2611294	23982.873
1575	3	RA GRO-5903-CECD1-CSHVR	Tractor Truck	5903	None	CECD1	CSHVR	10.808269	36.061836	35.697877	0.462258	0.4659691	1896.0887	6.7207332	4.9802048	25335.707
							AVERAGE	11.774977	37.665829	37.202366	0.4741293	0.4255077	1859.1402	6.7223374	5.0772748	24867.355
1576	2	RA GRO-5903-CARB-CSHVR	Tractor Truck	5903	None	CARB	CSHVR	13.025277	39.684537	39.607529	0.464416	0.4036711	2029.7773	6.7233233	4.8971715	26509.588
1576	3	RA GRO-5903-CARB-CSHVR	Tractor Truck	5903	None	CARB	CSHVR	13.257402	42.204731	39.556362	0.4704536	0.4154296	2027.3807	6.7247261	4.9019804	26483.582
1576	4	RA GRO-5903-CARB-CSHVR	Tractor Truck	5903	None	CARB	CSHVR	13.544665	41.631033	41.291142	0.4168154	0.3466944	1981.6698	6.722085	5.0125403	25899.443
							AVERAGE	13.275782	41.2402	40.151677	0.4505617	0.3885984	2013.016	6.7233766	4.9372307	26297.536
1618	2	RA GRO-5904-CECD1-2cshvr	Tractor Truck	5904	CRT	ECD1	2cshvr	0.91	40.7	43.7	X	0.0142	1730	13.44	5.51	22913
1618	3	RA GRO-5904-CECD1-2cshvr	Tractor Truck	5904	CRT	ECD1	2cshvr	1.1	36.7	35.4	0.018	0.0069	1749	13.44	5.45	23166
1618	4	RA GRO-5904-CECD1-2cshvr	Tractor Truck	5904	CRT	ECD1	2cshvr	1.82	36.3	22.7	0.021	0.0079	1742	13.44	5.47	23085
							AVERAGE	1.2766667	37.9	30.6	0.0195	0.0096667	1740.3333	13.44	5.4766667	23054.667
1619	2	RA GRO-5904-ECD-2cshvr	Tractor Truck	5904	CRT	ECD	2cshvr	2.19	38.4	73.8	X	0.0072	1687	13.45	5.64	22376
1619	3	RA GRO-5904-ECD-2cshvr	Tractor Truck	5904	CRT	ECD	2cshvr	2.07	39.6	29.2	0.0023	0.0025	1698	13.44	5.6	22514
1619	4	RA GRO-5904-ECD-2cshvr	Tractor Truck	5904	CRT	ECD	2cshvr	1.91	38.8	26.5	X	0.0034	1754	13.45	5.43	23257
							AVERAGE	2.0566667	38.933333	43.833333	0.0023	0.0043667	1713	13.446667	5.5566667	22715.667
1620	2	RAGRO-5904-ECD1-CSHVR	Tractor Truck	5904	none	ECD1	CSHVR	3.13	27.8	27	0.55	0.17	1906	6.72	4.98	25312
1620	3	RAGRO-5904-ECD1-CSHVR	Tractor Truck	5904	none	ECD1	CSHVR	2.81	29.1	27.7	0.54	0.16	1985	6.72	4.84	26078
1620	4	RAGRO-5904-ECD1-CSHVR	Tractor Truck	5904	none	ECD1	CSHVR	2.09	28.6	28.4	0.57	0.17	1930	6.72	4.93	25607
							AVERAGE	2.6766667	28.5	27.7	0.5533333	0.1666667	1933.6667	6.72	4.9166667	25665.667
1621	1	RAGRO-5904-CARB-CSHVR	Tractor Truck	5904	none	CARB	CSHVR	4.02	30.6	28.8	0.46	0.1	1950	6.72	5.13	25292
1621	2	RAGRO-5904-CARB-CSHVR	Tractor Truck	5904	none	CARB	CSHVR	3.68	32.1	31.2	0.48	0.14	1884	6.72	5.31	24439
1621	3	RAGRO-5904-CARB-CSHVR	Tractor Truck	5904	none	CARB	CSHVR	3.79	27.7	27.6	0.5	0.17	1930	6.71	5.19	25033
							AVERAGE	3.83	30.133333	29.2	0.48	0.1366667	1921.3333	6.7166667	5.21	24921.333
1596	2	RA GRO-5906-ECD-2cshvr	Tractor Truck	5906	DPX	ECD	2cshvr	4.8251429	27.418066	21.449436	0.0055152	0.0065407	1901.297	13.447076	4.9949718	25260.803
1596	3	RA GRO-5906-ECD-2cshvr	Tractor Truck	5906	DPX	ECD	2cshvr	4.4763603	27.505829	21.646933	0.0030446	0.0069561	1897.3741	13.443933	5.0066996	25201.637
1596	4	RA GRO-5906-ECD-2cshvr	Tractor Truck	5906	DPX	ECD	2cshvr	4.3934466	27.128426	21.466823	X	0.0067243	1893.1416	13.442261	5.0182362	25143.696
							AVERAGE	4.5816479	27.350773	21.520731	0.0042799	0.007407	1897.2709	13.444423	5.0066355	25202.045
1665	2	RA GRO-5906-ECD1-2cshvr	Tractor Truck	5906	DPX	ECD1	2cshvr	3.9056304	43.610137	45.420058	0.0464979	0.0110309	2117.1477	13.451669	4.7321105	27434.271
1665	3	RA GRO-5906-ECD1-2cshvr	Tractor Truck	5906	DPX	ECD1	2cshvr	3.9709053	45.097675	35.586147	0.0533449	X	2177.6235	13.449867	4.8009458	28216.986
1665	4	RA GRO-5906-ECD1-2cshvr	Tractor Truck	5906	DPX	ECD1	2cshvr	3.5603286	46.575535	38.50544	0.0545991	0.0124309	2124.1187	13.446638	4.7177987	27517.494
							AVERAGE	3.8456548	45.094116	39.837401	0.0521473	0.0121334	2139.63	13.448725	4.8503585	27722.917
1564	1	RA GRO-5909-ECD-2cshvr	Tractor Truck	5909	DPX	ECD	2cshvr	4.1691332	31.377002	24.240576	#	0.0048676	1964.8705	13.438604	4.8960709	25823.785
1564	2	RA GRO-5909-ECD-2cshvr	Tractor Truck	5909	DPX	ECD	2cshvr	4.7393889	30.661121	23.644588	#	0.0049906	1956.2445	13.449973	4.855547	25986.156
1564	3	RA GRO-5909-ECD-2cshvr	Tractor Truck	5909	DPX	ECD	2cshvr	4.7953138	27.337845	21.9604	0.0013729	0.0053012	2083.1448	13.446859	4.9006198	27666.635
1564	4	RA GRO-5909-ECD-2cshvr	Tractor Truck	5909	DPX	ECD	2cshvr	4.5577531	27.526016	21.653078	#	0.0055059	2028.6526	13.447106	4.6835294	26940.58
							AVERAGE	4.5653973	29.225996	22.079661	0.0013729	0.0054163	2003.2281	13.445186	4.7464433	26604.269

ROUND 3																	
Test ID	Test Run ID	WVU Ref No.	Vehicle Type	Vehicle Number	Particulate Filter	Fuel	Driving Schedule	CO (g/mile)	NOx (g/mile)	NO (g/mile)	HC (g/mile)	PM (g/mile)	CO2 (g/mile)	Miles	MPG	BTU
2175	1	RAGRO-5903-ECD1-2cshvr	Tractor Truck	5903	CRT	ECD1	2cshvr	3.13978	33.089451	33.699696	X	0.004661	1984.4619	13.4462	5.0505881	25704.334
2175	2	RAGRO-5903-ECD1-2cshvr	Tractor Truck	5903	CRT	ECD1	2cshvr	2.9523201	33.044716	18.051449	X	0.0031077	1945.5656	13.447039	5.1520839	25197.959
2175	3	RAGRO-5903-ECD1-2cshvr	Tractor Truck	5903	CRT	ECD1	2cshvr	2.8780031	33.018654	20.412771	X	X	1966.3679	13.442686	5.0980101	25465.23
							AVERAGE	2.9900344	33.05094	24.054639	BDL	0.0038843	1965.4651	13.445302	5.1002274	25455.841
2176	2	RAGRO-5903-CARB-CSHVR	Tractor Truck	5903	None	CARB	CSHVR	11.25141	35.427059	35.907104	0.4326764	0.5890282	1968.3309	6.718821	5.0557003	25678.342
2176	3	RAGRO-5903-CARB-CSHVR	Tractor Truck	5903	None	CARB	CSHVR	11.278783	34.440495	32.468834	0.3257538	0.5585057	1925.3163	6.7268182	5.1683331	25118.736
2176	4	RAGRO-5903-CARB-CSHVR	Tractor Truck	5903	None	CARB	CSHVR	11.254167	35.544724	33.788383	0.2746989	0.5570968	1962.2509	6.7193146	5.0724869	25593.363
							AVERAGE	11.261453	35.137426	34.055107	0.3443784	0.5682102	1951.966	6.7216506	5.0988401	25463.48
2172	1	RAGRO-5904-ECD1-2cshvr	Tractor Truck	5904	CRT	ECD1	2cshvr	2.2509942	25.959312	26.568439	0.0433269	0.0424165	1932.9242	13.447732	5.1886487	25020.387
2172	2	RAGRO-5904-ECD1-2cshvr	Tractor Truck	5904	CRT	ECD1	2cshvr	1.5095606	28.790319	28.773558	X	0.0130995	1873.4688	13.447551	5.356328	24237.127
2172	3	RAGRO-5904-ECD1-2cshvr	Tractor Truck	5904	CRT	ECD1	2cshvr	1.4888905	29.056057	18.469551	0.0176687	0.0057033	1849.5406	13.449504	5.4256306	23927.541
							AVERAGE	1.7498151	27.93523	24.603849	0.0304978	0.0204065	1885.3112	13.448262	5.3235358	24395.018
2173	3	RAGRO-5904-CARB-CSHVR	Tractor Truck	5904	None	CARB	CSHVR	9.9769907	22.973246	24.33462	0.2701618	0.6614845	1949.951	6.7276578	5.1094275	25408.326
2173	4	RAGRO-5904-CARB-CSHVR	Tractor Truck	5904	None	CARB	CSHVR	9.7484837	31.607718	31.118076	0.3615319	0.4480687	1911.8041	6.7242341	5.210691	24914.547
2173	5	RAGRO-5904-CARB-CSHVR	Tractor Truck	5904	None	CARB	CSHVR	9.523263	34.09396	31.699526	0.373533	0.4220777	1928.7333	6.7144394	5.1661811	25129.201
2173	6	RAGRO-5904-CARB-CSHVR	Tractor Truck	5904	None	CARB	CSHVR	7.8825183	34.994606	34.638904	0.3708181	0.4100687	1910.5747	6.7191291	5.2218814	24861.154
							AVERAGE	9.2828139	30.917382	30.447681	0.3440162	0.4854249	1925.2658	6.7213651	5.1770452	25078.307
2178	1	RAGRO-5908-ECD1-2cshvr	Tractor Truck	5908	DPX	ECD1	2cshvr	3.7371707	18.583414	18.382799	0.1479602	0.0027693	2102.186	13.444091	4.7662902	27237.535
2178	2	RAGRO-5908-ECD1-2cshvr	Tractor Truck	5908	DPX	ECD1	2cshvr	3.6178966	18.047895	13.583032	0.0478121	0.0066921	2065.6936	13.443131	4.8906813	26763.607
2178	3	RAGRO-5908-ECD1-2cshvr	Tractor Truck	5908	DPX	ECD1	2cshvr	3.8785229	18.296558	14.761916	0.0552443	0.0081345	2054.3704	13.447544	4.8763838	26822.598
							AVERAGE	3.74453	18.309289	15.575916	0.0836722	0.0058653	2074.0833	13.444922	4.8311218	26874.58
2179	1	RAGRO-5908-CARB-CSHVR	Tractor Truck	5908	None	CARB	CSHVR	9.38062	20.873652	21.342028	0.2219746	0.5854437	2033.9626	6.7204881	4.9026937	26479.729
2179	2	RAGRO-5908-CARB-CSHVR	Tractor Truck	5908	None	CARB	CSHVR	9.3277855	19.833652	19.296807	0.1755163	0.5968732	2042.3322	6.7223544	4.8833003	26584.891
2179	3	RAGRO-5908-CARB-CSHVR	Tractor Truck	5908	None	CARB	CSHVR	9.6562977	20.76244	21.231737	0.3091486	0.5602734	2071.8616	6.7142792	4.8120403	26978.576
							AVERAGE	9.4549011	20.489915	20.623191	0.2355465	0.5808301	2049.3855	6.7190409	4.8660115	26681.065
2191	1	RAGRO-5909-ECD1-2cshvr	Tractor Truck	5909	DPX	ECD1	2cshvr	4.341958	17.636812	16.744553	X	0.0738142	2174.3501	13.445056	4.6065207	28182.225
2191	2	RAGRO-5909-ECD1-2cshvr	Tractor Truck	5909	DPX	ECD1	2cshvr	3.5627301	17.252794	17.26733	X	0.0287422	2084.6333	13.433971	4.8069401	27007.201
2191	3	RAGRO-5909-ECD1-2cshvr	Tractor Truck	5909	DPX	ECD1	2cshvr	3.1374862	16.995106	16.368294	X	0.0269411	2043.5769	13.443261	4.9048491	26468.094
2191	4	RAGRO-5909-ECD1-2cshvr	Tractor Truck	5909	DPX	ECD1	2cshvr	3.4255071	18.132547	16.589201	X	0.0708336	2108.6872	13.44803	4.7527819	27314.949
							AVERAGE	3.6169204	17.504265	16.742344	BDL	0.0500808	2102.8069	13.44258	4.7677729	27243.117
2194	7	RAGRO-5909-CARB-CSHVR	Tractor Truck	5909	None	CARB	CSHVR	6.8280244	18.876083	19.605553	0.5571984	0.5342293	2011.6985	6.7208395	4.9637585	26153.973
2194	8	RAGRO-5909-CARB-CSHVR	Tractor Truck	5909	None	CARB	CSHVR	6.3677683	19.279541	19.653486	0.5932863	0.4207001	2006.8631	6.719883	4.9770956	26083.887
2194	9	RAGRO-5909-CARB-CSHVR	Tractor Truck	5909	None	CARB	CSHVR	7.6774211	18.929144	19.192383	0.6424673	0.428653	2046.892	6.7287593	4.8751316	26629.436
							AVERAGE	6.9577379	19.028256	19.483807	0.5976507	0.4611941	2021.8245	6.7231606	4.9386619	26289.098

Appendix D

General Performance Evaluation Data Summary

CRT Equipped Vehicles

Test ID	Test Run ID	WVU Ref No.	Vehicle Type	Fleet - Vehicle Number	Particulate Filter	Fuel	Driving Schedule	CO (g/mile)	NOx (g/mile)	NO (g/mile)	HC (g/mile)	PM (g/mile)	CO2 (g/mile)	Miles	MPG	BTU
3908	4	WCTA-479-ULSD1-BEELINE	Transit Bus	WCTA 479	None	ULSD1	BEELINE	7.9007502	39.486919	37.463734	0.3126024	0.6232539	2200.1418	6.6052966	4.481369	28630.674
3909	5	WCTA-479-ULSD1-BEELINE	Transit Bus	WCTA 479	None	ULSD1	BEELINE	8.3967574	39.613102	37.659115	0.3160755	0.6411537	2220.4167	6.54949	4.4194055	28902.529
3908	6	WCTA-479-ULSD1-BEELINE	Transit Bus	WCTA 479	None	ULSD1	BEELINE	7.5457821	39.057938	38.826363	X	0.6092626	2176.0354	6.664309	4.5087891	28329.559
							AVERAGE	7.9377632	39.385986	37.561424	0.314339	0.6245567	2198.8647	6.6063652	4.4631879	28620.921
3911	1	WCTA-479-ULSD1-2BEELINE	Transit Bus	WCTA 479	CRT	ULSD1	2BEELINE	0.5548742	37.372185	37.232117	e	0.144777	2255.7808	13.330826	4.3762469	29187.566
3911	2	WCTA-479-ULSD1-2BEELINE	Transit Bus	WCTA 479	CRT	ULSD1	2BEELINE	0.4305876	36.072952	20.563145	e	0.117286	2167.1936	13.408574	4.5596788	28037.973
3911	3	WCTA-479-ULSD1-2BEELINE	Transit Bus	WCTA 479	CRT	ULSD1	2BEELINE	0.5196285	38.12788	20.624088	e	0.11129	2221.9929	13.360743	4.4429307	28749.492
							AVERAGE	0.5016968	36.524339	20.593616	e	0.124451	2214.9891	13.366714	4.4529855	28658.344
3915	2	WCTA-568-ULSD1-BEELINE	Transit Bus	WCTA 568	None	ULSD1	BEELINE	1.5207306	32.264416	32.13784	0.3009721	0.3703938	2343.5049	6.6103668	4.2079644	30354.82
3915	3	WCTA-568-ULSD1-BEELINE	Transit Bus	WCTA 568	None	ULSD1	BEELINE	1.5997866	29.835917	29.276344	0.3631129	0.2654066	2284.5835	6.5199609	4.315614	29596.271
3915	4	WCTA-568-ULSD1-BEELINE	Transit Bus	WCTA 568	None	ULSD1	BEELINE	1.6891317	31.952698	31.3006	0.3638267	0.2406146	2338.0825	6.5328379	4.2168732	30290.691
							AVERAGE	1.5932196	31.350997	30.289472	0.3427372	0.2921384	2322.057	6.5543885	4.2468839	30080.594
3919	1	WCTA-568-ULSD1-2BEELINE	Transit Bus	WCTA 568	CRT	ULSD1	2BEELINE	0.225371	36.053684	35.977531	e	0.0596405	2750.2043	13.58332	3.5009872	35573.332
3919	2	WCTA-568-ULSD1-2BEELINE	Transit Bus	WCTA 568	CRT	ULSD1	2BEELINE	0.2694872	37.184269	18.777496	e	0.0811172	2791.9795	13.565816	3.5367773	36115.363
3919	3	WCTA-568-ULSD1-2BEELINE	Transit Bus	WCTA 568	CRT	ULSD1	2BEELINE	0.2409167	37.379162	18.612862	e	0.0833694	2786.6689	13.566429	3.5285118	36199.865
							AVERAGE	0.245259	36.872372	18.695179	e	0.0780424	2780.2846	13.571855	3.5519954	35962.887
3802	3	WMATA-3726-ULSD1-WMATA	Transit Bus	WMATA 3726	None	ULSD1	WMATA	1.4782145	16.163737	X	0.1632798	0.0966387	2238.2872	4.2262915	4.4064679	28987.389
3802	4	WMATA-3726-ULSD1-WMATA	Transit Bus	WMATA 3726	None	ULSD1	WMATA	1.4288781	16.167716	X	0.1480473	0.0977278	2115.4652	4.2364268	4.6622387	27397.15
3802	5	WMATA-3726-ULSD1-WMATA	Transit Bus	WMATA 3726	None	ULSD1	WMATA	1.4396571	16.071105	X	0.1479065	0.1001772	2224.2677	4.254333	4.4344234	28804.646
							AVERAGE	1.4489166	16.134186	X	0.1530779	0.0981613	2192.6734	4.2390636	4.5010427	28396.395
3806	1	WMATA-3726-ULSD1-2WMATA	Transit Bus	WMATA 3726	CRT	ULSD1	2WMATA	0.3003421	19.408252	19.19723	0	0.0028448	2296.9199	8.5507317	4.3010387	29697.941
3806	2	WMATA-3726-ULSD1-2WMATA	Transit Bus	WMATA 3726	CRT	ULSD1	2WMATA	0.454727	19.821965	19.476126	0	0.0030726	2345.6774	8.4749489	4.2097821	30341.713
3806	3	WMATA-3726-ULSD1-2WMATA	Transit Bus	WMATA 3726	CRT	ULSD1	2WMATA	0.2888084	18.794114	8.5795787	0.0100245	0.0024804	2209.9731	8.5808856	4.4678058	28590.707
							AVERAGE	0.3479591	19.341444	8.5795787	0.0033415	0.0027926	2284.1901	8.5354554	4.3261422	29543.454
3780	1	WMATA-5203-ULSD1-2WMATA	Transit Bus	WMATA 5203	CRT	ULSD1	2WMATA	1.5998328	39.928891	X	0.0482319	0.0095963	3654.6426	8.6976833	2.7001975	47304.688
3780	2	WMATA-5203-ULSD1-2WMATA	Transit Bus	WMATA 5203	CRT	ULSD1	2WMATA	1.54849	35.975833	X	0.0926819	0.0144099	3614.4464	8.614769	2.7301581	46785.57
3780	4	WMATA-5203-ULSD1-2WMATA	Transit Bus	WMATA 5203	CRT	ULSD1	2WMATA	1.8449387	35.407705	X	0.0829309	0.014318	3901.257	8.6450481	2.5293026	50600.879
							AVERAGE	1.6644205	37.104143	X	0.0746816	0.0127747	3723.4487	8.6525002	2.6532194	48197.046
3782	1	WMATA-5203-ULSD1-WMATA	Transit Bus	WMATA 5203	None	ULSD1	WMATA	4.2294508	36.816731	X	0.9897672	0.3048656	3663.1017	4.2943583	2.688745	47506.18
3782	2	WMATA-5203-ULSD1-WMATA	Transit Bus	WMATA 5203	None	ULSD1	WMATA	4.921425	36.113207	X	1.0600649	0.2909663	3670.5911	4.3007474	2.6823184	47620
3782	3	WMATA-5203-ULSD1-WMATA	Transit Bus	WMATA 5203	None	ULSD1	WMATA	5.2490212	37.782332	X	0.9844161	0.2899342	3744.8928	4.239448	2.629065	48584.57
							AVERAGE	4.7996323	36.904757	X	1.0114161	0.295222	3692.8619	4.2781849	2.6667085	47903.583
3728	1	NYCDOS-25CF042-D2-NYGTC3X	Refuse Truck	NYCDOS 25CF042	CRT	D2	NYGTC3X	1.3957316	124.22823	100.26445	1.2546827	0.6889607	7633.8398	1.1436392	1.3319147	97603.852
3728	3	NYCDOS-25CF042-D2-NYGTC3X	Refuse Truck	NYCDOS 25CF042	CRT	D2	NYGTC3X	1.2624719	123.62862	99.263847	1.1893122	0.7607692	7592.7051	1.1427212	1.3391953	97073.227
							AVERAGE	1.3241017	123.92842	99.764149	1.2219974	0.7248649	7613.2725	1.1431802	1.336555	97338.539
3730	1	NYCDOS-25CF042-D2-NYGTC3X	Refuse Truck	NYCDOS 25CF042	None	D2	NYGTC3X	11.475048	129.44873	119.61689	7.9004464	3.3824895	7816.8135	1.1361711	1.2946495	100413.28
3730	2	NYCDOS-25CF042-D2-NYGTC3X	Refuse Truck	NYCDOS 25CF042	None	D2	NYGTC3X	11.92857	127.94698	117.79655	8.477252	3.6521904	7881.0039	1.1427048	1.2837501	101265.82
3730	3	NYCDOS-25CF042-D2-NYGTC3X	Refuse Truck	NYCDOS 25CF042	None	D2	NYGTC3X	11.872091	126.7731	116.56904	8.4872751	3.6311398	7707.2603	1.1529016	1.3125819	99041.438
							AVERAGE	11.691903	128.05627	117.99082	8.2883245	3.5552729	7801.6925	1.1445925	1.2969938	100240.18
3732	1	NYCDOS-25CF043-D2-OCRTC2X	Refuse Truck	NYCDOS 25CF043	CRT	D2	OCRTC2X	1.1101534	48.762203	37.221741	0.4338014	0.119159	4387.9653	5.174305	2.3173819	56097.789
3732	2	NYCDOS-25CF043-D2-OCRTC2X	Refuse Truck	NYCDOS 25CF043	CRT	D2	OCRTC2X	1.038231	46.277462	35.020947	0.4338413	0.1342898	4260.1577	5.1817369	2.3699174	54463.555
3732	3	NYCDOS-25CF043-D2-OCRTC2X	Refuse Truck	NYCDOS 25CF043	CRT	D2	OCRTC2X	1.1234468	45.749191	34.298226	0.4229617	0.1190263	4184.5044	5.1698213	2.4299827	53498.324
							AVERAGE	1.0906104	46.929619	35.499838	0.4302548	0.1241581	4277.5425	5.1752877	2.378094	54686.556
3734	1	NYCDOS-25CF043-D2-OCRTC2X	Refuse Truck	NYCDOS 25CF043	None	D2	OCRTC2X	5.157793	47.171249	44.079792	3.2052305	1.0153888	4264.4517	5.197	2.3760166	54713.422
3734	2	NYCDOS-25CF043-D2-OCRTC2X	Refuse Truck	NYCDOS 25CF043	None	D2	OCRTC2X	5.3280472	46.667477	43.475082	3.2622323	0.8973534	4245.3652	5.2003467	2.3864012	54475.332
3734	3	NYCDOS-25CF043-D2-OCRTC2X	Refuse Truck	NYCDOS 25CF043	None	D2	OCRTC2X	5.2577448	47.630096	44.389305	3.3988633	0.9240998	4243.8472	5.2116814	2.3870711	54460.043
							AVERAGE	5.248195	47.156264	43.981393	3.2887754	0.945603	4251.2214	5.2040127	2.383163	54549.599

DPX Equipped Vehicles

Test ID	Test Run ID	WVU Ref No.	Vehicle Type	Fleet - Vehicle Number	Particulate Filter	Fuel	Driving Schedule	CO (g/mile)	NOx (g/mile)	NO (g/mile)	HC (g/mile)	PM (g/mile)	CO2 (g/mile)	Miles	MPG	BTU
3905	1	WCTA-479-ULSD1-2BEELINE	Transit Bus	WCTA 479	DPX	ULSD1	2BEELINE	0.2733495	40.37204	40.2831123	e	0.0627051	2195.5149	13.145769	4.49758629	28400.143
3905	2	WCTA-479-ULSD1-2BEELINE	Transit Bus	WCTA 479	DPX	ULSD1	2BEELINE	0.2388986	37.651806	18.623613	e	0.0639776	2053.1348	13.214984	4.8099947	26555.539
3905	4	WCTA-479-ULSD1-2BEELINE	Transit Bus	WCTA 479	DPX	ULSD1	2BEELINE	0.5936021	37.403152	18.110235	e	0.0390696	2195.6711	13.040664	4.4999221	28406.213
							AVERAGE	0.3576171	38.475666	18.366924	e	0.0619174	2148.1069	13.133806	4.6013999	27787.298
3908	4	WCTA-479-ULSD1-BEELINE	Transit Bus	WCTA 479	None	ULSD1	BEELINE	7.9007502	39.486919	37.463734	0.3126024	0.6232539	2200.1418	6.6052966	4.461369	28630.674
3908	5	WCTA-479-ULSD1-BEELINE	Transit Bus	WCTA 479	None	ULSD1	BEELINE	8.3967574	39.613102	37.699115	0.3160755	0.6411537	2220.4167	6.54949	4.4194055	28902.529
3908	6	WCTA-479-ULSD1-BEELINE	Transit Bus	WCTA 479	None	ULSD1	BEELINE	7.5457821	39.057938	38.826363	X	0.6092626	2176.0354	6.664309	4.5087891	28329.559
							AVERAGE	7.9377632	39.385986	37.561424	0.314339	0.6245567	2198.8647	6.6663652	4.4631879	28620.921
3915	2	WCTA-568-ULSD1-BEELINE	Transit Bus	WCTA 568	None	ULSD1	BEELINE	1.5207306	32.264416	32.13784	0.3009721	0.3703938	2343.5049	6.6103668	4.2079644	30354.82
3915	3	WCTA-568-ULSD1-BEELINE	Transit Bus	WCTA 568	None	ULSD1	BEELINE	1.5697866	29.835917	29.276344	0.3633129	0.2654066	2284.5835	6.5199609	4.315814	29596.271
3915	4	WCTA-568-ULSD1-BEELINE	Transit Bus	WCTA 568	None	ULSD1	BEELINE	1.6891317	31.952658	31.3006	0.3639267	0.2406146	2336.0825	6.5326379	4.2169732	30290.691
							AVERAGE	1.5932196	31.350997	30.289472	0.3427372	0.2921384	2322.057	6.5543885	4.2469839	30080.594
3916	2	WCTA-568-ULSD1-2BEELINE	Transit Bus	WCTA 568	DPX	ULSD1	2BEELINE	0.1093813	36.127045	35.941769	e	0.0351377	2784.3994	13.606891	3.5468206	36013.098
3916	3	WCTA-568-ULSD1-2BEELINE	Transit Bus	WCTA 568	DPX	ULSD1	2BEELINE	0.1492219	35.682167	23.050547	e	0.0325715	2711.3455	13.376979	3.6423087	35068.965
3916	4	WCTA-568-ULSD1-2BEELINE	Transit Bus	WCTA 568	DPX	ULSD1	2BEELINE	0.0768302	37.374432	23.720747	e	0.0336799	2799.1123	13.586918	3.5282571	36202.578
							AVERAGE	0.1118145	36.394548	23.385647	e	0.0337964	2764.9524	13.523596	3.5724822	35761.547
3774	1	WMATA-5229-ULSD1-2WMATA	Transit Bus	WMATA 5229	DPX	ULSD1	2WMATA	1.4691888	42.779972	X	0.1074993	0.0192676	3819.0873	8.504014	2.5840232	49431.445
3774	2	WMATA-5229-ULSD1-2WMATA	Transit Bus	WMATA 5229	DPX	ULSD1	2WMATA	1.1622926	40.192536	X	0.084452	0.0195249	3864.0818	8.5217962	2.5543218	50006.23
3774	3	WMATA-5229-ULSD1-2WMATA	Transit Bus	WMATA 5229	DPX	ULSD1	2WMATA	0.5888288	39.958124	X	0.0833892	0.0226142	3880.3863	8.4969501	2.5441875	50205.418
							AVERAGE	1.0734367	40.976877	X	0.0917802	0.0204689	3854.5185	8.5075866	2.5608442	49881.031
3777	1	WMATA-5229-ULSD1-WMATA	Transit Bus	WMATA 5229	None	ULSD1	WMATA	3.8770394	39.486539	X	1.1742205	0.2014925	3743.8712	4.2933593	2.630868	48651.277
3777	2	WMATA-5229-ULSD1-WMATA	Transit Bus	WMATA 5229	None	ULSD1	WMATA	3.7939406	38.424762	X	1.0732263	0.1791557	3647.551	4.3139749	2.7004869	47299.617
3777	3	WMATA-5229-ULSD1-WMATA	Transit Bus	WMATA 5229	None	ULSD1	WMATA	3.7974569	38.502299	X	1.1287159	0.1803496	3699.507	4.3295422	2.6897245	47844.637
							AVERAGE	3.8228123	38.807867	X	1.1253876	0.1869992	3697.8431	4.3122921	2.6870284	47998.51
3795	1	WMATA-3724-ULSD1-2WMATA	Transit Bus	WMATA 3724	DPX	ULSD1	2WMATA	0.2668085	16.069053	X	0	0.010742	2016.7007	8.7101517	4.891232	26114.484
3795	2	WMATA-3724-ULSD1-2WMATA	Transit Bus	WMATA 3724	DPX	ULSD1	2WMATA	0.2714219	16.883435	X	0.1063895	0.0104527	2077.1592	8.6344366	4.7525616	26876.453
3795	3	WMATA-3724-ULSD1-2WMATA	Transit Bus	WMATA 3724	DPX	ULSD1	2WMATA	0.202237	16.591791	X	0.0368681	0.0110322	1934.3387	8.7251797	5.1041927	25024.916
							AVERAGE	0.2467558	17.180093	X	0.0477526	0.0107423	2010.0662	8.6899227	4.8159954	26005.285
3796	3	WMATA-3724-ULSD1-WMATA	Transit Bus	WMATA 3724	None	ULSD1	WMATA	2.0237846	18.662679	X	0.1943269	0.1576901	2223.0512	4.3060187	4.4347248	28802.689
3796	4	WMATA-3724-ULSD1-WMATA	Transit Bus	WMATA 3724	None	ULSD1	WMATA	1.991073	17.707339	X	0.2006153	0.1435812	2217.5224	4.3108077	4.4458265	28730.766
3796	5	WMATA-3724-ULSD1-WMATA	Transit Bus	WMATA 3724	None	ULSD1	WMATA	2.1911636	17.688826	X	0.1955504	0.1487632	2142.5685	4.2972507	4.6004424	27765.156
							AVERAGE	2.0686737	18.019615	X	0.1967976	0.1500115	2194.3807	4.305359	4.4936646	28432.87
3719	2	NYCDOS-25CF045-D2-NYGTC3X	Refuse Truck	NYCDOS 25CF045	DPX	D2	NYGTC3X	2.1931176	115.54144	129.39076	1.4117553	0.0405637	7695.2324	1.1268885	1.3209939	98410.75
3719	3	NYCDOS-25CF045-D2-NYGTC3X	Refuse Truck	NYCDOS 25CF045	DPX	D2	NYGTC3X	1.8139172	115.81574	128.54462	1.3742445	0.0374865	7558.041	1.1346478	1.3450744	96848.93
3719	4	NYCDOS-25CF045-D2-NYGTC3X	Refuse Truck	NYCDOS 25CF045	DPX	D2	NYGTC3X	3.0239227	113.78798	127.04073	1.4059228	0.1467258	7467.1094	1.1329216	1.3610737	95512.828
							AVERAGE	2.3436525	115.04839	128.32537	1.3973075	0.075582	7573.4609	1.131412	1.3423807	96857.503
3722	1	NYCDOS-25CF045-D2-NYGTC3X	Refuse Truck	NYCDOS 25CF045	None	D2	NYGTC3X	12.7	119.91319	129.0148	7.5515137	3.1416454	7470.5146	1.148439	1.3541719	95899.633
3722	2	NYCDOS-25CF045-D2-NYGTC3X	Refuse Truck	NYCDOS 25CF045	None	D2	NYGTC3X	12.216476	121.28515	130.77827	7.7190075	3.0964077	7506.6978	1.1360607	1.3477232	96458.977
3722	3	NYCDOS-25CF045-D2-NYGTC3X	Refuse Truck	NYCDOS 25CF045	None	D2	NYGTC3X	11.766148	119.5512	128.85121	7.5629468	2.8887794	7469.8564	1.1468488	1.3545485	95972.945
							AVERAGE	12.227541	120.24984	129.5481	7.611156	3.0422775	7482.3563	1.1437829	1.3521479	96143.852
3724	1	NYCDOS-25CF044-D2-OCRTC2X	Refuse Truck	NYCDOS 25CF044	DPX	D2	OCRTC2X	0.8944548	45.018326	30.647865	X	0.1409825	3860.2673	5.0317025	2.6357734	49321.387
3724	2	NYCDOS-25CF044-D2-OCRTC2X	Refuse Truck	NYCDOS 25CF044	DPX	D2	OCRTC2X	0.768316	43.679958	29.389933	X	0.1106838	3756.616	5.1622548	2.7082226	48001.961
3724	3	NYCDOS-25CF044-D2-OCRTC2X	Refuse Truck	NYCDOS 25CF044	DPX	D2	OCRTC2X	0.7061269	42.674782	28.493665	X	0.0932558	3737.0481	5.2269829	2.7223425	47752.992
							AVERAGE	0.7896332	43.791022	29.510155	X	0.1149907	3784.6436	5.1409801	2.6887795	48358.78
3726	1	NYCDOS-25CF044-D2-OCRTC2X	Refuse Truck	NYCDOS 25CF044	None	D2	OCRTC2X	4.9668012	43.214355	40.460411	3.0416317	0.6826055	3631.7424	5.2443075	2.7885113	46619.859
3726	2	NYCDOS-25CF044-D2-OCRTC2X	Refuse Truck	NYCDOS 25CF044	None	D2	OCRTC2X	4.8963294	43.520157	40.7393	3.1042418	0.7038816	3719.8342	5.2433567	2.7227192	47746.387
3726	3	NYCDOS-25CF044-D2-OCRTC2X	Refuse Truck	NYCDOS 25CF044	None	D2	OCRTC2X	4.872942	43.681725	40.812763	3.222755	0.7801871	3708.5244	5.2762103	2.7307348	47606.234
							AVERAGE	4.9120242	43.472079	40.670825	3.1228762	0.7255248	3686.7004	5.2546248	2.7473218	47324.16